# Sarcolemmal lipid analysis from mechanically skinned rat muscle fibres.

Val Andrew Miciano Fajardo, BSc Biomedical Sciences

Submitted in partial fulfillment of the requirements for the degree
Master of Science in Applied Health Sciences
(Health Science)

Under the supervision of Paul LeBlanc, PhD

Faculty of Applied Health Sciences
Brock University, St. Catharines, Ontario

MASTER OF SCIENCE (2011)

TITLE: Sarcolemmal lipid analysis from mechanically skinned rodent EDL muscle fibres.

AUTHOR: Val Andrew Fajardo

SUPERVISOR: Dr. Paul J. LeBlanc

SUPERVISORY COMMITTEE: Dr. Brian Roy

Dr. Thad Harroun

Dr. Robert Grange (External examiner)

NUMBER OF PAGES: 197

ABSTRACT

Membrane lipid composition, which includes phospholipid (PL) headgroup, and fatty acid (FA) saturation, has been shown to affect cellular function. The sarcolemma (SL) membrane is integral to skeletal muscle function and health. Previous studies assessing SL lipid composition are limited as they have 1) restricted analysis to a PL level and neglected FA composition and 2) relied on aggressive membrane isolation procedures resulting in t-tubule and sarcoplasmic reticulum contamination and unknown levels of nuclear and mitochondrial contamination. Thus, to overcome these limitations, this study assessed a method of individually skinned skeletal muscle fibres as an alternative to analyze complete sarcolemmal membrane lipid composition. The major findings of this study were 1) complete SL lipid composition can be obtained 2) the SL had higher sphingomyelin content than previous studies and 3) the SL membrane had minimal nuclear and mitochondrial contamination and was void of contamination from sarcoplasmic reticulum and t-tubules.

# ACKNOWLEDGEMENTS

My family, thank you for your love and support. To Beth who has been extremely supportive and patient. To my Mom and Dad who have continued to push me throughout my academic career. To the Eppendorf family, thank you for all the Sunday night dinners which helped me debrief from some very hard weeks.

To Paul, an excellent mentor and friend, thank your patience and wisdom. Thank you for leading me through my transition from student to researcher.

To the Muscle Physiology Group at La Trobe University, thank you for teaching me how to skin single muscle fibres and biochemically analyze them.

To my committee, thank you for your time and valuable feedback.

To my lab mates and friends, thank you for the good times! I think we can all say we have truly learned from each other.

To Bailey and Elmo, I'll never forget my best mates.

Thank you!

**TABLE OF CONTENTS**

LIST OF TABLES

LIST OF FIGURES

LIST OF ABBREVIATIONS

PL - Phospholipid

PC – Phosphatidylcholine

PS – Phosphatidylserine

PE – Phosphatidylethanolamine

PA – Phosphatidic acid

CL – Cardiolipin

SM - Sphingomyelin

FA – Fatty acid

SFA – Saturated fatty acid

MUFA – Monounsaturated fatty acid

PUFA – Polyunsaturated fatty acid

ATP – Adenosine triphosphate

MHC – myosin heavy chain

SO – Slow oxidative

FOG – Fast oxidative glycolytic

FG – Fast glycolitic

SR – Sarcoplasmic reticulum

DHPR – Dihydropyridine receptor

SL – Sarcolemma

ECC – Excitation contraction coupling

DGC – Dystrophin glycoprotein complex

TLC – Thin layer chromatography

HPTLC – High performance thin layer chromatography

GC – Gas chromatography

GLUT 4 – Glucose uptake transporter 4

EDL – extensor digitorum longus

PVDF – Polyvinylidene difluoride

CaV 1.1 – DHPR skeletal muscle isoform

CaV 1.2 – DHPR cardiac muscle isoform

SERCA1 – Sarco(endo)plasmic reticulum $Ca^{2+}$-ATPase 1

SERCA1 – Sarco(endo)plasmic reticulum $Ca^{2+}$-ATPase 2

GM130 – Golgi marker 130

HEPES - 4-(2-hydroxyethyl)-1-piperazineethanesulfonic acid

BHT – Butylated hydroxytoluene

PBS – Phosphate buffer saline

FAME – Fatty acid methyl ester

FFID – Fast flame ionizing detector

SE – Standard error

BMR – basal metabolic rate

DG –dystroglycan

# Chapter 1.0: General Introduction

## 1.1 Biological membranes

Membranes are essential cellular components of life as they provide semi-permeable barriers between cells' internal milieu and their external environment. Importantly, the lipid membrane bilayer, as well as partitioning cells into various subcompartments, also provides a dynamic environment in which much of the important chemistry of life occurs (Hulbert, et al., 2005). These events include metabolism, cell signalling, and fuel storage. In order for them to occur, biological membranes house proteins that perform the roles for these vital functions. As a result, membrane-associated protein function may ultimately be influenced by membrane structure. Importantly, membrane structure can be influenced by membrane lipid, carbohydrate and protein composition.

## 1.2 Membrane lipids

Membranes are comprised of three main classes of lipids; i) phospholipids (PL), ii) glycolipids and iii) cholesterol which all exhibit the same bipolar nature that is responsible for the bilayer structure. The PLs represent the most dominant membrane lipid and their bilayer formation is oriented such that non-polar fatty acyl tails of two distinct lipids are adjacent and attracted to one another with van der Waals forces, and their respective polar head groups are facing a hydrophilic environment. The three classes, more importantly, differ with regards to their structure and importantly their localization, which evidentially partially accounts for the various combinations in membrane composition. Additional variation within membrane composition occurs due

to the different combinations of fatty acyl chains that bind to the backbones of PLs and glycolipids.

*Phospholipids*

Phospholipids may either be derived from glycerol or sphingosine forming glycerophospholipids and sphingophospholipids, respectively (Dannenberger, et al., 2007). The differences within PL species, importantly, are not limited to backbone, but also depend on the phosphate head group. The phosphoryl group consists of choline, serine, inositol, or ethanolamine resulting in phosphatidylcholine (PC), phosphatidylserine (PS), phosphatidylinositol (PI), and phosphatidylethanolamine (PE), respectively. Phosphatidic acid (PA) is unique and represents the most simple glycerophospholipid where there is no head group attached to the phosphate head. Importantly most PLs contain two non-polar fatty acid tails with the exception of lysophospholipids that have only one and cardiolipin (CL), which represents a dimer of phospholipids whereby there are 2 phosphorus groups and four fatty acyl chains. Similar to glycerophospholipids, alcohol groups such as choline and ethanolamine can bind to the polar phosphate heads on sphingophospholipids. Sphingomyelin (SM) is a sphingophospholipid comprised of a ceramide backbone with a choline attached to the phosphate head (Ramstedt & Slotte, 2002). Ceramide is a fatty acyl chain attached to an amide group on the sphingosine; an 18-carbon chain with an amino alcohol terminal (Ramstedt & Slotte, 2002). Taken together, the aforementioned phospholipids represent the majority of phospholipids found in cellular membranes, which vary by percent composition, location, and predominant fatty acyl chain (Table 1.0**)**.

**Table 1. 1.** Characteristics of the main phospholipids found in biological membranes.

| PL | Composition | Charge | Primary Fatty Acids | Dominant location |
|---|---|---|---|---|
| PC | 30-35%[2] | Neutral[1] | High 16:0, 18:2n6[3], and low 22:6n3[2] | Outer monolayer (66%)[3] |
| PE | 15-25%[4,5] | Neutral[4,5] | High 18:0[3], 20:4n6[3] | Inner monolayer (~20%)[3,6] |
| SM | 2-15%[8,9] | Neutral[8] | High 16:0 and 18:0, low unsaturated FA, 24:1 and 22:0[1,8] | Extracellular monolayer of sarcolemma[8,9] |
| PI | 10-15%[1] | Acidic[1] | 18:0 in sn-1, 20:4 in sn-2[1] 18:2n6[3] | Inner monolayer |
| PS | 2-10% | Acidic[1] | High 22:6n3 | Inner monolayer of plasma membranes, sarcolemma |
| CL | 2-5%[7] | Acidic | 18:2n6[6], high levels (80%) Of unsaturation[6] | Inner monolayer of mitochondria[6] |
| PA | Trace Amounts[10] | Acidic[11] | High 16:0 and 18:0[1] | Present only in small amounts in biological membranes |

Table derived from: (Stefanyk, 2008).
Original data obtained from: [1](Voet, 2004), [2](Mitchell, et al., 2007), [3] (Clore, et al., 1998), [4] (Bell GH, 1976), [5] (Bleijerveld, et al., 2007), [6] (Ritov, et al., 2006), [8] (Tsalouhidou, et al., 2006),[9] (Ramstedt & Slotte, 2002), [10] (Nikolaidis & Mougios, 2004), [11](Mahrla & Zachar, 1974), [12] (Dalton, et al., 1998). PL, phospholipids; SM, sphingomyelin; PC, phosphatidylcholine; PS, phosphatidylserine; PI, phosphatidylinositol; PE, phosphatidylethanolamine; sn stereospecific numbering.

*Glycolipids*

Glycolipids are lipids that have a carbohydrate or small carbohydrate chains attached to the backbone by a glycoside linkage in contrast to the phosphate group found in phospholipids (Bell GH, 1976; Voet, 2004). Similar to phospholipids, these glycolipids are either glycero- or sphingoglycolipids depending on the backbone. This lipid species is exclusively located on the outer monolayer of membranes (Degroote, et al., 2004).

*Fatty Acids*

Fatty acids (FA) commonly found in cellular membranes are long-chain hydrocarbons (most commonly 14-20 carbons) with a carboxyl group at one end and a methyl group at the other (Voet, 2004). Indeed the differences within FAs lie not only on the length of the carbon chain, but also on the saturation of these chains with hydrogen ions. Saturated fatty acids (SFA) are those that are fully "saturated" with hydrogen (Figure 1.1 a). Monounsaturated fatty acids (MUFA) have one double bond along the carbon-carbon chain (Figure 1.1 b). In contrast, more than one double bond results in polyunsaturated fatty acids (PUFA) (Figure 1.1 c). Recent attention has been drawn to the essential fatty acids, n3 and n6 PUFA, named due to the presence of the first double bond from the methyl end ($3^{rd}$ and $6^{th}$, respectively). These two PUFAs are essential fatty acids since mammalian cells are unable to synthesize these FA (Voet, 2004). Aside from the number and position of double bonds within a FA, the double bond has two possible configurations, *cis* or *trans* (Voet, 2004) . The *cis* configuration has the hydrogens on the same side of the carbon-carbon double bond causing a kink in the chain, whereas, the *trans* configuration has the hydrogens on opposite sides (Figure 1.2).

*Cholesterol*

Cholesterol is composed of a hydrophobic four ring steroid structure branched by hydrocarbon chains and bipolarized with a hydroxyl group (Bell GH, 1976). It is located predominantly at the outer monolayer of cell membranes, and to a lesser extent in the membranes of subcellular organelles (Voet, 2004). Cholesterol can bind with the fatty acyl chains of different PLs, but most commonly interacts with SM within lipid raft domains (cholesterol enriched micro domains) (Pike, 2004). These microdomains within

membranes are important in signal transduction, protein activity and membrane trafficking (M'Baye, et al., 2008).

a.
b.
c.

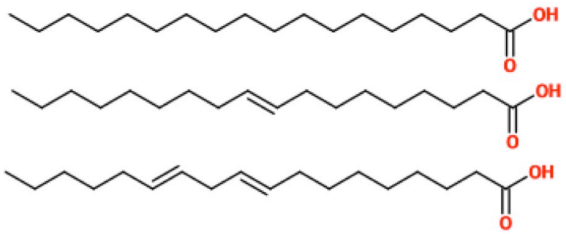


**Figure 1. 1.** Chemical structures of fatty acids: a. saturated fatty acid (18:0, stearic acid), b. monounsaturated fatty acid (18:1, oleic acid), c. polyunsaturated fatty acid (18:2n:6, linoleic acid (image created on www.emolecules.com).

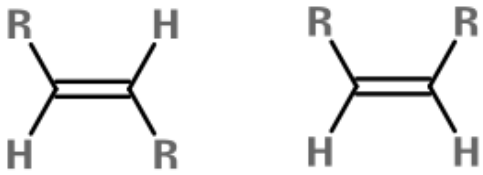


Trans Cis

**Figure 1. 2.** Chemical structures of *cis* and *trans* configured carbon double bonds (image created on www.emolecules.com).

### 1.3 Membrane proteins

Membrane proteins, either integral or peripheral, carry out the dynamic processes associated with membranes from different tissues (Voet, 2004). Integral proteins are those that span the membrane and as such, are embedded within the lipid bilayer by hydrophobic forces, and along with lipids account for the majority of membrane weight. Conversely, peripheral proteins are anchored to lipid bilayers by hydrophilic forces on PL heads or on hydrophilic residues of the integral proteins. Both groups of proteins can act as enzymes, receptors, or transporters that ultimately play roles in the overall function of the cell including cell communication (ie. G-proteins), fuel uptake (ie. Glucose transporters), and adhesion (ie. SNARE proteins). Recent studies reveal that certain membrane areas differ in their protein composition where the selection can be based upon chemical (hydrophobicity) or physical (membrane thickness, microviscosity) properties of the lipid micro domain (Marguet, et al., 2006), and thus indicate that protein composition can vary across membranes due to its relation with lipids.

### 1.4 Membrane carbohydrates

The proportion of carbohydrates on biological membranes never exceeds 10% by mass and is often much less (Bretscher & Raff, 1975). Membrane carbohydrates are mainly oligosaccharides; small chains of monosaccharides and are attached to proteins and lipids, thus constituting glycoproteins and glycolipids, the latter of which was described above (section 1.2 ii). Although hundreds of monosaccharides occur in nature, only about 10 are seen within membrane glyolipids and glycoproteins including the principal sugars: galactose, mannose, fucose, galactosamine, glucosamine, glucose and sialic acid (Bretscher & Raff, 1975). Indeed, the differing combinations between fatty

acyl chains and carbohydrate head group accounts for variability in membrane glycolipid composition. Furthermore, although the oligosaccharides are usually no longer than 15 sugars, they can be branched in different combinations and thus adds more structural complexity and variation in membranes (Bretscher & Raff, 1975). Glycoproteins and glycolipids are both important acting as biological markers for cell-to-cell signalling, cell growth regulation, development and differentiation (Bretscher & Raff, 1975; Voet, 2004).

### 1.5 The membrane structure-protein function relationship

Throughout sections 1.2 – 1.4 it was highlighted that lipids and proteins are the major components of biological membranes. As such, the relationship between lipids and proteins is important for many biological processes and the foundation of this interaction between lipids and proteins is based upon membrane structure. Moreover, membrane structure can be divided into two components: 1) chemical structure and 2) physical structure. Chemical structure includes lipid composition, which may have direct (ie. lipid species activation/inactivation of specific proteins) and indirect (lipid composition correlation to physical properties of membrane structure, see *Membrane physical structure: fluidity* section) influences on protein function (Figure 1.3). Physical properties are those that are directly linked to protein function, and this includes membrane bending, thickness and fluidity (Pabst, et al., 2010). Taken together, membrane lipid composition can affect protein function directly with specific lipids and indirectly via changes in membrane physical structure.

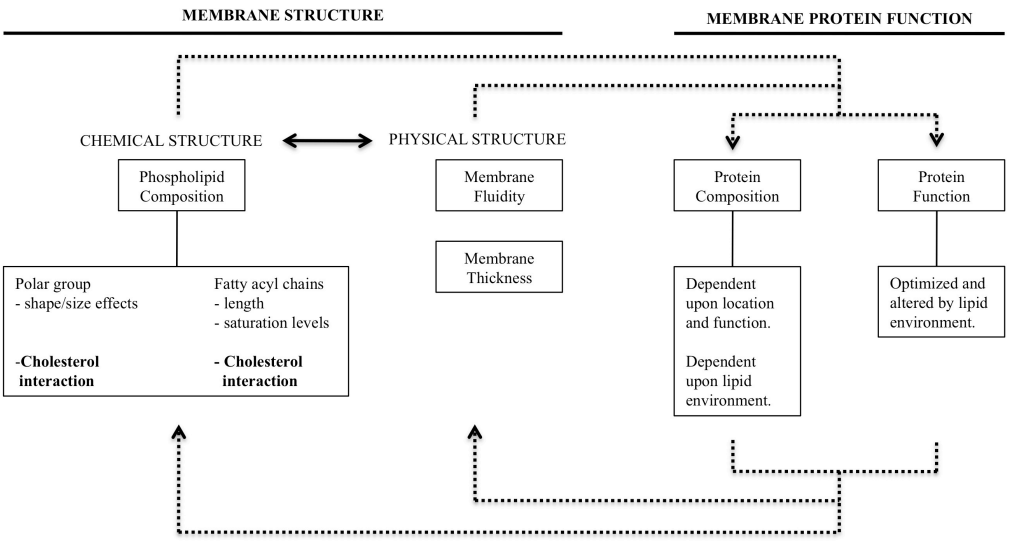


**Figure 1. 3.** Schematic diagram of the membrane structure-protein function relationship.

*Membrane physical structure: fluidity*

The term membrane fluidity can be defined as the viscosity of the bilayer, which may determine the ease of movement within the membrane. Membrane lipids can adopt various fluid and solid phases and is known to be important for membrane function (van Meer, et al., 2008). There are many factors that alter membrane fluidity, including chemical structure through lipid composition; i) PL characteristics, ii) FA composition and iii) cholesterol content.

i) PL characteristics

As discussed above, membranes are comprised of different phospholipids including; PA, PE, PS, PI, PC, CL and SM. The molecular shape of each phospholipid varies according to their respective head group (Cullis & de Kruijff, 1979). Briefly, phospholipids with relatively small polar heads (PE, CL, and PA) have an up-right oriented cone shaped molecule, thus result in a reduced area per molecule at the lipid-water interface ((Cullis & de Kruijff, 1979); Figure 1.4). In contrast, phospholipids with relatively large polar heads (PI), compared to FA chains, have an inverted cone shaped molecule ((Alberts, et al., 2002; Figure 1.4)). In contrast, PC, SM, PS all adopt a cylindrical shape (Cullis & de Kruijff, 1979); Figure 1.4). The size of the head group of the PL can influence membrane packing, whereby PLs with small head groups can pack more tightly than PLs with larger head groups (Hazel & Williams, 1990). Thus these shapes may predict packing nature of the membrane affecting membrane fluidity such that cone conformation will reduce membrane fluidity while cylinder conformation will increase membrane fluidity. Importantly, the dominant phospholipids in general

biological membranes are PC, SM, and PE, accounting for up to ~80% (Borochov, et al., 1977; Escriba, et al., 2008) explaining why most research assessing PL influence on membrane fluidity have used them as the focus group. Indeed, membranes rich in PC were found to be more fluid than membranes rich in PE (Ladbrooke & Chapman, 1969). However, PC and SM share the same head group, choline, yet membranes rich in SM are known to be less fluid than membranes rich in PC (Cooper, et al., 1977; Sunshine & McNamee, 1994). In addition to shape and size of the PL headgroup, hydration, may also affect lipid packing. Hydration is the binding of water to the PL head group as well as its fatty acyl chains, which prevents packing of lipids increasing membrane fluidity (Hazel & Williams, 1990; M'Baye, et al., 2008). Not surprisingly, PC is more hydrated than SM and PE, (Hazel & Williams, 1990; M'Baye, et al., 2008).

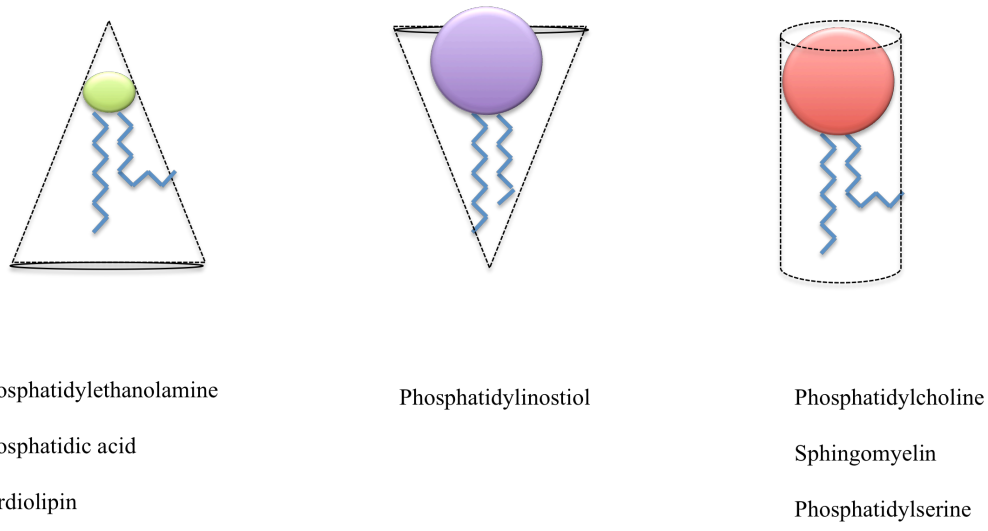


**Figure 1. 4**. Dynamic molecular shapes of component lipids adapted from Cullis & de Kruijff, (1979) and Alberts, et al., (2002).

ii) FA Composition

The fatty acyl chains associated with PLs can affect membrane fluidity by its length and saturation. Short fatty acyl chains are more fluid than longer acyl chains whereby longer fatty acyl chains, have higher transition temperatures; temperature in which the membrane becomes a gel-like solid and loses its fluidity (Voet, 2004). Shorter fatty acyl chains have less carbon chains, and thus experience less van der Waals force explaining the increase in fluidity and lower temperature required to transition from gel to fluid. Similarly, SFAs and *trans* FAs also exhibit higher transition temperatures since they can pack tightly together with many hydrophobic interactions, which would therefore increase rigidity of the membrane (Nikolaidis & Mougios, 2004). In contrast, unsaturated FAs with the *cis* configuration contain kinks, preventing the ability of lipids to pack tightly together resulting in an increase in membrane fluidity. The effect *cis* double bonds have on membrane fluidity is additive, whereby, more *cis* double bonds per FA will further increase membrane fluidity.

iii) Cholesterol

Cholesterol has a general effect of decreasing membrane fluidity, by interacting with surrounding PL groups and restricting movement (Voet, 2004). Of importance cholesterol has a high affinity for SFAs where it can form both van der Waals interactions and hydrogen bonds (M'Baye, et al., 2008; Sprong, et al., 2001). The tight interactions with SFAs causes cholesterol to increase packing of these membrane lipids and thus decreases membrane fluidity (Sprong, et al., 2001). Not surprisingly, cholesterol rich regions are known to have high transition temperatures (Voet, 2004).

Lipid composition can influence proteins by altering the physical structure of the membrane such as membrane fluidity (Figure 1.3). Importantly, it is known that the function of proteins often depends on the shape they take. Some proteins involved in ion transport across membranes must conform to their substrate, and then must undergo a conformational change to release the substrate. Some enzymes rely on conformational changes to increase or decrease affinity for certain substrates. It is therefore evident that those proteins that are embedded in the membrane must have an optimal environment to undergo these conformational changes to allow for their respective activities. Taken together, combinations of PL, FA and cholesterol on membranes can differ between various membranes, and can mediate an effect on membrane function by altering membrane fluidity (Nikolaidis & Mougios, 2004).

In addition to the proteins requiring more fluid membrane domains, some proteins including G-proteins (7-transmembrane spanning protein), require less fluid membrane domains and are thus sorted to lipid rafts. Lipid rafts, seen in section 1.2, are known as sphingolipid-cholesterol rich domains, and thus by sorting proteins to domains of this specific lipid composition some functions of the membrane can be optimized (McIntosh & Simon, 2006; Sprong, et al., 2001).

*Membrane chemical structure on protein function*

The schematic diagram in Figure 1.3 indicates that membrane chemical structure through lipid composition may pose a direct effect on protein function. Specifically, certain lipid species can enhance protein function by acting as substrates, catalysts, signals and/or secondary messengers. For example, PI is intricately involved in signalling

as a secondary messengers for many processes including signal transduction corresponding to its asymmetric distribution to the inner membrane leaflet (van Meer, et al., 2008).

Biological membranes are structured as bilayers, where there is a non-symmetrical distribution of specific lipids. This is exemplified with the fact that most SM and PC on the plasma membrane and Golgi appear on the non-cytosolic leaflet while the majority of PS, PI and PE are on the cytosolic leaflet (van Meer & Vaz, 2005). Moreover, lipid asymmetry is present in both the outer and inner mitochondrial membranes. Specifically, PE + PC are dominant on the external and leaflet of the outer mitochondrial membrane (Hovius, et al., 1993). In contrast, CL + PI, and PE + PC are dominant on the matrix- and cytosolic side of the inner mitochondrial membrane, respectively (Daum, 1985; Nilsson & Dallner, 1977). Furthermore, CL is more present within the inner mitochondrial membrane relative to the outer mitochondrial membrane partly due to its synthesis there (Daum, 1985). The CL asymmetric distribution favouring the matrix side of the inner mitochondrial membrane has functional relevance by binding and enhancing complex III of the respiratory chain enzymes (Beattie, et al., 1981). Lipid asymmetry can be functionally important also within red blood cells, since PS on the outer monolayer could signal for apoptosis and vascular coagulation (Mohandas & Gallagher, 2008; Yamaji-Hasegawa & Tsujimoto, 2006). It is clear that lipid asymmetry within membranes do not occur randomly, and shows the impact chemical structure can have on protein function and recruitment (Sprong, et al., 2001).

*Protein-mediated influence on membrane structure*

In addition to membrane structural impact on protein function, Figure 1.3 indicates a reciprocated influence mediated by protein on membrane structure. Of importance, proteins mediate an effect on membrane physicochemical structure. That is, the influence proteins have on physical structure is interrelated with its effect on membrane chemical structure.

A majority of the biological processes in the body including signal transduction, and ion/molecular transport involves transmembrane proteins. In order for these functions to occur the local membrane domains that house these proteins must undergo some sort of deformation. The integral proteins within biological membranes can alter the thickness of a membrane by hydrophobic matching (Figure 1.3). Hydrophobic matching occurs when the length of the hydrophobic residues of a specific protein associate with the lipids of the membrane. Transmembrane proteins with hydrophobic thickness that do not match that to the bilayer causes the bilayer FAs to bend, compress and tilt in order to compensate for the size of the proteins' hydrophobic residues, thus altering the thickness of the membrane within that domain (McIntosh & Simon, 2006; Pabst, et al., 2010). Interestingly, through other non-membrane-spanning proteins, PLs and FAs can be transferred within the bilayer to either increase or decrease membrane thickness according to the transmembrane protein (Sprong, et al., 2001). Therefore proteins can alter the membrane physicochemical structure within a specific domain by altering the lipid composition to fit a certain degree of thickness.

Thus it is clear that membrane lipid composition can alter membrane protein function, and also protein function can mediate an influence on lipid composition. The sorting of proteins by lipids can be reciprocated by the sorting of lipids by proteins (Figure 1.3). Importantly, since biological membranes from cells of different tissues will have different functions, lipid composition could be useful in defining these various membranes and more importantly in maintaining their respective roles.

**1.6 Skeletal muscle**

The majority of energy expenditure in humans is accounted for by basal metabolic rate (BMR), where energy is utilized to maintain vital organ function, ion homeostasis, protein synthesis, cellular turnover, repair and other cellular processes (Harper, et al., 2008). Importantly, ~20-30% of whole body BMR is accounted for by skeletal muscle (Norris, et al., 2010). The majority of the energy expenditure at rest in skeletal muscle is used to maintain ion homeostasis with the $Na^+/K^+$ ATPase and sarco(endo)plasmic reticulum $Ca^{2+}$ ATPase (SERCA) (Asahi, et al., 2003; Cornelius & Mahmmoud, 2003; Tupling, 2009), both of which are membrane integral proteins.

Indeed energy expenditure must be counter-acted by energy production and skeletal muscle produces energy from two main sources; carbohydrate and fat by degrading them into their single units, namely glucose, and fatty acids, so that they may be metabolized to produce adenosine triphosphate (ATP). Moreover, skeletal muscle has been identified as the major tissue in glucose metabolism, accounting for approximately 75% of whole-body insulin-stimulated glucose uptake (DeFronzo, et al., 1981; Shulman, et al., 1990). Indeed type II diabetes and insulin resistance have been correlated with skeletal muscle insulin action impairment (Pan, et al., 1995). Further, although there are

some fat stores within skeletal muscle, most of the fat stores are found in adipose tissue, whereby various proteins function to transport fats into skeletal muscle to be metabolized (Bonen, et al., 2004). Importantly, the complex pathways that produce ATP from carbohydrate and fat involves membrane spanning proteins as early as entry into the muscle cell and as late as the electron transport chain within the mitochondria (Voet, 2004).

Taken together, it is evident that skeletal muscle is an importance metabolic tissue. Many of the metabolic proteins involved in energy expenditure and production span the lipid membranes within skeletal muscle. With the understanding that lipids may influence protein function, skeletal muscle is an appropriate subject for membrane structure-protein function analysis.

*Skeletal muscle fibre types*

Skeletal muscle fibre identification is based on their twitch and metabolic characteristics; whereby slow fibres contract and relax slowly and rely on oxidative phosphorylation from carbohydrates and lipids, for ATP production, therefore, these fibres are classified as slow oxidative or type I (Voet, 2004). In contrast, fast fibres contract and relax rapidly (Bottinelli & Reggiani, 2000; Trinh & Lamb, 2006), and rely on glycogen stores for ATP production, therefore these fibres are labelled as fast glycolytic or broadly type II (Voet, 2004). In addition, type II fibres can be divided into 3 subtypes: 1) type IIa (fast oxidative glycolytic [FOG]) which combine fast-twitch responses with aerobic fatigue-resistant metabolism (Saladin, 2004), 2) type IIb (fast glycolytic [FG]) which are defined by the characteristics seen in Table 1.,2 and, 3) a type

IId/x which is a hybrid of FOG and FG (type IId/x) (Delp & Duan, 1996). Table 1.2 summarizes the differences seen between type I and type II skeletal muscle fibres.

**Table 1. 2**. Classification of skeletal muscle fibre types adapted from Saladin (2004).

| **Properties** | **Type I** | **Type IIa** | **Type IId/x** | **Type IIb** |
|---|---|---|---|---|
| MHC isoform | MHC I[1] | MHC IIa[1] | MHC IId/x[1] | MHCIIb[1] |
| Relative diameter | Smallest[1] | Large[1] | Larger[1] | Largest[1] |
| ATP synthesis | Aerobic[2] | Aerobic[2] | Anaerobic[3] | Anaerobic[2] |
| Glycolysis | Moderate[3] | Moderate[3] | Fast[3] | Fastest[3] |
| Myoglobin content | Abundant[3,4] | Moderate[3,4] | Low[3,4] | Low[3,4] |
| Glycogen content | Low[2,5] | Low[2,5] | Abundant[2,5] | Abundant[2,5] |
| Mitochondria | Abundant and large[2,4] | Abundant and large[2,4] | Fewer and smaller[2,4] | Fewer and smaller[2,4] |
| Capillaries | Abundant[5] | Moderate[5] | Fewer[5] | Fewer[5] |
| Color | Red[5] | Red[5] | White, pale[5] | White, pale[5] |

[1](Delp & Duam, 1996), [2](Saladin, 2004), [3](Bamford et al., 2003), [4](Harms & Hickson, 1983), [5](Engel & Franzini-Armstron, 2004)

*Membrane subcompartments of skeletal muscle*

Skeletal muscle subcompartments represent a variety of membranes that house a variety of proteins providing their own respective functions that ultimately contribute to the overall function of skeletal muscle. Specifically, the t-tubules have important roles in insulin-stimulated glucose uptake by housing a vast distribution of insulin receptors (Kanzaki, 2006). Along with the sarcoplasmic reticulum (SR), the t-tubules are fundamental in the excitation-contraction coupling process (ECC) (Dombrowski, et al., 1996; Zorzano & Camps, 2006). The dihydropyridine receptors (DHPR) within the t-tubule membranes translates action potentials so that subsequent calcium release can occur (Malouf, et al., 1986). The SR is a highly specialised form of smooth endoplasmic reticulum that is dedicated to $Ca^{2+}$ homeostasis in the muscle (Malouf, et al., 1986;

Sorrentino, 2004). The t-tubules and SR are intimately connected so that action potentials can be converted to calcium release, which can then be used for muscle contraction. The mitochondria are responsible for the majority of ATP production and therefore provide energy to the muscle. The sarcolemma (SL) is central to all of the above functions because this membrane encases each and every muscle fibre ultimately controlling metabolite entry and action potential propagation to the t-tubules. Therefore, the SL is central for skeletal muscle metabolism and contraction, justifying itself as a subject for this present study. Importantly, the sarcolemma is generally defined as a three-layer surface membrane, which includes a plasma membrane situated between a basement membrane and a submembranous cytoskeletal network (Ozawa, et al., 2001; Sanes, 1982). For the purpose of this thesis, the lipid analysis will focus only on the plasma membrane component of the sarcolemma, and will be termed as sarcolemma throughout this document.

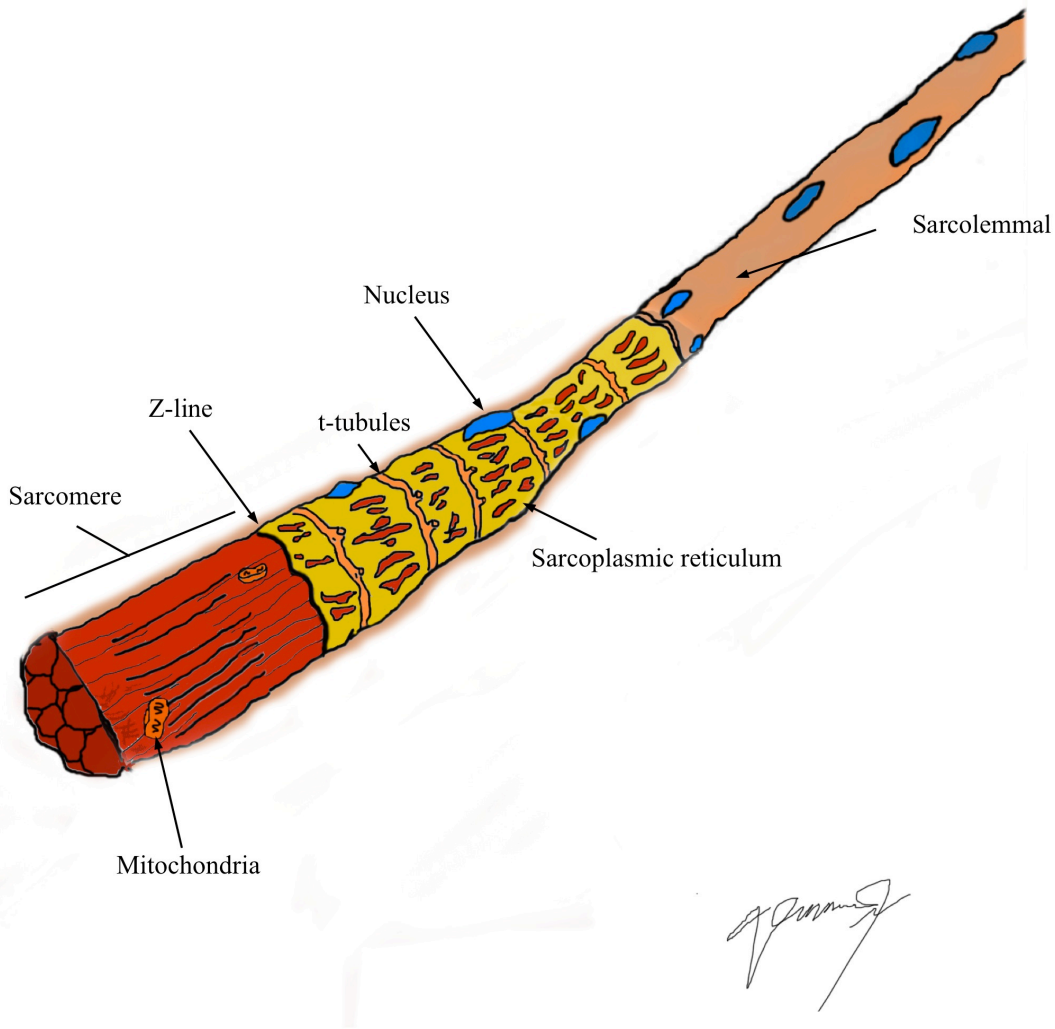


**Figure 1. 5**. Structure of a skeletal muscle fibre revealing the various subcellular compartments.

## 1.7 The sarcolemma

*Functions of the sarcolemma*

After contraction, the SL has an innate role in maintaining structural integrity in order to protect muscle fibres from stress induced by contraction via its intimate connection with the dystrophin glycoprotein complex (DCG) (Campbell & Kahl, 1989; DeWolf, et al., 1997; Lapidos, et al., 2004; Ohlendieck, et al., 1991). Specifically, the

DGC is part of the network of proteins, namely, the costameres, which connect the SL to the sarcomere Z-lines and M-lines (Bloch & Gonzalez-Serratos, 2003; Engel & Franzini-Armstron, 2004). Along with these cytoplasmic interactions, the DGC is connected to the extracellular matrix (ECM) through laminin, and thereby links the SL membrane to the ECM and cytoskeletal network (Bloch & Gonzalez-Serratos, 2003; Engel & Franzini-Armstron, 2004). Indeed, it is the connections to the ECM and cytoskeletal network, that protects the SL membrane from the stresses induced by contraction, and also serves as mechanism to transmit force laterally for uniform contraction (Bloch & Gonzalez-Serratos, 2003; Engel & Franzini-Armstron, 2004).

The SL also provides important metabolic functions including non-insulin and insulin-mediated glucose uptake, and fatty acid uptake. It is evident that the SL membrane participates in a large number of vital biological processes and importantly, much of it is due to SL membrane integral proteins. Therefore, there is raised interest in examining the SL membrane lipid composition, in order to get a clear understanding of the SL membrane structure-protein function relationship.

*Sarcolemmal membrane lipid composition*

Most skeletal membrane lipid analyses has utilized whole muscle (Abbott, et al., 2010; Blackard, et al., 1997) however recent data suggests that mitochondrial membrane lipid profiles significantly differ from a whole muscle perspective (Stefanyk, et al., 2010; Tsalouhidou, et al., 2006). Indeed, it is plausible for other subcompartmental levels to differ in lipid profile from whole muscle including the SL. Throughout the literature there have been rare attempts at assessing the SL lipid composition. To this date, it has been

found that rodent SL membranes were comprised mostly of PC and PE, followed by PS and SM with SFA being the dominant FA species (de Kretser & Livett, 1977; Fiehn, et al., 1971). There is also few data indicating that SL membrane lipid composition differs from other subcompartments including SR, t-tubules and mitochondria in rodent skeletal muscle (Fiehn, et al., 1971; Stefanyk, 2008). In addition, recent data indicates lipid composition differences between mitochondria from plantaris, soleus and red gastrocnemius (Stefanyk, et al., 2010) raising potential for SL lipid composition to also differ between muscle fibre types. However, despite attempts at assessing SL lipid composition (de Kretser & Livett, 1977; Fiehn, et al., 1971; Mahrla & Zachar, 1974; Pilarska, et al., 1991; Stefanyk, 2008), the results from these studies are limited because of two factors. Firstly, most studies assessing SL lipid composition are incomplete as they only provide data on PL species distribution and neglect the FA composition of individual PL species (Lau, et al., 1979; Rosemblatt, et al., 1981; Smith & Appel, 1977; Sumnicht & Sabbadini, 1982). Secondly, their isolation protocols have shown to be contaminated with t-tubules , nuclei, and sarcoplasmic reticulum (Dombrowski, et al., 1996; Fiehn, et al., 1971; Liu, et al., 1994; Ohlendieck, et al., 1991; Smith & Appel, 1977; Sumnicht & Sabbadini, 1982; Zorzano & Camps, 2006; Stefanyk, 2008).

*Sarcolemmal isolation & purification*

Most procedures in retrieving SL membranes involve three fundamental steps: 1) homogenization, 2) differential centrifugation and 3) purification through some form of membrane concentration. Homogenization allows the muscle to undergo constant suspension within a solution. Differential centrifugation is based on a form of density-

gradient centrifugation, whereby SL membrane fractions can be isolated from certain density levels (Dombrowski, et al., 1996; Ohlendieck, et al., 1991). The purification of SL membranes have involved some form of membrane concentration, which could use antibodies to bind to membrane specific proteins or lectin to bind to outside-oriented sarcolemmal glycoproteins (Munoz, et al., 1995; Ohlendieck, et al., 1991; Zorzano & Camps, 2006). The binding to either glycoproteins or SL-specific proteins allows SL fractions to segregate into pellets after centrifugation (Munoz, et al., 1995; Ohlendieck, et al., 1991; Zorzano & Camps, 2006). Taken together, the previous protocols used to isolate SL membranes from whole muscle through both mechanical and chemical processes, may be too aggressive.

The aggressive nature of previous isolation protocols may partially explain the contamination from t-tubule, SR and the nuclear membranes (Dombrowski, et al., 1996; Ohlendieck, et al., 1991; Zorzano & Camps, 2006; Stefanyk, 2008). Therefore, the limitations with regards to FA lipid composition and subcellular contamination in previous SL isolation protocols stress the importance of improving SL isolation to provide complete lipid composition data. To better understand and depict the membrane structure-protein function relationship of the sarcolemma, a microscopic manipulative approach for isolating sarcolemmal membranes which minimizes subcellular contamination is needed to assess the lipid composition inclusive of both PL and FA.

*Sarcolemmal cuffs from mechanically skinned fibres*

The mechanically skinned fibre preparation has been utilized for decades, whereby, its main use was to provide insight on the chemical signalling in relation to the mechanical output of skeletal muscle (Lamb & Stephenson, 1990a; Posterino, et al.,

2000). By applying these mechanically skinned fibres to solutions mimicking different physiological states, researchers have increased knowledge in the process of ECC, especially with t-tubular - SR calcium control and contractile apparatus activity. In brief, a single fibre segment is teased from a skeletal muscle, such as EDL, and from that, two myofibril bundles are pulled away from each other which results in SL cuff formation (Figure 1.6). This membrane skin comprises the plasma membrane, basement membrane as well as their respective embedded proteins and is peeled off without disturbing the still functioning internal environment (Lamb & Stephenson, 1990a; Robyn M. Murphy, et al., 2009). The t-tubules have been said to reseal and repolarize, allowing for analysis of t-tubule excitability and the translation into contraction via SR $Ca^{+}$ release (Lamb & Stephenson, 1990a) (Figure 1.7). By utilizing this method, researchers gained access and ability to control the internal environment of a single muscle fibre, which led to various insights of muscle physiology. However, more information can be extracted using such preparations, and may involve the sarcolemmal membrane that is peeled off. Given that the mechanical skinning approach involves peeling the surface of individual muscle fibre segments it would be more meticulous in obtaining SL membranes rather than previous protocols that process a whole muscle through homogenization, differential centrifugation and membrane purification.

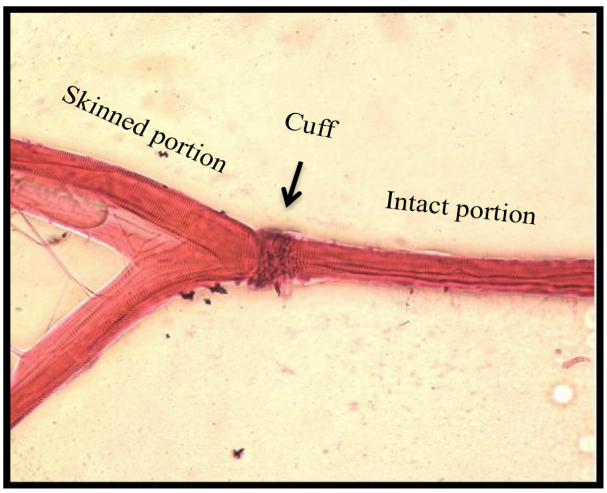


**Figure 1. 6**. Single fibre segment ½ skinned and stained with hematoxylin & eosin stain (40x magnification).

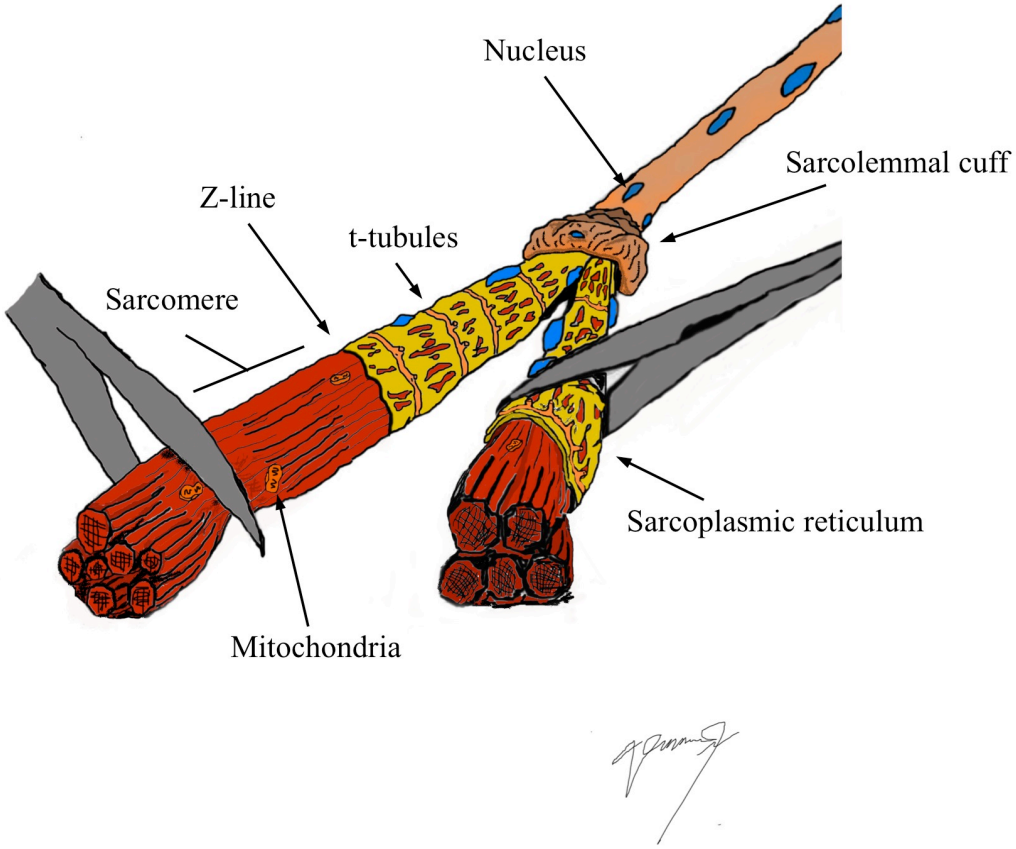


**Figure 1. 7**. Cellular illustration of the mechanical skinning technique, depicting the subcellular structures left within the skinned segments.

Throughout the literature, the analysis of the sarcolemmal membrane after mechanically skinning a muscle fibre is limited (Murphy, et al., 2009; Murphy, et al., 2006; Rybakova, et al., 2000). One investigation focused on the location of calveolin-3 after applying highly sensitive Western blotting and immunohistochemistry techniques on the peeled sarcolemmal membrane (Murphy, et al., 2009). Caveolins are proteins that are imperative for the formation of caveolae which are small invaginations of the plasma membrane of many cells and are involved in compartmentalizing and integrating cell signal transduction events (Cohen, et al., 2004). Importantly, caveolin-3 was thought to be restricted to the SL, but by mechanically skinning single muscle fibres, it was found that the majority of caveolin-3 was in fact in the t-tubular regions and not the SL (Murphy, et al., 2009). Moreover, it was found that after mechanically skinning single muscle fibres, dystrophin, a common SL intracellular marker situated in the submembranous cytoskeletal network, and laminin a common SL extracellular marker found in the basal lamina were both detected solely in the isolated cuff and not in the skinned fibres using immunohistochemistry (Murphy, et al., 2009; Rybakova, et al., 2000).

Currently, there is a limitation within the literature with regards to an exclusive SL membrane-spanning marker, which may be due to the continuous nature with the t-tubule membrane. However, dystrophin and laminin are connected to each other through linkages to a protein named, dystroglycan (Draviam, et al., 2006; Ozawa, et al., 2001; Sotgia, et al., 2003). Specifically, dystroglycan is made of two subunits, α and β (Ozawa, et al., 2001; Sotgia, et al., 2003). Laminin is bound to α-dystroglycan, which is the extracellular subunit bound to the β-dystroglycan subunit that does span the SL

membrane and is further bound to dystrophin in the submembranous cytoskeletal network ((Ozawa, et al., 2001; Sotgia, et al., 2003), Figure 1.7). Since immunohistochemistry has shown dystrophin and laminin only in the skinned cuffs (Murphy, et al., 2009; Rybakova, et al., 2000), and these two proteins are connected to each other through the dystroglycan protein, it was chosen as a membrane-spanning marker for the SL cuffs (Ozawa, et al., 2001). Because β-dystroglycan is the subunit that spans the SL membrane, it was used as a potential SL membrane-spanning marker in this study.

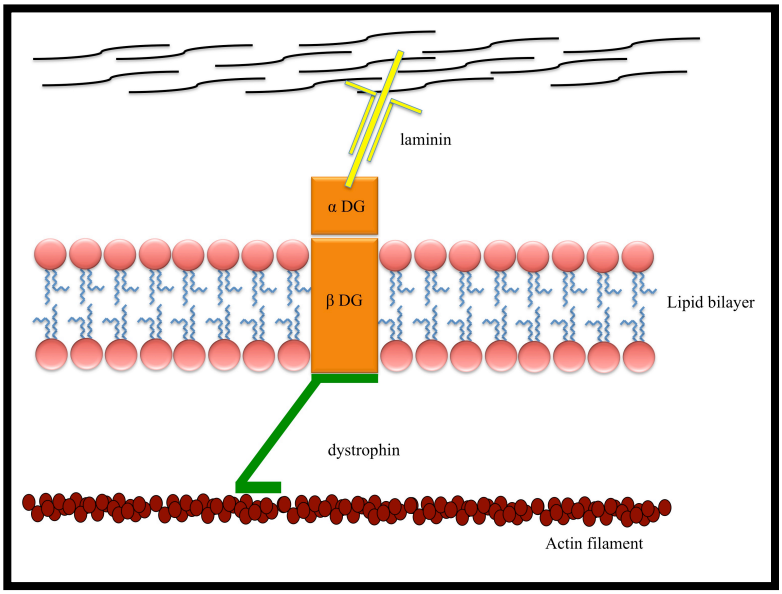


**Figure 1. 8**. Illustrative representation revealing the laminin connection to dystrophin via dystroglycan (αDG and βDG) adapted from Ozawa, et al., (2001). SCG, sarcoglycan complex.

*Lipid analysis of sarcolemmal cuffs from mechanically skinned fibres*

PL and FA membrane composition traditionally involves separation of PLs via thin-layer chromatography (TLC) followed by gas chromatography (GC) to determine FA profile. Importantly, TLC utilizes a range of 10 – 100 μg of lipid (Oberkochen, 1977),

which may not be sensitive enough to detect lipids from sarcolemmal cuffs. One 3 mm single fibre segment is approximately 8 -16 μg of muscle mass (Murphy, et al., 2009). The SL is approximately 1% of muscle mass (Murphy, et al., 2006) corresponding to 80 ng from a 3 mm single fibre segment. In general ~ 50% of plasma membranes is protein (Voet, 2004) corresponding to 40 ng of protein in a 3 mm single fibre segment (Mollica, et al., 2009). Moreover, a 0.50 – 0.55 phospholipid/protein ratio has been suggested (Fiehn, et al., 1971), corresponding to ~20 ng of phospholipid from a 3 mm single muscle fibre segment. It is clear with this crude estimation that mechanically skinning single fibre segments for sarcolemmal PL and FA composition analysis would require techniques sensitive enough to detect ~ 20 ng of PL.

High performance thin-layer chromatography (HPTLC) is similar to TLC, but is highly sensitive partly due to the fact that silica particles in HPTLC plates are finer when compared to TLC plates (Oberkochen, 1977; Ramstedt & Slotte, 2002). In practice applying more than 15 μg of lipids would overload the HPTLC plate and would not provide sufficient separation of phospholipids (Oberkochen, 1977). Indeed the fact that HPTLC requires smaller samples makes it suitable for the sarcolemmal cuff lipid analysis. Within the literature, HPTLC has been able to detect nanograms of PL, but has been restricted, for the most part, to a PL level where the development of the HPTLC plate involved charring preventing any subsequent analysis of FA profile (Morgan, et al., 2008; Ponec, et al., 2003; Rissmann, et al., 2006). Nonetheless, the ability to detect ng of PL makes HPTLC a valid tool for SL cuff lipid analysis. One study successfully coupled HPTLC and GC to examine sphingomyelin fatty acyl composition, whereby the development of the HPTLC plate involved a non-destructive dye, Rhodamine 6G

(Ramstedt et al., 1999). Therefore, the PL and FA profile from SL cuffs may be determined by coupling HPTLC with GC provided a non-destructive dye is used.

**Statement of the Problem**

The sarcolemmal membrane, as aforementioned, is a very important membrane that is involved with many biological processes. Specifically, the SL acts as a site for insulin-mediated and exercise-induced GLUT-4 translocation (Kanzaki, 2006; Kendall & Eston, 2002), and houses fatty acid transporters (Bonen, et al., 2004) to promote carbohydrate and lipid metabolism, respectively. In addition, SL plays an intricate role in excitation-contraction coupling as it aids in the propagation of action potentials down to the t-tubules to promote calcium release from the SR and subsequent muscle contraction (Melzer, et al., 2006; J. Nielsen, et al., 2009). Furthermore, the SL and muscle fibre must be protected from stress induced from contractions, and this is mediated by the DGC. (Deconinck & Dan, 2007; Lapidos, et al., 2004). With the understanding that membrane structure can alter protein function (section 1.5), there has been growing interest in the study of the sarcolemmal membrane lipid profile in relation to protein function, especially in disease states such as muscular dystrophy and diabetes.

Importantly, most skeletal muscle membrane lipid composition analysis has been done using a whole muscle model. The few studies that have assessed SL lipid profile are limited because they 1) neglected FA analysis of individual PL species and 2) relied on aggressive multi-step isolation methods producing SL membranes contaminated with t-tubules, nuclei and SR membranes. Thus, in order to gain knowledge on SL membrane structure-protein function relationship, priority must be allotted to improving techniques that isolate SL membranes to allow for lipid analysis that is inclusive of FA and PL.

**Purpose**

The purpose of this thesis was to assess the possibility of using mechanically skinning fibres as an alternative isolation protocol in the analysis of SL lipid (PL and FA) composition by 1) developing a method to analyze SL cuff lipid composition and 2) examining contamination from other subcellular membranes (t-tubule, nucleus, mitochondria, and sarcoplasmic reticulum) via Western blotting.

**Hypothesis**

It was hypothesized that the sarcolemmal cuffs collected from mechanically skinned fibres would provide sufficient membranes for lipid compositional data including PL and FA, while minimizing contamination from other skeletal muscle subcompartmental membranes.

**References**

Abbott, S. K., Else, P. L., & Hulbert, A. J. (2010). Membrane fatty acid composition of rat skeletal muscle is most responsive to the balance of dietary n-3 and n-6 PUFA. *The British journal of nutrition*, 1-8.

Alberts, B., Johnson, A., Lewis, J., Raff, M., Roberts, K., & Walter, P. (2002). *Molecular Biology of the Cell* (4 ed.): Garland Science.

Asahi, M., Sugita, Y., Kurzydlowski, K., De Leon, S., Tada, M., Toyoshima, C., et al. (2003). Sarcolipin regulates sarco(endo)plasmic reticulum Ca2+-ATPase (SERCA) by binding to transmembrane helices alone or in association with phospholamban. *Proc Natl Acad Sci U S A, 100*(9), 5040-5045.

Bamford, J. A., Lopaschuk, G. D., MacLean, I. M., Reinhart, M. L., Dixon, W. T., & Putman, C. T. (2003). Effects of chronic AICAR administration on the metabolic and contractile phenotypes of rat slow- and fast-twitch skeletal muscles. *Can J Physiol Pharmacol, 81*(11), 1072-1082.

Beattie, D. S., Clejan, L., Chen, Y. S., Lin, C. I., & Sidhu, A. (1981). Orientation of complex III in the yeast mitochondrial membrane: labeling with [125I] diazobenzenesulfonate and functional studies with the decyl analogue of coenzyme Q as substrate. *J Bioenerg Biomembr, 13*(5-6), 357-373.

Bell GH, E.-S. K., & Paterson CR (1976). *Textbook of PHysiology and Biochemistry,* (9th ed.). Edinburgh: Churchill Livingston.

Blackard, W. G., Li, J., Clore, J. N., & Rizzo, W. B. (1997). Phospholipid fatty acid composition in type I and type II rat muscle. *Lipids, 32*(2), 193-198.

Bleijerveld, O. B., Brouwers, J. F., Vaandrager, A. B., Helms, J. B., & Houweling, M. (2007). The CDP-ethanolamine pathway and phosphatidylserine decarboxylation

generate different phosphatidylethanolamine molecular species. *J Biol Chem, 282*(39), 28362-28372.

Bloch, R. J., & Gonzalez-Serratos, H. (2003). Lateral force transmission across costameres in skeletal muscle. *Exerc Sport Sci Rev, 31*(2), 73-78.

Bonen, A., Parolin, M. L., Steinberg, G. R., Calles-Escandon, J., Tandon, N. N., Glatz, J. F., et al. (2004). Triacylglycerol accumulation in human obesity and type 2 diabetes is associated with increased rates of skeletal muscle fatty acid transport and increased sarcolemmal FAT/CD36. *FASEB J, 18*(10), 1144-1146.

Borochov, H., Zahler, P., Wilbrandt, W., & Shinitzky, M. (1977). The effect of phosphatidylcholine to sphingomyelin mole ratio on the dynamic properties of sheep erythrocyte membrane. *Biochim Biophys Acta, 470*(3), 382-388.

Bottinelli, R., & Reggiani, C. (2000). Human skeletal muscle fibres: molecular and functional diversity. *Prog Biophys Mol Biol, 73*(2-4), 195-262.

Bretscher, M. S., & Raff, M. C. (1975). Mammalian plasma membranes. *Nature, 258*(5530), 43-49.

Campbell, K. P., & Kahl, S. D. (1989). Association of dystrophin and an integral membrane glycoprotein. *Nature, 338*(6212), 259-262.

Clore, J. N., Li, J., Gill, R., Gupta, S., Spencer, R., Azzam, A., et al. (1998). Skeletal muscle phosphatidylcholine fatty acids and insulin sensitivity in normal humans. *Am J Physiol, 275*(4 Pt 1), E665-670.

Cohen, A. W., Hnasko, R., Schubert, W., & Lisanti, M. P. (2004). Role of caveolae and caveolins in health and disease. *Physiological reviews, 84*(4), 1341-1379.

Cooper, R. A., Durocher, J. R., & Leslie, M. H. (1977). Decreased fluidity of red cell membrane lipids in abetalipoproteinemia. *J Clin Invest, 60*(1), 115-121.

Cornelius, F., & Mahmmoud, Y. A. (2003). Functional modulation of the sodium pump: the regulatory proteins "Fixit". *News Physiol Sci, 18*, 119-124.

Cullis, P. R., & de Kruijff, B. (1979). Lipid polymorphism and the functional roles of lipids in biological membranes. *Biochimica et biophysica acta, 559*(4), 399-420.

Dalton, K. A., East, J. M., Mall, S., Oliver, S., Starling, A. P., & Lee, A. G. (1998). Interaction of phosphatidic acid and phosphatidylserine with the Ca2+-ATPase of sarcoplasmic reticulum and the mechanism of inhibition. *Biochem J, 329 ( Pt 3)*, 637-646.

Dannenberger, D., Nuernberg, G., Scollan, N., Ender, K., & Nuernberg, K. (2007). Diet alters the fatty acid composition of individual phospholipid classes in beef muscle. *J Agric Food Chem, 55*(2), 452-460.

Daum, G. (1985). Lipids of mitochondria. *Biochim Biophys Acta, 822*(1), 1-42.

de Kretser, T. A., & Livett, B. G. (1977). Skeletal-muscle sarcolemma from normal and dystrophic mice. Isolation, characterization and lipid composition. *The Biochemical journal, 168*(2), 229-237.

Deconinck, N., & Dan, B. (2007). Pathophysiology of duchenne muscular dystrophy: current hypotheses. *Pediatric neurology, 36*(1), 1-7.

DeFronzo, R. A., Jacot, E., Jequier, E., Maeder, E., Wahren, J., & Felber, J. P. (1981). The effect of insulin on the disposal of intravenous glucose. Results from indirect calorimetry and hepatic and femoral venous catheterization. *Diabetes, 30*(12), 1000-1007.

Degroote, S., Wolthoorn, J., & van Meer, G. (2004). The cell biology of glycosphingolipids. *Semin Cell Dev Biol, 15*(4), 375-387.

Delp, M. D., & Duan, C. (1996). Composition and size of type I, IIA, IID/X, and IIB fibers and citrate synthase activity of rat muscle. *J Appl Physiol, 80*(1), 261-270.

DeWolf, C., McCauley, P., Sikorski, A. F., Winlove, C. P., Bailey, A. I., Kahana, E., et al. (1997). Interaction of dystrophin fragments with model membranes. *Biophysical journal, 72*(6), 2599-2604.

Dombrowski, L., Roy, D., Marcotte, B., & Marette, A. (1996). A new procedure for the isolation of plasma membranes, T tubules, and internal membranes from skeletal muscle. *The American Journal of Physiology, 270*(4 Pt 1), E667-676.

Draviam, R. A., Wang, B., Shand, S. H., Xiao, X., & Watkins, S. C. (2006). Alpha-sarcoglycan is recycled from the plasma membrane in the absence of sarcoglycan complex assembly. *Traffic, 7*(7), 793-810.

Engel, A., & Franzini-Armstron, C. (2004). *Myology* (3 ed. Vol. 1). New York: McGraw Hill.

Escriba, P. V., Gonzalez-Ros, J. M., Goni, F. M., Kinnunen, P. K., Vigh, L., Sanchez-Magraner, L., et al. (2008). Membranes: a meeting point for lipids, proteins and therapies. *J Cell Mol Med, 12*(3), 829-875.

Fiehn, W., Peter, J. B., Mead, J. F., & Gan-Elepano, M. (1971). Lipids and fatty acids of sarcolemma, sarcoplasmic reticulum, and mitochondria from rat skeletal muscle. *J Biol Chem, 246*(18), 5617-5620.

Harms, S. J., & Hickson, R. C. (1983). Skeletal muscle mitochondria and myoglobin, endurance, and intensity of training. *J Appl Physiol, 54*(3), 798-802.

Harper, M. E., Green, K., & Brand, M. D. (2008). The efficiency of cellular energy transduction and its implications for obesity. *Annu Rev Nutr, 28*, 13-33.

Hazel, J. R., & Williams, E. E. (1990). The role of alterations in membrane lipid composition in enabling physiological adaptation of organisms to their physical environment. *Prog Lipid Res, 29*(3), 167-227.

Hovius, R., Thijssen, J., van der Linden, P., Nicolay, K., & de Kruijff, B. (1993). Phospholipid asymmetry of the outer membrane of rat liver mitochondria. Evidence for the presence of cardiolipin on the outside of the outer membrane. *FEBS Lett, 330*(1), 71-76.

Hulbert, A. J., Turner, N., Storlien, L. H., & Else, P. L. (2005). Dietary fats and membrane function: implications for metabolism and disease. *Biological reviews of the Cambridge Philosophical Society, 80*(1), 155-169.

Kanzaki, M. (2006). Insulin receptor signals regulating GLUT4 translocation and actin dynamics. *Endocrine journal, 53*(3), 267-293.

Kendall, B., & Eston, R. (2002). Exercise-induced muscle damage and the potential protective role of estrogen. *Sports medicine (Auckland, N.Z.), 32*(2), 103-123.

Ladbrooke, B. D., & Chapman, D. (1969). Thermal analysis of lipids, proteins and biological membranes. A review and summary of some recent studies. *Chem Phys Lipids, 3*(4), 304-356.

Lamb, G. D., & Stephenson, D. G. (Writer) (1990). Calcium release in skinned muscle fibres of the toad by transverse tubule depolarization or by direct stimulation, *The Journal of physiology*. ENGLAND.

Lapidos, K. A., Kakkar, R., & McNally, E. M. (2004). The dystrophin glycoprotein complex: signaling strength and integrity for the sarcolemma. *Circ Res, 94*(8), 1023-1031.

Lau, Y. H., Caswell, A. H., Brunschwig, J. P., Baerwald, R., & Garcia, M. (1979). Lipid analysis and freeze-fracture studies on isolated transverse tubules and sarcoplasmic reticulum subfractions of skeletal muscle. *J Biol Chem, 254*(2), 540-546.

Liu, S., Baracos, V. E., Quinney, H. A., & Clandinin, M. T. (1994). Dietary omega-3 and polyunsaturated fatty acids modify fatty acyl composition and insulin binding in skeletal-muscle sarcolemma. *Biochem J, 299 ( Pt 3)*, 831-837.

M'Baye, G., Mely, Y., Duportail, G., & Klymchenko, A. S. (2008). Liquid ordered and gel phases of lipid bilayers: fluorescent probes reveal close fluidity but different hydration. *Biophys J, 95*(3), 1217-1225.

Mahrla, Z., & Zachar, J. (1974). Lipid composition of isolated external and internal skeletal muscle membranes. *Comparative Biochemistry and Physiology Part B: Biochemistry and Molecular Biology, 47*(2), 493-502.

Malouf, N. N., Taylor, S., Gillespie, G. Y., Bynum, J. M., Wilson, P. E., & Meissner, G. (1986). Monoclonal antibody specific for the T-tubule of skeletal muscle. *J Histochem Cytochem, 34*(3), 347-355.

Marguet, D., Lenne, P. F., Rigneault, H., & He, H. T. (2006). Dynamics in the plasma membrane: how to combine fluidity and order. *The EMBO journal, 25*(15), 3446-3457.

McIntosh, T. J., & Simon, S. A. (2006). Roles of bilayer material properties in function and distribution of membrane proteins. *Annu Rev Biophys Biomol Struct, 35*, 177-198.

Melzer, W., Andronache, Z., & Ursu, D. (2006). Functional roles of the gamma subunit of the skeletal muscle DHP-receptor. *Journal of muscle research and cell motility, 27*(5-7), 307-314.

Mitchell, T. W., Buffenstein, R., & Hulbert, A. J. (2007). Membrane phospholipid composition may contribute to exceptional longevity of the naked mole-rat (Heterocephalus glaber): a comparative study using shotgun lipidomics. *Exp Gerontol, 42*(11), 1053-1062.

Mohandas, N., & Gallagher, P. G. (2008). Red cell membrane: past, present, and future. *Blood, 112*(10), 3939-3948.

Mollica, J. P., Oakhill, J. S., Lamb, G. D., & Murphy, R. M. (2009). Are genuine changes in protein expression being overlooked? Reassessing Western blotting. *Anal Biochem, 386*(2), 270-275.

Morgan, W. A., Nk, T., & Ding, Y. (2008). The use of High Performance Thin-Layer Chromatography to determine the role of membrane lipid composition in bile salt-induced kidney cell damage. *J Pharmacol Toxicol Methods, 57*(1), 70-73.

Munoz, P., Rosemblatt, M., Testar, X., Palacin, M., & Zorzano, A. (1995). Isolation and characterization of distinct domains of sarcolemma and T-tubules from rat skeletal muscle. *The Biochemical journal, 307 ( Pt 1)*(Pt 1), 273-280.

Murphy, R. M., Mollica, J. P., & Lamb, G. D. (2009). Plasma membrane removal in rat skeletal muscle fibers reveals caveolin-3 hot-spots at the necks of transverse tubules. *Experimental cell research, 315*(6), 1015-1028.

Murphy, R. M., Verburg, E., & Lamb, G. D. (2006). Ca2+ activation of diffusible and bound pools of mu-calpain in rat skeletal muscle. *The Journal of physiology, 576*(Pt 2), 595-612.

Nielsen, J., Schroder, H. D., Rix, C. G., & Ortenblad, N. (2009). Distinct effects of subcellular glycogen localization on tetanic relaxation time and endurance in mechanically skinned rat skeletal muscle fibres. *The Journal of physiology, 587*(Pt 14), 3679-3690.

Nikolaidis, M. G., & Mougios, V. (2004). Effects of exercise on the fatty-acid composition of blood and tissue lipids. *Sports Med, 34*(15), 1051-1076.

Nilsson, O. S., & Dallner, G. (1977). Enzyme and phospholipid asymmetry in liver microsomal membranes. *J Cell Biol, 72*(3), 568-583.

Norris, S. M., Bombardier, E., Smith, I. C., Vigna, C., & Tupling, A. R. (2010). ATP consumption by sarcoplasmic reticulum Ca2+ pumps accounts for 50% of resting metabolic rate in mouse fast and slow twitch skeletal muscle. *Am J Physiol Cell Physiol, 298*(3), C521-529.

Oberkochen, C. Z. (1977). Potential and experience in quantitative "high performance thin-layer chromatography" HPTLC. In I. A. Zlatis, Kaiser, R. E. (Ed.), *HPTLC high performance thin-layer chromatography* (Vol. 9, pp. 147-167): Elseveir Scientific Publishing Company.

Ohlendieck, K., Ervasti, J. M., Snook, J. B., & Campbell, K. P. (1991). Dystrophin-glycoprotein complex is highly enriched in isolated skeletal muscle sarcolemma. *The Journal of cell biology, 112*(1), 135-148.

Ozawa, E., Nishino, I., & Nonaka, I. (2001). Sarcolemmopathy: muscular dystrophies with cell membrane defects. *Brain Pathol, 11*(2), 218-230.

Pabst, G., Kucerka, N., Nieh, M. P., Rheinstadter, M. C., & Katsaras, J. (2010). Applications of neutron and X-ray scattering to the study of biologically relevant model membranes. *Chem Phys Lipids, 163*(6), 460-479.

Pan, D. A., Lillioja, S., Milner, M. R., Kriketos, A. D., Baur, L. A., Bogardus, C., et al. (1995). Skeletal muscle membrane lipid composition is related to adiposity and insulin action. *J Clin Invest, 96*(6), 2802-2808.

Pike, L. J. (2004). Lipid rafts: heterogeneity on the high seas. *Biochem J, 378*(Pt 2), 281-292.

Pilarska, M., Wrzosek, A., Pikula, S., & Famulski, K. S. (1991). Thyroid hormones control lipid composition and membrane fluidity of skeletal muscle sarcolemma. *Biochim Biophys Acta, 1068*(2), 167-173.

Ponec, M., Weerheim, A., Lankhorst, P., & Wertz, P. (2003). New acylceramide in native and reconstructed epidermis. *J Invest Dermatol, 120*(4), 581-588.

Posterino, G. S., Lamb, G. D., & Stephenson, D. G. (2000). Twitch and tetanic force responses and longitudinal propagation of action potentials in skinned skeletal muscle fibres of the rat. *The Journal of physiology, 527 Pt 1*, 131-137.

Ramstedt, B., Leppimaki, P., Axberg, M., Slotte, J.P. 1999. Analysis of natural and synthetic sphingomyelins using high-performance thin-layer chromatography. *Eur J Biochem* **266:**997-100

Ramstedt, B., & Slotte, J. P. (2002). Membrane properties of sphingomyelins. *FEBS Lett, 531*(1), 33-37.

Rissmann, R., Groenink, H. W., Weerheim, A. M., Hoath, S. B., Ponec, M., & Bouwstra, J. A. (2006). New insights into ultrastructure, lipid composition and organization of vernix caseosa. *J Invest Dermatol, 126*(8), 1823-1833.

Ritov, V. B., Menshikova, E. V., & Kelley, D. E. (2006). Analysis of cardiolipin in human muscle biopsy. *J Chromatogr B Analyt Technol Biomed Life Sci, 831*(1-2), 63-71.

Rosemblatt, M., Hidalgo, C., Vergara, C., & Ikemoto, N. (1981). Immunological and biochemical properties of transverse tubule membranes isolated from rabbit skeletal muscle. *J Biol Chem, 256*(15), 8140-8148.

Rybakova, I. N., Patel, J. R., & Ervasti, J. M. (2000). The dystrophin complex forms a mechanically strong link between the sarcolemma and costameric actin. *J Cell Biol, 150*(5), 1209-1214.

Saladin, K. (2004). *Anatomy & Physiology: The Unity of Form and Function* (3 ed.). New York, NY: McGraw-Hill.

Sanes, J. R. (1982). Laminin, fibronectin, and collagen in synaptic and extrasynaptic portions of muscle fiber basement membrane. *J Cell Biol, 93*(2), 442-451.

Shulman, G. I., Rothman, D. L., Jue, T., Stein, P., DeFronzo, R. A., & Shulman, R. G. (1990). Quantitation of muscle glycogen synthesis in normal subjects and subjects

with non-insulin-dependent diabetes by 13C nuclear magnetic resonance spectroscopy. *N Engl J Med, 322*(4), 223-228.

Smart, E. J., Graf, G. A., McNiven, M. A., Sessa, W. C., Engelman, J. A., Scherer, P. E., et al. (1999). Caveolins, liquid-ordered domains, and signal transduction. *Mol Cell Biol, 19*(11), 7289-7304.

Smith, P. B., & Appel, S. H. (1977). Isolation and characterization of the surface membranes of fast and slow mammalian skeletal muscle. *Biochim Biophys Acta, 466*(1), 109-122.

Sorrentino, V. (2004). Molecular determinants of the structural and functional organization of the sarcoplasmic reticulum. *Biochimica et biophysica acta, 1742*(1-3), 113-118.

Sotgia, F., Bonuccelli, G., Bedford, M., Brancaccio, A., Mayer, U., Wilson, M. T., et al. (2003). Localization of phospho-beta-dystroglycan (pY892) to an intracellular vesicular compartment in cultured cells and skeletal muscle fibers in vivo. *Biochemistry, 42*(23), 7110-7123.

Sprong, H., van der Sluijs, P., & van Meer, G. (2001). How proteins move lipids and lipids move proteins. *Nat Rev Mol Cell Biol, 2*(7), 504-513.

Stefanyk, L.E. (2008). *Skeletal Muscle Fibre-Type Comparison of Whole tissue and Subcellular Phospholipids and Fatty Acids.* Brock University, St. Catharines.

Stefanyk, L. E., Coverdale, N., Roy, B. D., Peters, S. J., & LeBlanc, P. J. (2010). Skeletal muscle type comparison of subsarcolemmal mitochondrial membrane phospholipid fatty acid composition in rat. *J Membr Biol, 234*(3), 207-215.

Sumnicht, G. E., & Sabbadini, R. A. (1982). Lipid composition of transverse tubular membranes from normal and dystrophic skeletal muscle. *Arch Biochem Biophys, 215*(2), 628-637.

Sunshine, C., & McNamee, M. G. (1994). Lipid modulation of nicotinic acetylcholine receptor function: the role of membrane lipid composition and fluidity. *Biochim Biophys Acta, 1191*(1), 59-64.

Trinh, H. H., & Lamb, G. D. (2006). Matching of sarcoplasmic reticulum and contractile properties in rat fast- and slow-twitch muscle fibres. *Clin Exp Pharmacol Physiol, 33*(7), 591-600.

Tsalouhidou, S., Argyrou, C., Theofilidis, G., Karaoglanidis, D., Orfanidou, E., Nikolaidis, M. G., et al. (2006). Mitochondrial phospholipids of rat skeletal muscle are less polyunsaturated than whole tissue phospholipids: implications for protection against oxidative stress. *J Anim Sci, 84*(10), 2818-2825.

Tupling, A. R. (2009). The decay phase of Ca2+ transients in skeletal muscle: regulation and physiology. *Appl Physiol Nutr Metab, 34*(3), 373-376.

van Meer, G., & Vaz, W. L. (2005). Membrane curvature sorts lipids. Stabilized lipid rafts in membrane transport. *EMBO Rep, 6*(5), 418-419.

van Meer, G., Voelker, D. R., & Feigenson, G. W. (2008). Membrane lipids: where they are and how they behave. *Nat Rev Mol Cell Biol, 9*(2), 112-124.

Voet, V. (2004). *Biochemistry* (3rd ed.). Pennsylvannia: John Wiley and Sons, Inc.

Yamaji-Hasegawa, A., & Tsujimoto, M. (2006). Asymmetric distribution of phospholipids in biomembranes. *Biol Pharm Bull, 29*(8), 1547-1553.

Zorzano, A., & Camps, M. (2006). Isolation of T-tubules from skeletal muscle. *Current protocols in cell biology / editorial board, Juan S.Bonifacino ...[et al.], Chapter 3*, Unit 3.24.

**Chaper 2: Developing a method for sarcolemmal cuff lipid analysis.**

**Introduction**

In general, when analyzing membrane PL and FA membrane composition, most studies have employed TLC for the separation of PLs followed by GC to determine FA profile of the individual PL species (Stefanyk, et al., 2010; Tsalouhidou, et al., 2006). Flame ionizing detectors (FID) coupled to GC is the most widely favoured system for lipid analysis (Dodds, et al., 2005). Specifically, commercial suppliers of the GC-FID system suggest sensitivity as low as 20 pg. In contrast, TLC utilizes a range of 10 – 100 μg of lipid (Oberkochen, 1977), which may not be sensitive enough to detect lipids from sarcolemmal cuffs. One 3 mm single fibre segment is approximately 8 -16 μg of muscle mass (Murphy, et al., 2009). The SL is approximately 1% of muscle mass (Murphy, et al., 2006) corresponding to 80 ng from a 3 mm single fibre segment. In general ~ 50% of plasma membranes is protein (Voet, 2004) corresponding to 40 ng of protein in a 3 mm single fibre segment (Mollica, et al., 2009). Moreover, a 0.50 – 0.55 phospholipid/protein ratio has been suggested (Fiehn, et al., 1971), corresponding to ~20 ng of phospholipid from a 3 mm single muscle fibre segment. It is clear with this crude estimation that mechanically skinning single fibre segments for sarcolemmal PL and FA composition analysis would require techniques sensitive enough to detect ~ 20 ng of PL.

High performance thin-layer chromatography (HPTLC) is similar to TLC, but is highly sensitive partly due to the fact that silica particles in HPTLC plates are finer when compared to TLC plates (Oberkochen, 1977; Ramstedt & Slotte, 2002). In practice applying more than 15 μg of lipids would overload the HPTLC plate and would not provide sufficient separation of phospholipids (Oberkochen, 1977). Indeed the fact that HPTLC requires smaller samples makes it suitable for the sarcolemmal cuff lipid analysis. Within the literature, HPTLC has been able to detect nanograms of PL, but has

been restricted, for the most part, to a PL level where the development of the HPTLC plate involved charring preventing any subsequent analysis of FA profile (Morgan, et al., 2008; Ponec, et al., 2003; Rissmann, et al., 2006). Nonetheless, the ability to detect ng of PL makes HPTLC a potential tool for SL cuff lipid analysis. One study successfully coupled HPTLC and GC to examine sphingomyelin fatty acyl composition, whereby the development of the HPTLC plate involved a non-destructive dye, Rhodamine 6G (Ramstedt et al., 1999). Therefore, the purpose of the experiments in these sections was to develop the HPTLC coupled to GC method for the analysis of SL cuff PL and FA profile. In general, there were four main areas that needed development: mechanical skinning solution, lipid extraction, HPTLC, and GC (Figure 2.1).

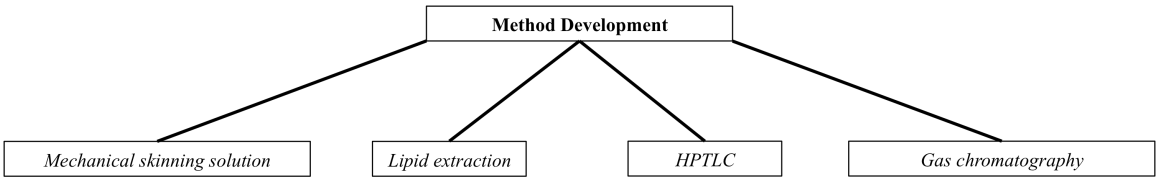


**Figure 2. 1**. Schematic flow-chart indicating the four main areas that were developed for SL cuff lipid analysis.

Before, any of the four areas could be assessed, it had to be determined if the nondestructive dye, dichlorofluoroscein (DCF) would be successful on HPTLC plates since the majority of the literature using HPTLC plates has often used charring method to detect lipids. Figure 2.1 illustrates that DCF was successful and could be used for HPTLC plate lipid detection.

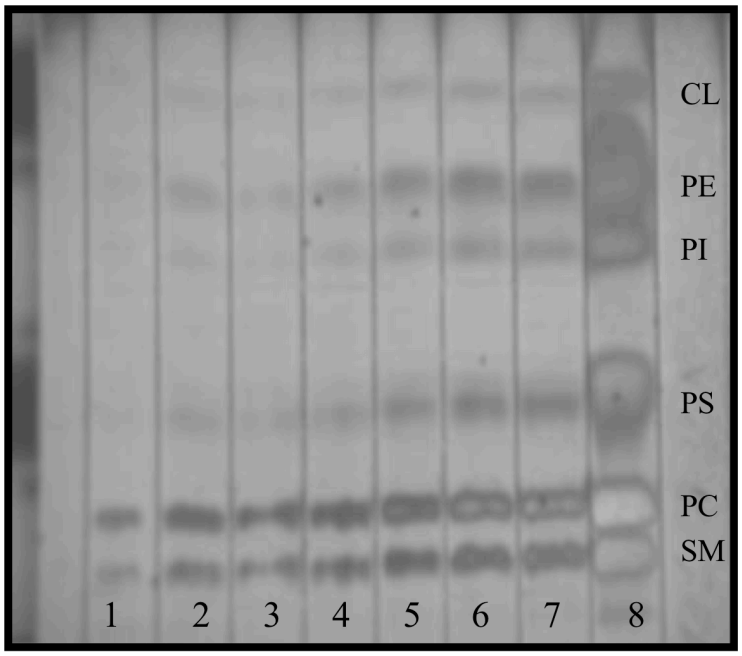


**Figure 2. 2**. HPTLC plate of a standard phospholipid mixture developed with DCF. Sphingomyelin (SM), phosphatidylcholine (PC), phosphatidylserine (PS), phosphatidylinositol (PI), phosphatidylethanolamine (PE) and cardiolipin (CL). Total lipid weights of each lane were 1: 2.74 µg, 2: 5.49 µg, 3: 10.97 µg, 4: 16.45 µg, 5: 21.94 µg 6: 27.43 µg, 7: 32.92 µg, 8: 219.5 µg. Concentration of total lipids in standard mix is 21.945 µg/µl.

Specifically with DCF detection the lowest level of detection when spotting lipids as 8 mm bands was in lane 2 with 5.49 µg of total lipid (Figure 2.2). Interestingly, lane 8 is a common load on standard TLC plates, and Figure 2.2 reveals that separation of phospholipid species was unsuccessful which can be explained by HPTLC's smaller silica particles that can easily be overloaded.

*Method development: Mechanical skinning solution*

Initially, the mechanical skinning protocol involved skinning single fibres under paraffin oil. Researchers in the muscle physiology lab group (La Trobe University,

Melbourne, Australia), including Dr. Graham Lamb, Dr. Robyn Murphy and Dr. George Stephenson used this technique to keep all the cellular components (ions and unbound proteins) within the cell after the fibre was mechanically skinned (due to hydrophobic interactions). The collection of cuffs involved pipetting out a droplet of paraffin oil onto a piece of parafilm. A pin was used to collect the cuff from the dish. Next, the pin with the cuff adhered to it, was plunged back and forth into the droplet of paraffin oil until the cuff was displaced from the pin into the oil (can be seen under a dissecting scope 40X magnification). Finally, the oil droplet housing the cuff was pipetted into an eppendorf tube and stored for future analysis. With this method, various pools of cuffs were spotted onto an HPTLC plate (Figure 2.3).

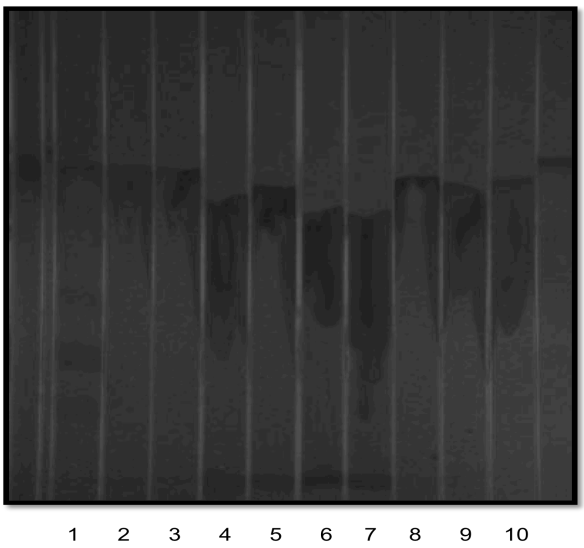


**Figure 2. 3**. HPTLC plate of a variety of cuff pools spotted as 8 mm bands. (Chloroform (100): Methanol (60): Acetic acid (16): Water (8)). Lane 1: phospholipid standard, Lane 2: 1 cuff, Lane 3: 1 cuff, Lane 4: 1 cuffs, Lane 5: 2 cuffs, Lane 6: 2 cuffs, Lane 7: 3 cuffs, Lane 8: 3 cuffs, Lane 9: 4 cuffs, Lane 10: 5 cuffs.

Figure 2.3 reveals streaking upon spotting samples. This streaking was first thought to be a result of mechanically skinning fibres under paraffin oil, which contaminate the SL cuff lipids and causing overload and streaking on the HPTLC plate. With the help of Dr. Graham Lamb, an aqueous solution for mechanically skinning was then implemented into the lipid analysis protocol of sarcolemmal cuffs: $Na^+$-based resting solution ( 90 mM HEPES, 50 mM EGTA, 10.3 mM MgO, 8 mM ATP, 10 mM creatine phosphate, pH 7.1 with 4 M NaOH, ~295 mOsmoles) (Figure 2.4).

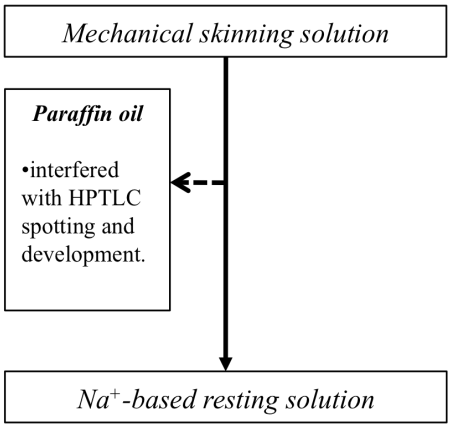


**Figure 2. 4**. Diagrammatic flow illustrating the exclusion of paraffin oil and inclusion of $Na^+$-based resting solution as the mechanical skinning solution. Dashed arrow = excluded.

With the new solution for mechanical skinning, the protocol for collecting cuffs after skinning was in need of re-invention. Thus, pools of cuffs were collected either using a small piece (<5mm) of 4.0 black braided silk suture or one end of Dumont inox forceps. It was determined that brushing the sylgard layer with the suture to collect the cuff was easier than using the other end of the forceps. Furthermore, using the other end of the forceps did not ensure that the cuff had adhered onto the forceps and then displaced from

the forceps into the Eppendorf tube. With the suture method, sutures were simply placed into the Eppendorf tube with the membrane buffer solution (Buffer A).

*Method development: Lipid extraction*

Despite the change in mechanical skinning solution the development of HPTLC plates were unsuccessful. Figure 2.5 reveals that despite using an aqueous solution for skinning, streaking of samples occurred. It was then thought that prior to lipid extraction there was no form of membrane disruption such as freeze-thaw cycles. Therefore, the lipid analysis protocol started implementing a 3x freeze-thaw cycle.

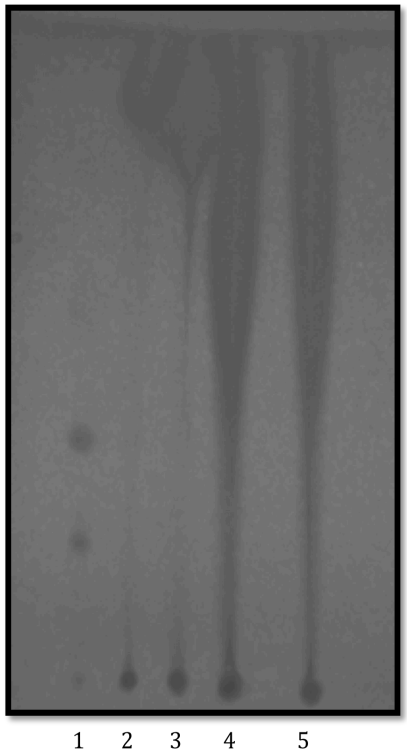


**Figure 2. 5**. HPTLC plate of a pool of 5 cuffs (2), 15 cuffs (3), 20 cuffs (4) and 20 cuffs (4) collected using the new aqueous skinning solution. (Chloroform (100): Methanol (60): Acetic acid (16): Water (8)). Lane 1: phospholipid standard.

However, despite this change, and many others outlined in the below sections, the PL specie distribution determined by both HPTLC plates and GC analysis was unexpected. This led to the thought that there was incomplete lipid extraction, and thus SL cuffs were treated with 1% Triton-X100 and were homogenized (Figure 2.6).

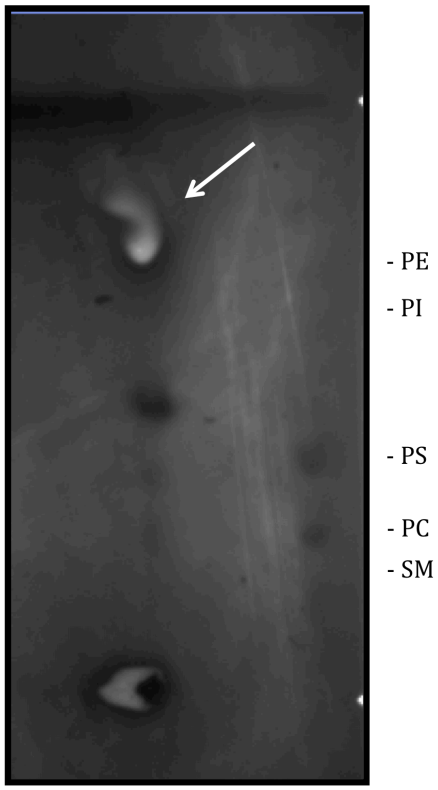


**Figure 2. 6**. Charred HPTLC plate of 10 EDL sarcolemmal cuffs lipid extracted with hand homogenization and 1% Triton-X100. White arrow points to Triton-X100 artefact on the plate.

Indeed with this lipid extraction protocol, the phospholipids PC, SM and PS were present on the HPTLC plate, however, the treatment with Triton-X100, seemed to affect the HPTLC plate along the PE area, and there was concern that this would detriment the GC apparatus (Figure 2.6). Therefore, lipid extraction was carried out with the hand homogenization without Triton-X100 treatment. In summary, for lipid extraction, 3

freeze-thaw cycles and homogenization were included in the protocol to help disrupt and release the membrane lipids from the SL cuffs, while Triton-X100 was excluded due to contaminating artefacts (Figure 2.7).

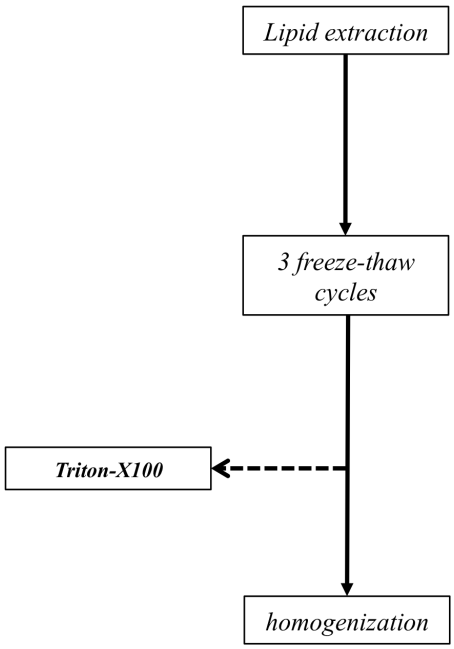


**Figure 2. 7**. Diagrammatic flow-chart illustrating the included and excluded steps utilized for Lipid extraction. Dashed arrow = excluded.

*Method development: HPTLC*

Since the estimated amount of lipids from a pool of 10 cuffs was 200 ng of phospholipid, it was clear that the 5.49 µg as the lowest level of detection indicated Figure 2.2 would not be sensitive enough. The next step was to try to establish the phospholipid detection threshold of the HPTLC plates (Figure 2.8).

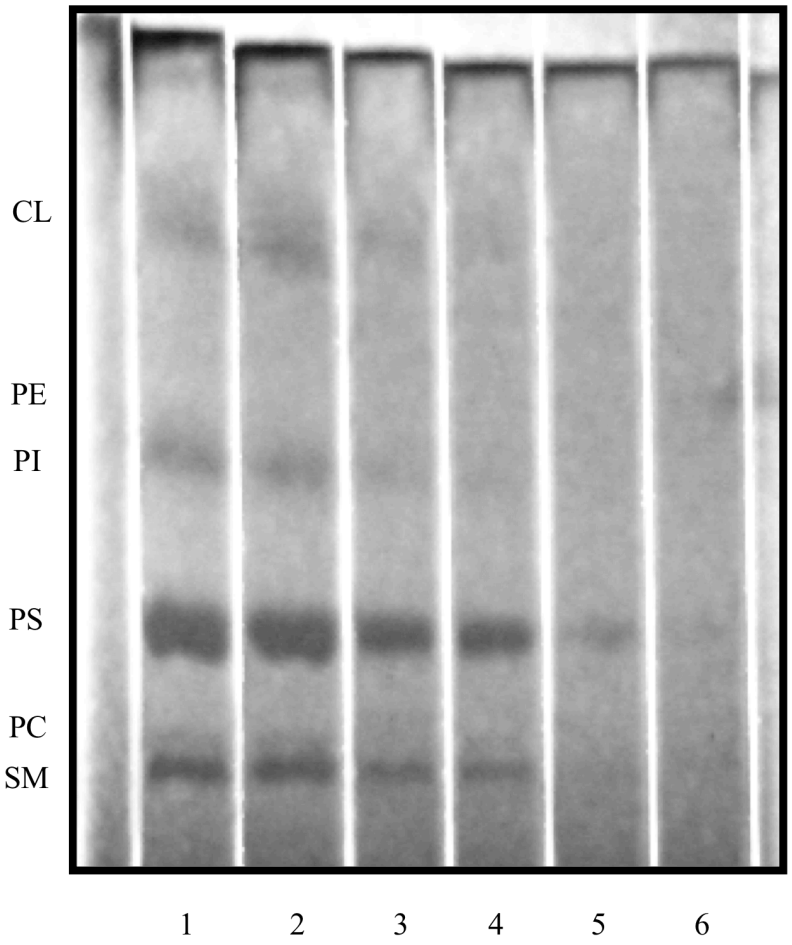


**Figure 2. 8**. HPTLC plate developed with a standard phospholipid mixture containing sphingomyelin (SM), phosphatidylcholine (PC), phosphatidylserine (PS), phosphatidylinositol (PI), phosphatidylethanolamine (PE) and cardiolipin (CL). Total lipid weights of each lane were 1: 21.94 µg, 2: 10.97 µg, 3: 5.49 µg, 4: 2.74 µg, 5: 1.37 µg 6: 0.685 µg. Concentration of total lipids in standard mix is 21.945 µg/µl.

Figure 2.8 reveals that with 8 mm bands the lowest level of detection of lipids was lane 4 (2.74 µg total lipid). This is at least 10-fold higher than what was expected to be present in 10 sarcolemmal cuffs (200 ng). Thus, an increase in sensitivity was needed and it was thought that by spotting the plate as ~1mm dots rather than 8mm bands would concentrate the signal using the same phospholipid mixture and solvent system (Figure 2.9).

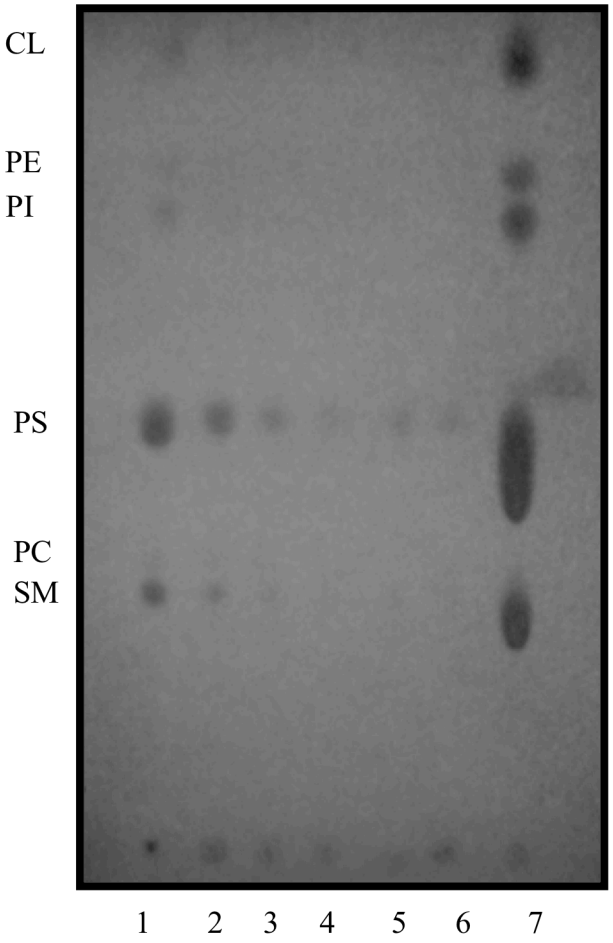


**Figure 2. 9**. HPTLC plate developed with a standard phospholipid mixture containing sphingomyelin (SM), phosphatidylcholine (PC), phosphatidylserine (PS), phosphatidylinositol (PI), phosphatidylethanolamine (PE) and cardiolipin (CL) spotted as 1mm dots. Total lipid weights of each lane were 1: 1.37 µg, 2: 685 ng, 3: 342.5 ng, 4: 274 ng, 5: 204 ng 6: 137 ng, 7: 10.97 µg. Concentration of total lipids in standard mix is 21.945 µg/µl.

When lipids were spotted as ~1mm dots, the lowest level of detection decreased to 342.5 ng of total lipid (Figure 2.9, lane 3). However, lanes 4,5,6 and 7 still have the possibility of having lipids that are just not detected with the less sensitive DCF technique. Therefore, the lipid analysis protocol included spotting samples as ~1mm dots not bands.

Despite the increased sensitivity of the HPTLC plates, the aqueous skinning solution, freeze-thaw cycles in lipid extraction, the development of sarcolemmal cuffs was unsuccessful, as there was still streaking (Figure 2.5). In general, streaking that occurs on HPTLC plates is thought to be a result of overloading the silica particles. Phospholipids along with glycolipids belong to a group, namely, the polar lipids, and, separate from this group are the neutral lipids (cholesterol, free fatty acids). There are several investigations that utilize HPTLC and TLC to separate these lipids all one on plate, using different solvent systems varying in polarity and run times. We then tried to implement a "push" strategy, which simply pushes the neutral lipids higher on the plate allowing for better separation of phospholipids on the lower portion of the plate. Lipids were spotted as 1mm dots and the plate was developed in a chamber containing dichloromethane (80): ethyl acetate (16): acetone (4) for 7 cm to separate cholesterol, free fatty acids and triglycerides from phospholipids to prevent overloading of the silica particles in accordance with a previous study (Weerheim, et al., 2002). Using a new solvent system for phospholipids (Choloform (60): Ethyl acetate (12): Acetone (12): Isopropanol (12): Ethanol (32): Methanol (56): Water (12): Acetic Acid (2)), phospholipids were separated by incubation in saturating tank until the solvent front ran 5.5 cm (Figure 2.10).

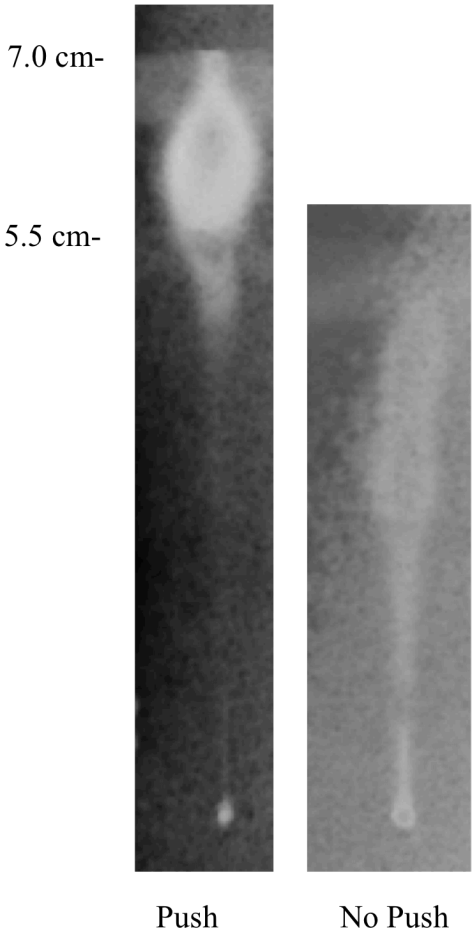


**Figure 2. 10**. HPTLC plate of a pool of 20 cuffs with and without the "push" system.

Using the new "push" strategy, the bulk of the streak was brought up higher (Figure 2.10). However, there was still a thin streak occurring with the push. Furthermore the push method did not reveal phospholipid bands, which may also be due to the low sensitivity of the DCF technique. It was then thought that the sample needed to be cleaned up prior to spotting onto HPTLC plates. We then sought out solid phase extraction to possibly alleviate these problems.

Solid phase extraction (SPE) is a common protocol utilized in the analysis of lipids. It is most commonly used as cleaning strategy in preparation for various techniques including HPTLC and gas chromatography. In brief, it utilizes a solid

stationary phase that bind lipids, and with the use of solvents varying in polarity, neutral lipids (neutral solvent) can be separated from polar lipids (polar solvents). For our purposes, the stationary phase was silica, and the glass columns were custom made (diameter: 8 – 10 mm, length: 20 cm) with a stopcock.

The validity of this technique for our purposes was first tested with two separate pools of 10 cuffs. In this test DCF detection of lipids was not used and instead the charring method (3% copper sulfate in 8% phosphoric acid) was used in order to ensure that there was lipid present in the sarcolemmal cuffs. Lipids were developed in neutral lipid solvent system (Hexane (80) : diethyl ether (20): acetic acid (15) (Kupke & Zeugner, 1978)) alongside two neutral lipid standards 13:0 free fatty acid and triglycerides obtained from vegetable oil extract (Figure 2.11).

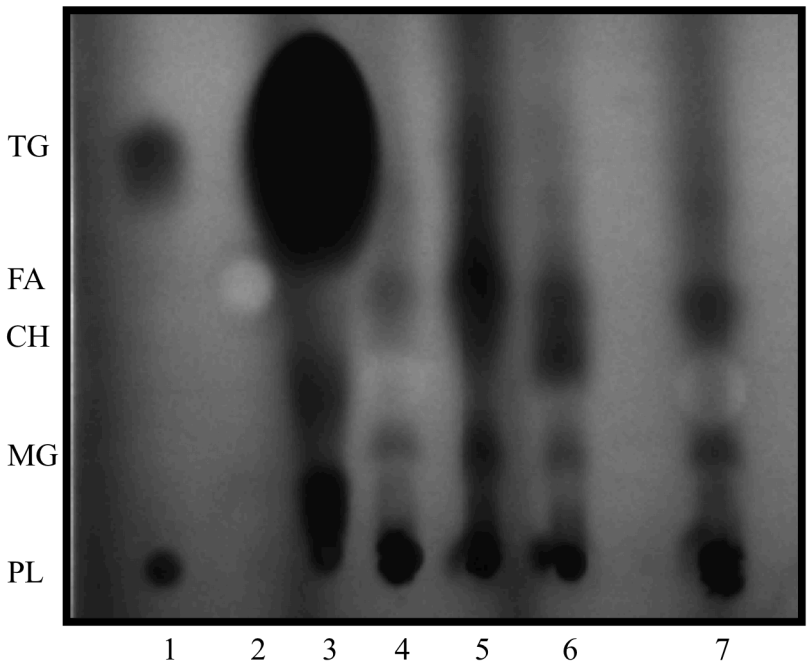


**Figure 2. 11**. HPTLC plate testing the applicability of solid phase extraction to sarcolemmal cuffs lipid analysis. Lane 1: Lipid mix (phospholipids + triglyceride + free fatty acid), Lane 2: 13:0 free fatty acid standard, Lane 3: triglyceride standard, Lane 4: SPE neutral lipid fraction, Lane 5 :SPE Glycolipid fraction, Lane 6: SPE phospholipid fraction, Lane 7: 10 cuffs applied directly without SPE. TG: triglyceride; FA: fatty acid; CH: cholesterol; MG: monoglyceride; PL: phospholipids.

After using the charring method on HPTLC plates it was evident that there were lipids present in the pool of 10 sarcolemmal cuffs, thereby justifying the pool of 10 (Figure 2.11). It was also evident that the cuffs were enriched in neutral lipids specifically free fatty acids and most likely cholesterol and monoglycerides (two bands below fatty acids based on a previous study) (Yao & Rastetter, 1985). These results indicate that despite the solid phase extraction, there was still neutral lipid contamination in the glycolipid and phospholipid fractions (Lane 5 and 6, respectively). Furthermore, lane 1 indicates that phospholipids and polar lipids are immobile in this solvent system.

Interestingly, there are still polar lipids in the neutral lipid fraction after SPE (Lane 4). There are some practical benefits to solid phase extraction which include: time to plate samples, whereby the application of samples onto the HPTLC plate without SPE was prolonged (> 1 hr). Furthermore, by splitting lipid samples into fractions you can prevent any possible overload onto the silica particles. Therefore, SPE was implemented into the lipid analysis protocol.

Next, two different strategies were tested to separate phospholipids after SPE 1) push method and 2) plate-scrape-plate (PSP) method. The latter, in brief, involves developing the neutral lipids on an HPTLC plate (plate), scraping the silica particles with the immobile polar lipids (scrape), extracting those polar lipids and finally, spotting onto another HPTLC plate for phospholipid development (plate). So the next step was to determine which strategy worked best. After the lipid extract of 10 EDL cuffs underwent SPE, they were spotted and developed with the push strategy (Figure 2.12). Likewise, after 10 EDL cuffs underwent SPE, they were spotted and developed with the PSP strategy (Figure 2.13 & 2.14).

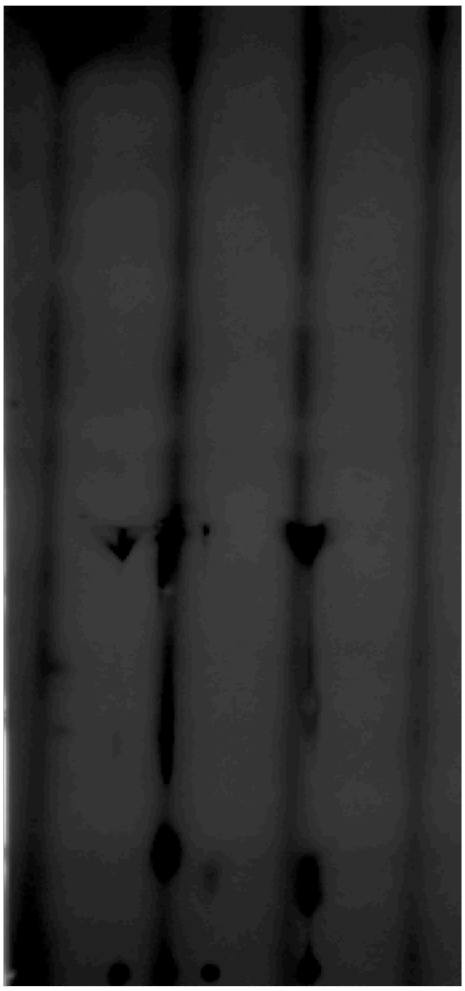

NL GL PL SPE-

**Figure 2. 12**. HPTLC plate testing the applicability of solid phase extraction with neutral lipid "push". NL: neutral lipid fraction; GL: glycolipid fraction; PL: phospholipid fraction; SPE- : no solid phase extraction. Neutral lipid solvent (Hexane (80) : Diethyl ether (20): Acetic acid (1.5)), phospholipid solvent (Chloroform (100): Methanol (75): Water (4)).

It was evident that the push did work to some extent. The PL fraction had a signal at the PC/SM area. The GL and SPE- fractions both also had a signal in the proximity of PC/SM bands but there was streaking occurring in these bands.

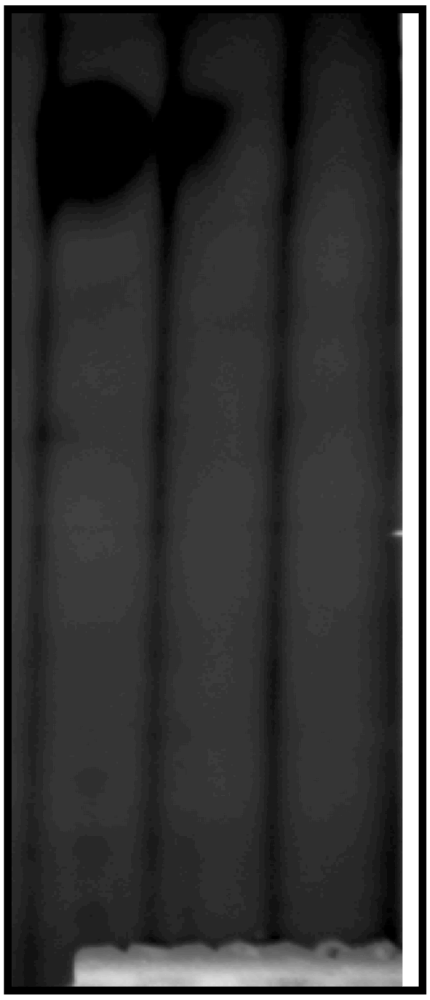


**Figure 2. 13**. HPTLC plate testing the applicability of solid phase extraction with neutral lipid development then phospholipid extraction. NL: neutral lipid fraction; GL: glycolipid fraction; PL: phospholipid fraction; SPE- : no solid phase extraction. Neutral lipid solvent (Hexane (80) : Diethyl ether (20): Acetic acid (1.5)).

Of no surprise, neutral lipid development after SPE indicates that the neutral lipid had the most neutral lipids (Figure 2.13). After this development the immobile phospholipids were scraped and lipids were extracted from the silica using the Bligh and Dyer method (1959). After, the lipid extract was spotted onto a separate plate, developed in a phospholipid solvent system, and visualized through charring (Figure 2.14).

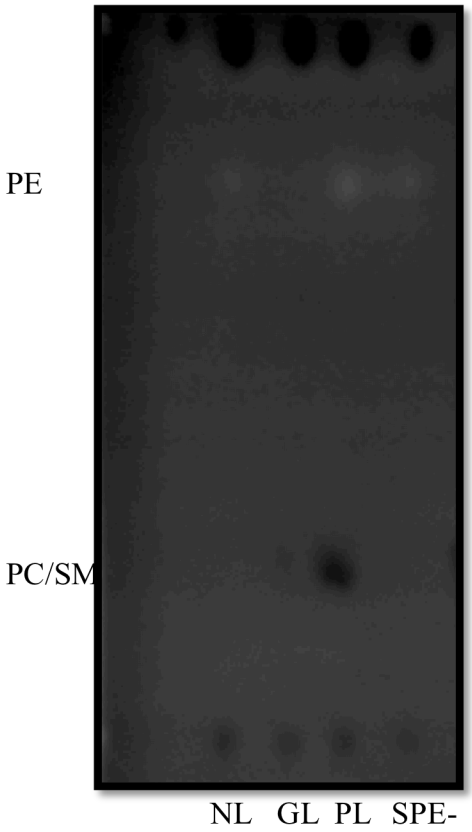


**Figure 2. 14**. HPTLC plate of phospholipids scraped from a prior neutral lipid development. NL: neutral lipid fraction; GL: glycolipid fraction; PL: phospholipid fraction; SPE- : no solid phase extraction. Phospholipid solvent (Chloroform (100) : Methanol (75): Water (4)).

Solid phase extraction was successful whereby the PL fraction had the most phospholipids (Figure 2.14). However, there seemed to be phospholipids in both the NL and GL fractions. Unlike, the push method shown in Figure 2.12, there are no streaks in the two step development. Therefore, with the PSP method, the NL, GL and PL fractions could be combined after neutral lipid development to maximize recovery of the phospholipids. Although, the push method showed some signs of phospholipids in the PL fraction, the summation of PL, GL and NL would not be possible due to the streaking that

occurs in the NL and GL lanes. Therefore, the PSP method was implemented into the sarcolemmal cuff lipid analysis protocol.

After SL cuff lipid extract PL development with the PSP method, PLs were scraped and methylated for GC analysis. It is important to note that due to DCF sensitivity, phospholipid bands were rarely seen, and thus phospholipids were scraped in correspondence to phospholipid standards regardless of visual detection (ghost lanes). An of 3 was analyzed with the PSP method, and interestingly, analysis revealed that PS was the most abundant phospholipid (Figure 2.15).

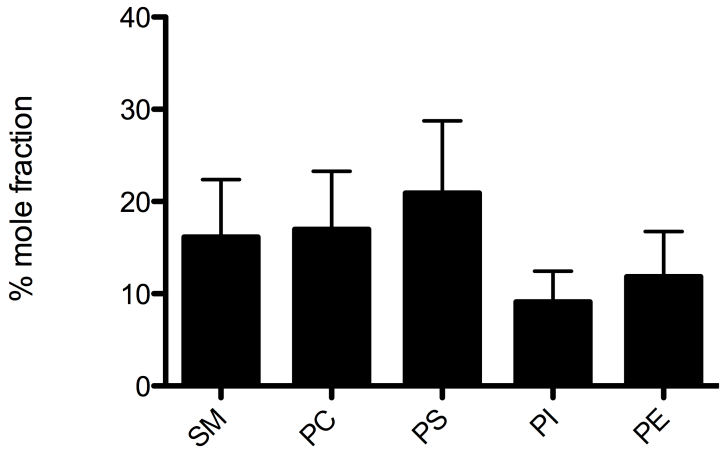


**Figure 2. 15**. Phospholipid specie distribution from sarcolemmal cuffs utilizing the PSP development (n=3). SM: sphingomyelin; PC: phosphatidylcholine; PS: phosphatidylserine: PI: phosphatidylinositol; PE: phosphatidylethanolamine.

These results were confirmed with sets of sarcolemmal cuffs extracted from soleus muscle that was processed with SPE and the PSP method. After phospholipid development the HPTLC plate was charred (Figure 2.16).

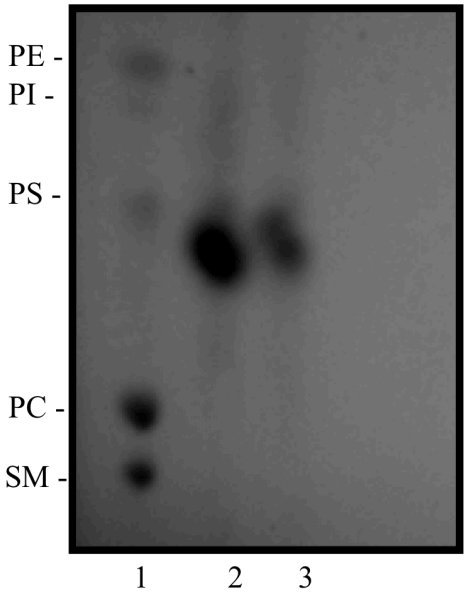


**Figure 2. 16**. Sarcolemmal cuff phospholipid analysis from soleus muscle fibres. Lane 1: Phospholipid standard; Lane 2: Phospholipid extract from 10 soleus cuffs; Lane 3: Phospholipid extract from 10 soleus cuffs.

The results from the soleus cuffs confirm that PC and SM are not present, while PS, PI and PE were (image is not as clear). Also, there is presence of an unknown lipid, which may be a result of overloaded silica preventing sufficient separation. The presence of this unknown PL, may have been unintentionally scraped for PS, possibly explaining its high relative abundance after GC analysis.

With SM and PC being less abundant than expected, it was thought that two step development was minimizing recovery of the phospholipids. It is well known that SM and PC bind strongest to silica particles due to choline's high polarity (Pernet, et al., 2006). Thus it was plausible that lipid extraction from silica after the first neutral lipid development would not have extracted all PC and SM. In addition, since solid phase extraction also utilizes silica particles, the loss in recovery could have happened at this stage in the protocol. Therefore, in order to try and maximize recovery, 2-dimensional

(2d) HPTLC was tested for our purposes. In brief, sample was spotted onto the HPTLC plate and neutral lipid separation was run. Subsequently, the plate was rotated 90° before running the phospholipid separation. With red gastrocnemius whole muscle lipid extract, an experiment was set to compare the recoveries of phospholipids using the PSP method and the 2d HPTLC (Figure 2.17).

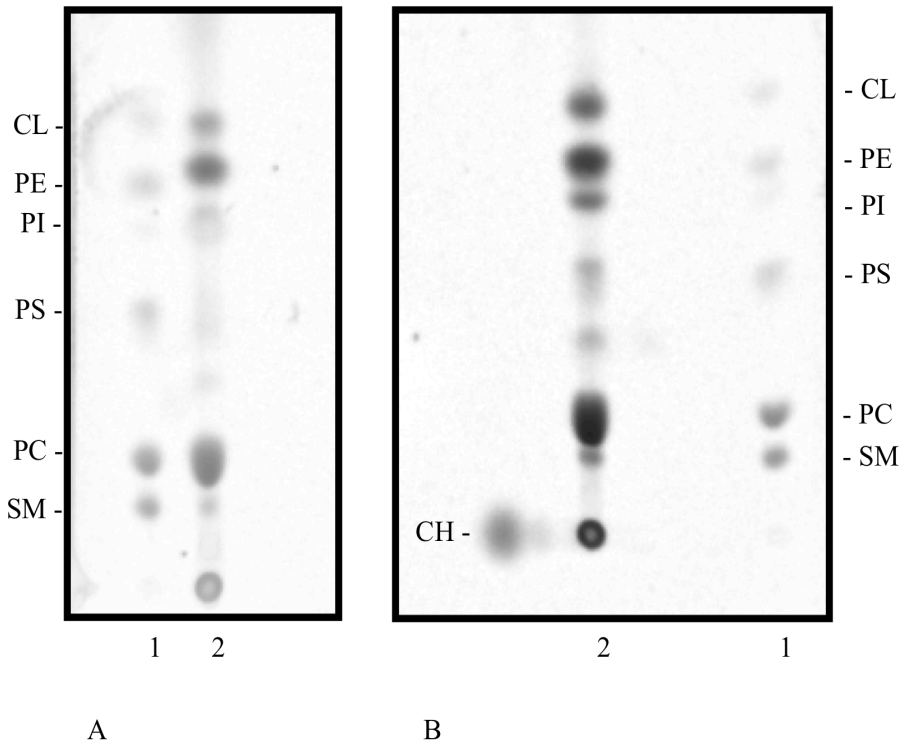


**Figure 2. 17**. HPTLC analysis comparing phospholipids using either PSP method (A) and 2d analysis (B) with lipids extracted from red gastrocnemius whole muscle (150 µL of lipid extract). Lane 1: Phospholipid standard; Lane 2: Red gastrocnemius sample. SM: sphingomyelin; PC: phosphatidylcholine; PS: phosphatidylserine; PI: phosphatidylinositol; PE: phosphatidylethanolamine; CH: cholesterol.

The bands were visually darker with the 2d HPTLC compared to the PSP method, despite starting with the same volume of lipid extract (150 µl) and charring for the same amount

of time at 180°C (10 min). When assessing the densitometries, 2d had consistently higher density bands than PSP (Figure 2.18).

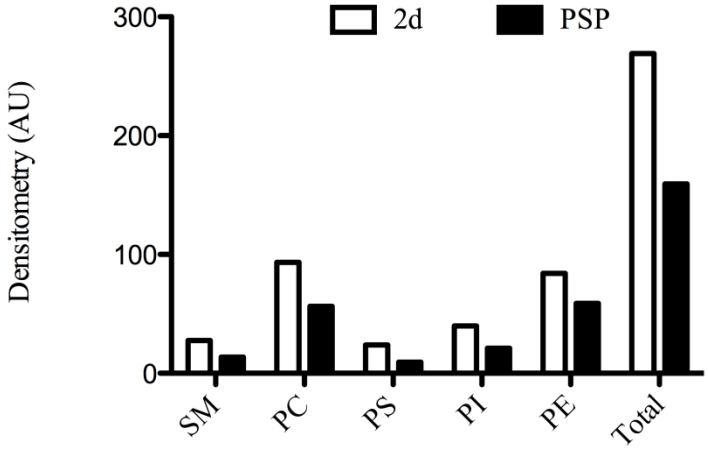


**Figure 2. 18**. Densitometric analysis of phospholipid species after 2-dimensional (2d) HPTLC and plate-scrape-plate method (PSP). Values are arbitrary units per µl of lipid used.

When considering 2d as total, percent recovery of the PSP method ranged from 40 – 68 % (Figure 2.19).

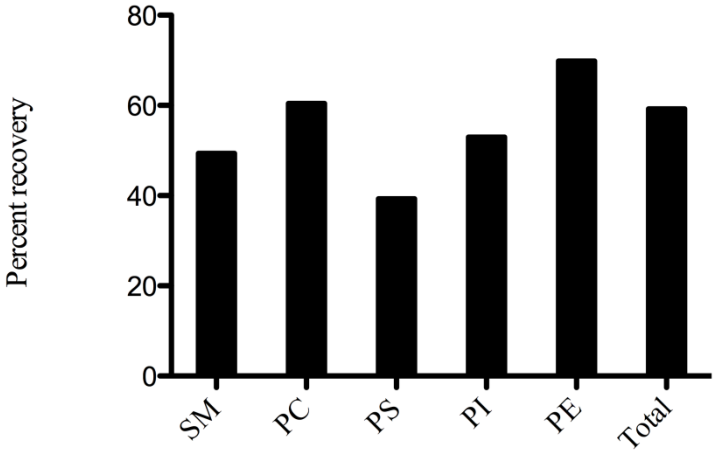


**Figure 2. 19**. Percent recovery of phospholipid species using the PSP method when considering 2d analysis as 100%.

Given the results that 2d HPTLC had greater amount of lipids relative to PSP, 2d HPTLC was implemented into the sarcolemmal lipid analysis protocol while PSP was eliminated. In addition Figure 2.20 reveals that cardiolipin migrates to an unknown artefact on HPTLC. Therefore, cardiolipin was not included in lipid analysis.

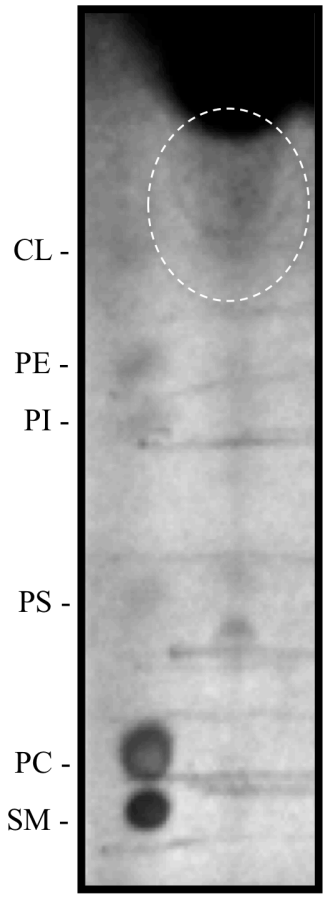


**Figure 2. 20**. HPTLC plate of 10 EDL sarcolemmal cuffs indicating CL's migration to a potential contaminating artefact, marked by the dashed circle.

Figure 2.21 summarizes the included and excluded steps for sarcolemmal cuff phospholipid separation using HPTLC.

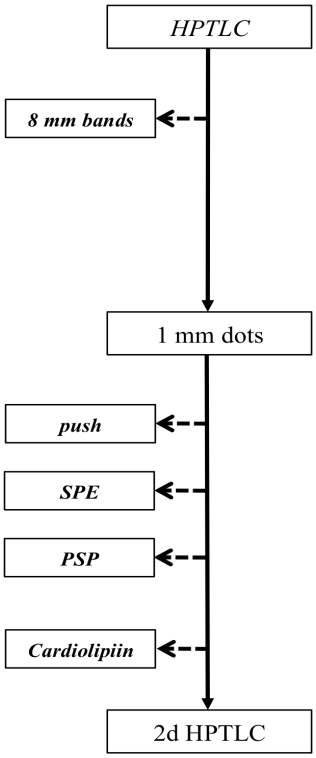


**Figure 2. 21**. Diagrammatic flow-chart illustrating the included and excluded steps for the separation of phospholipid species on HPTLC. Dashed arrows = excluded.

*Method development: Gas Chromatography*

Despite the changes in HPTLC methodology, upon GC analysis, phospholipid species distribution was still not as expected, with PS and SM being major lipids (Figure 2.22).

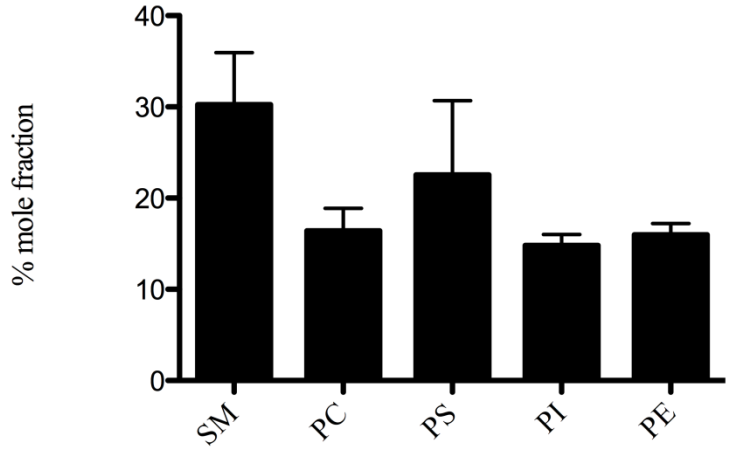


**Figure 2. 22**. Phospholipid specie distribution upon utilizing 2d HPTLC from EDL cuffs. SM: sphingomyelin; PC: phosphatidylcholine; PS: phosphatidylserine; PI: phosphatidylinositol; PE: phosphatidylethanolamine.

The next step was to determine what could be the cause of these results. We then tested the GC contamination and assessed what blank silica particles (particles expected to not have bound lipids) after phospholipid development would like under GC analysis. An experiment was set out with 2d analysis with 10 EDL cuffs, and their phospholipids were collected along with a blank area on the HPTLC plate. Upon GC analysis, it was surprising that the blank lane and the phospholipid lanes had similar peak patterns (Figure 2.23A – E compared to Figure 2.23F).

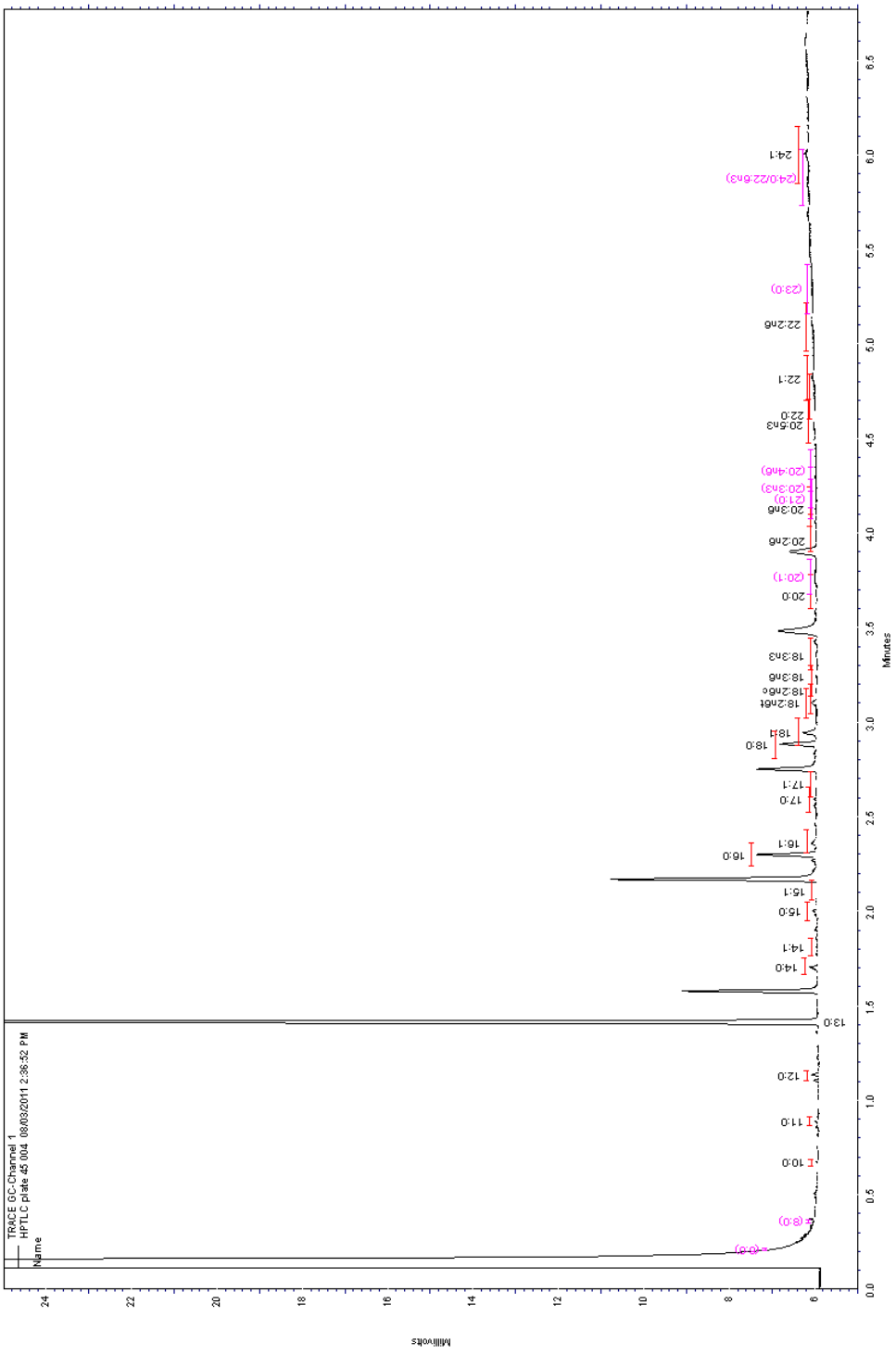


**Figure 2.23 A**. Gas chromatograph of sphingomyelin from a pool 10 EDL cuffs that underwent 2d HPTLC.

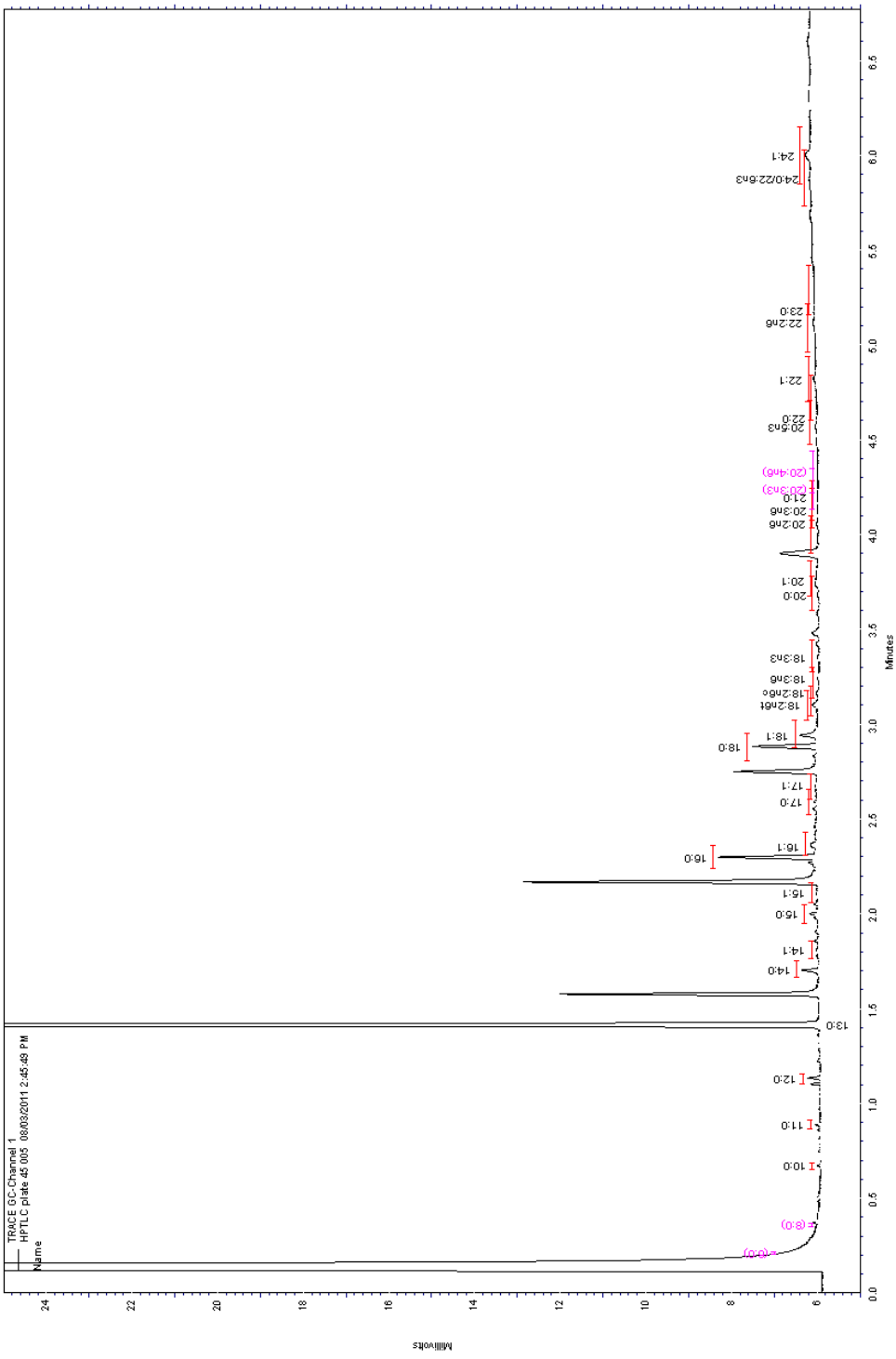


**Figure 2.23 B**. Gas chromatograph of phosphatidylcholine from a pool 10 EDL cuffs that underwent 2d HPTLC.

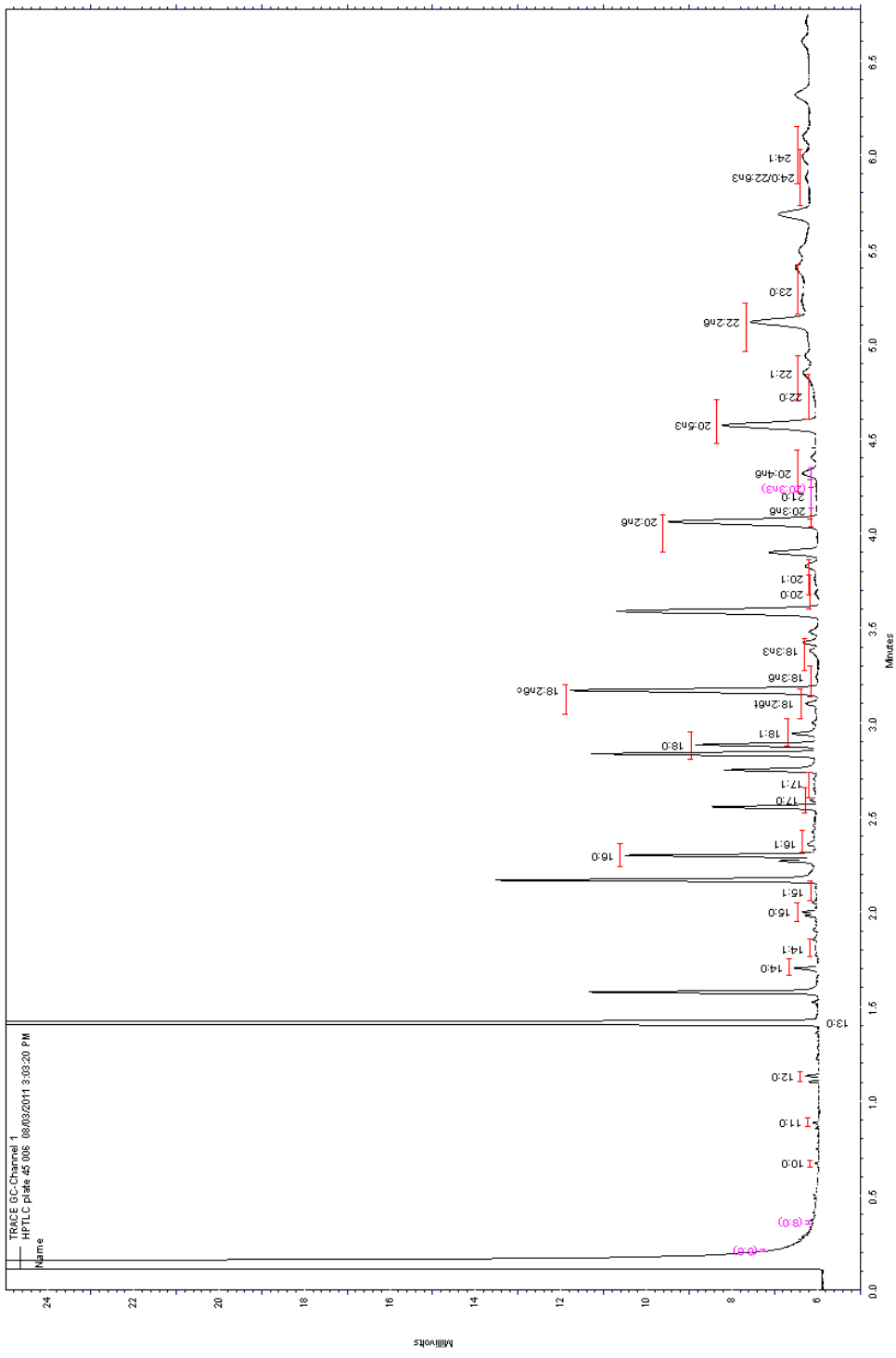


**Figure 2.23 C**. Gas chromatograph of phosphatidylserine from a pool 10 EDL cuffs that underwent 2d HPTLC.

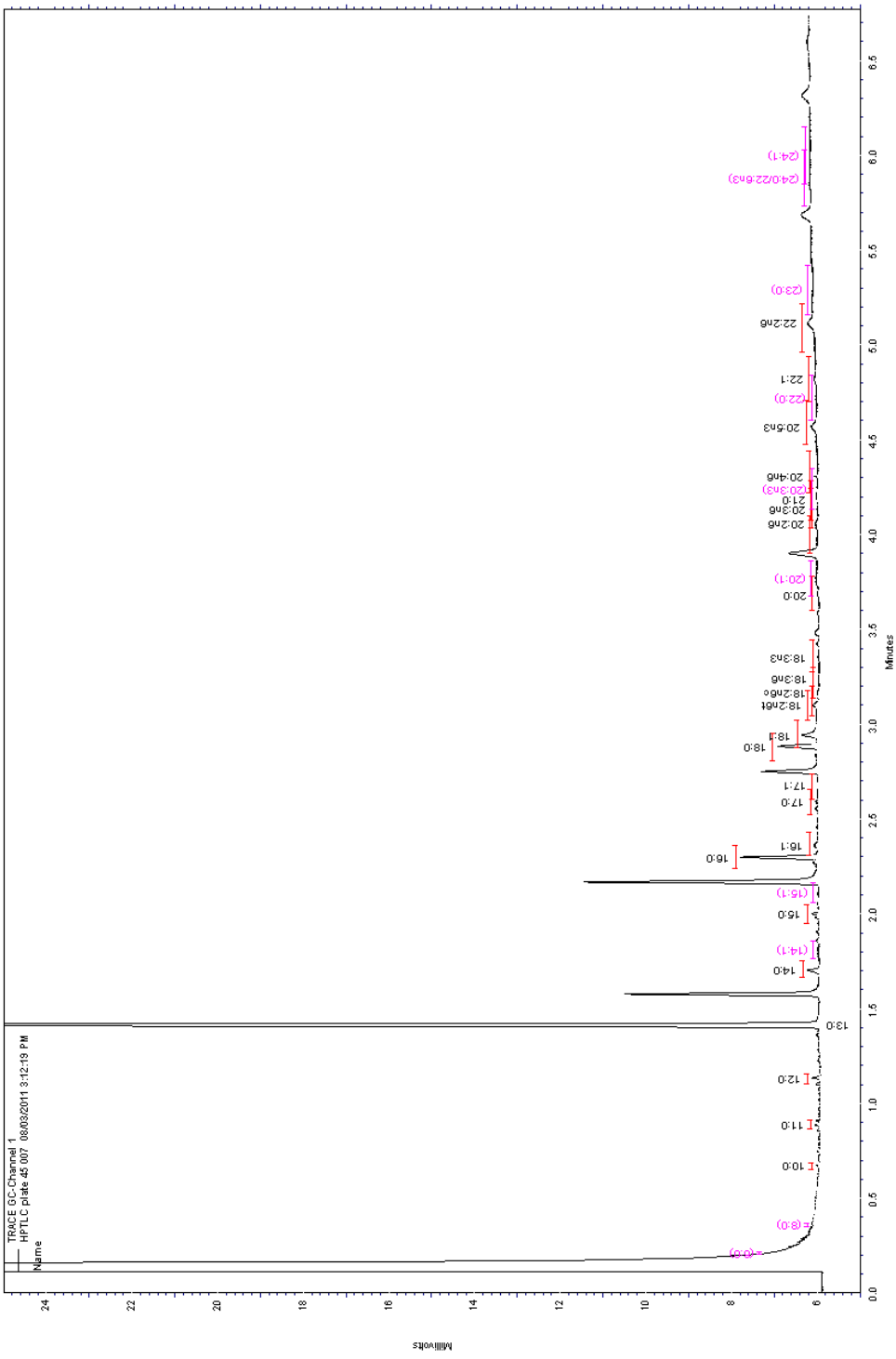


**Figure 2.23 D**. Gas chromatograph of phosphatidylinositol from a pool 10 EDL cuffs that underwent 2d HPTLC.

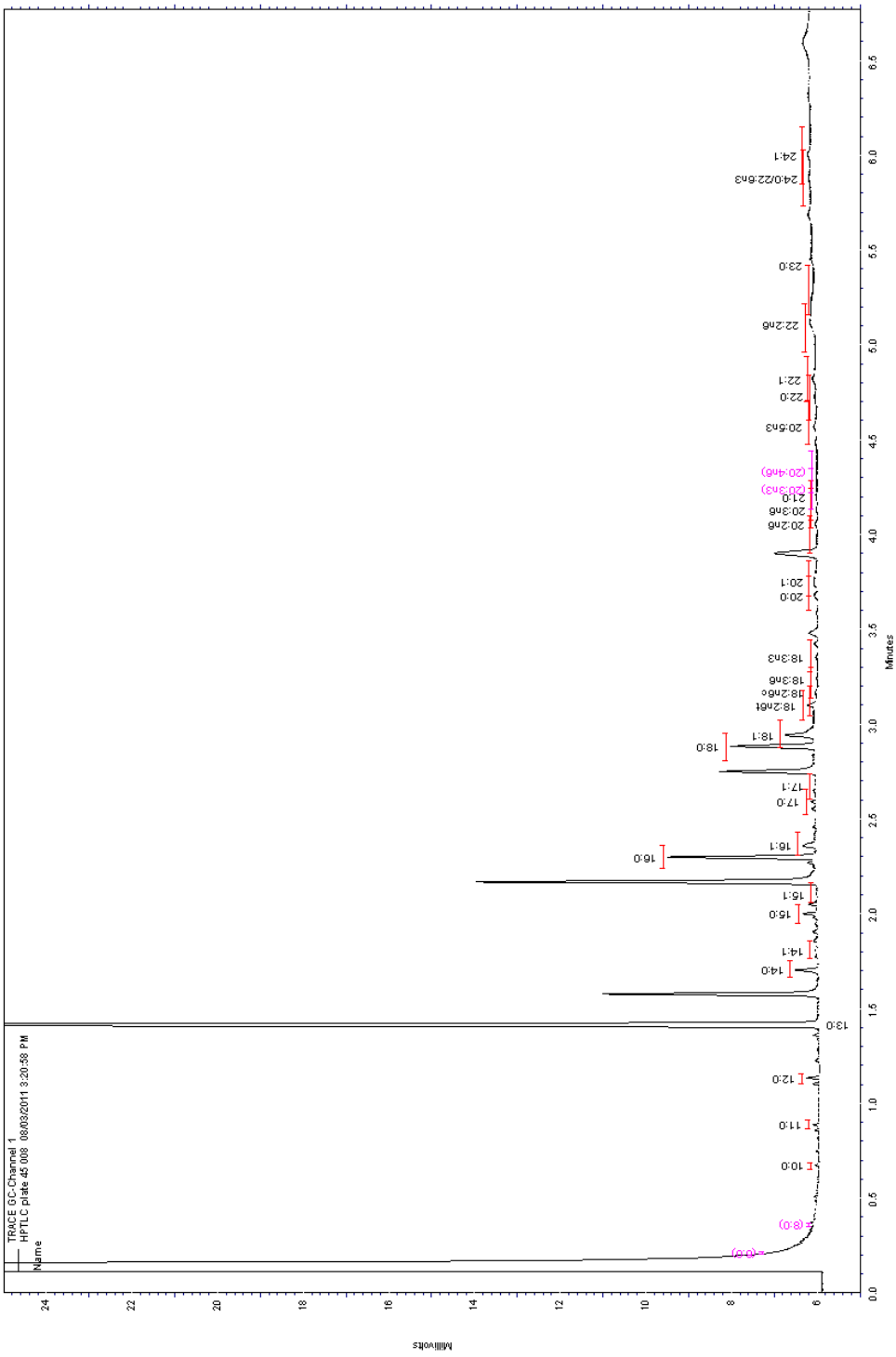


**Figure 2.23 E**. Gas chromatograph of phosphatidylethanolamine from a pool 10 EDL cuffs that underwent 2d HPTLC.

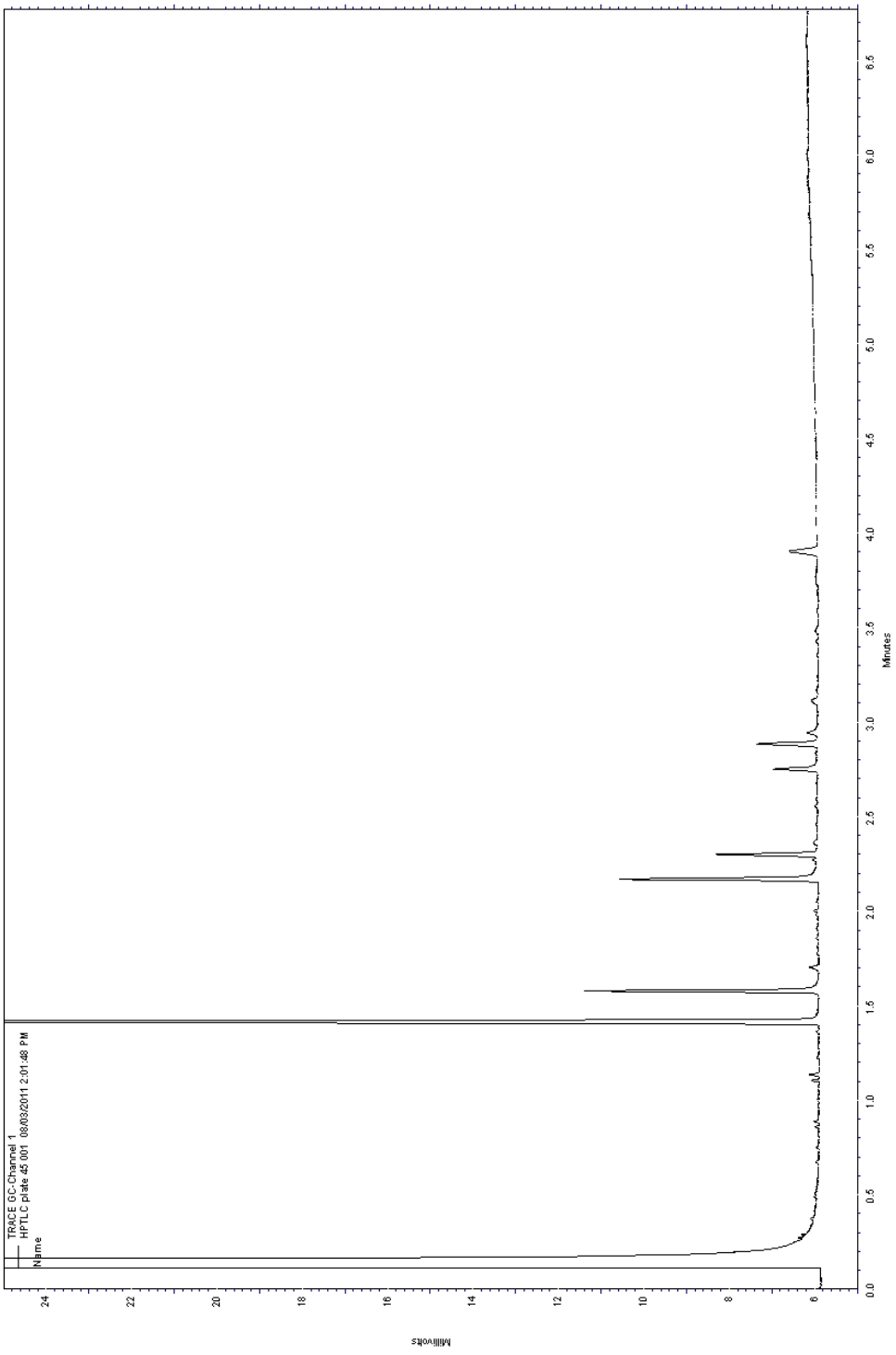


**Figure 2.23 F**. Gas chromatograph of silica particles without any lipids from a pool 10 EDL cuffs that underwent 2d HPTLC.

With the results in Figure 2.23 A - F, it was evident that there was a source of contamination.

All solvents used in the analysis of FA from lipid extraction to GC analysis were tested to determine causing factor in the formation of peaks in the blank silica lanes and possibly causing the problems seen in the phospholipid distributions. The list of solvents included: chloroform, methanol, diethyl ether, ethanol, isopropanol, and ethyl acetate. Each of these solvents (1 ml) were dried down under a stream of nitrogen and were then processed through the methylation protocol. After methylation, samples underwent GC analysis. The chromatographs of the solvents reveal that all solvents have the same peak patterns, which are also similar to the phospholipid peaks seen in Figure 2.23 (Figure 2.24 A – F).

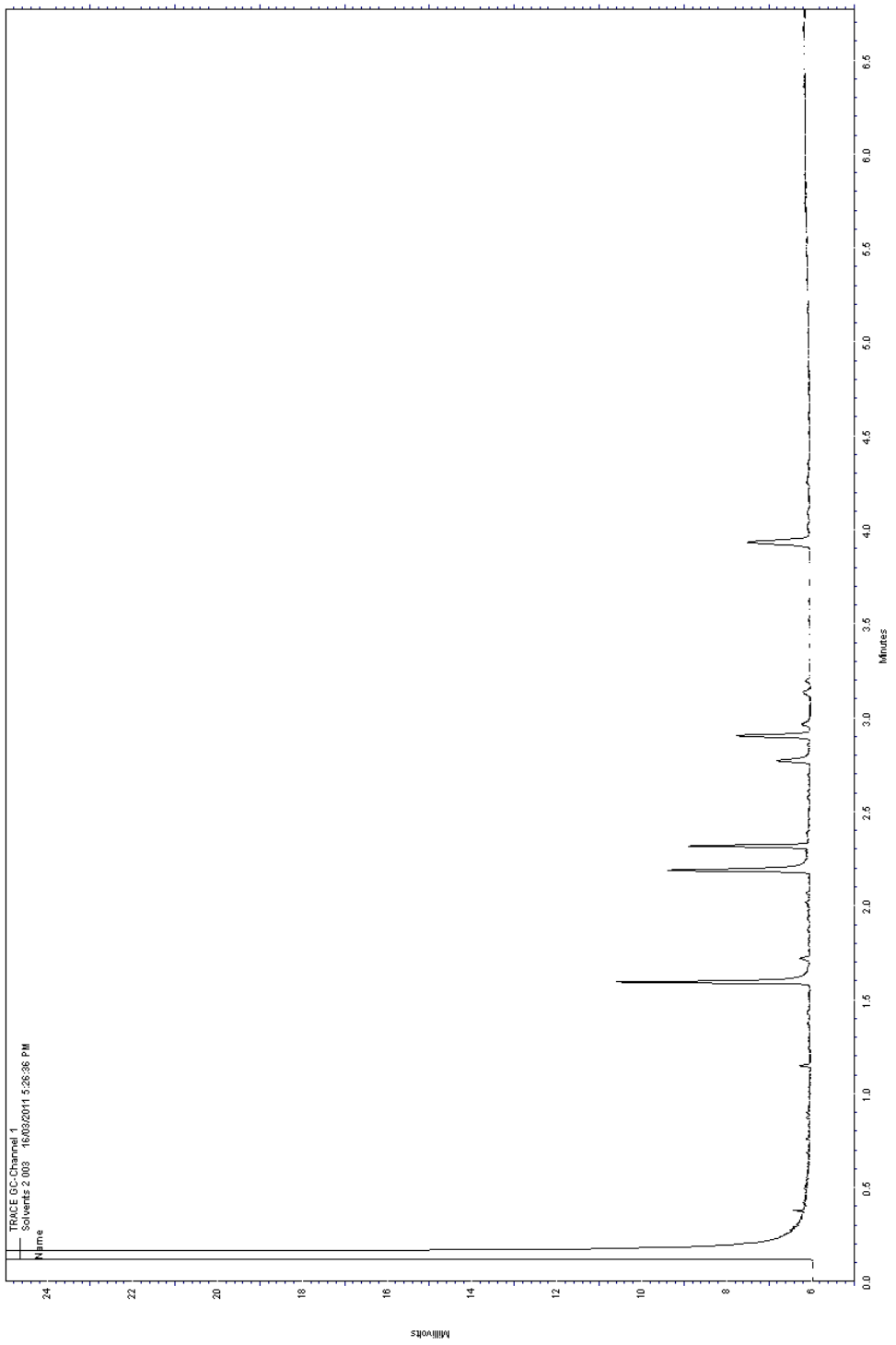


**Figure 2.24 A**. Gas chromatograph of chloroform solvent.

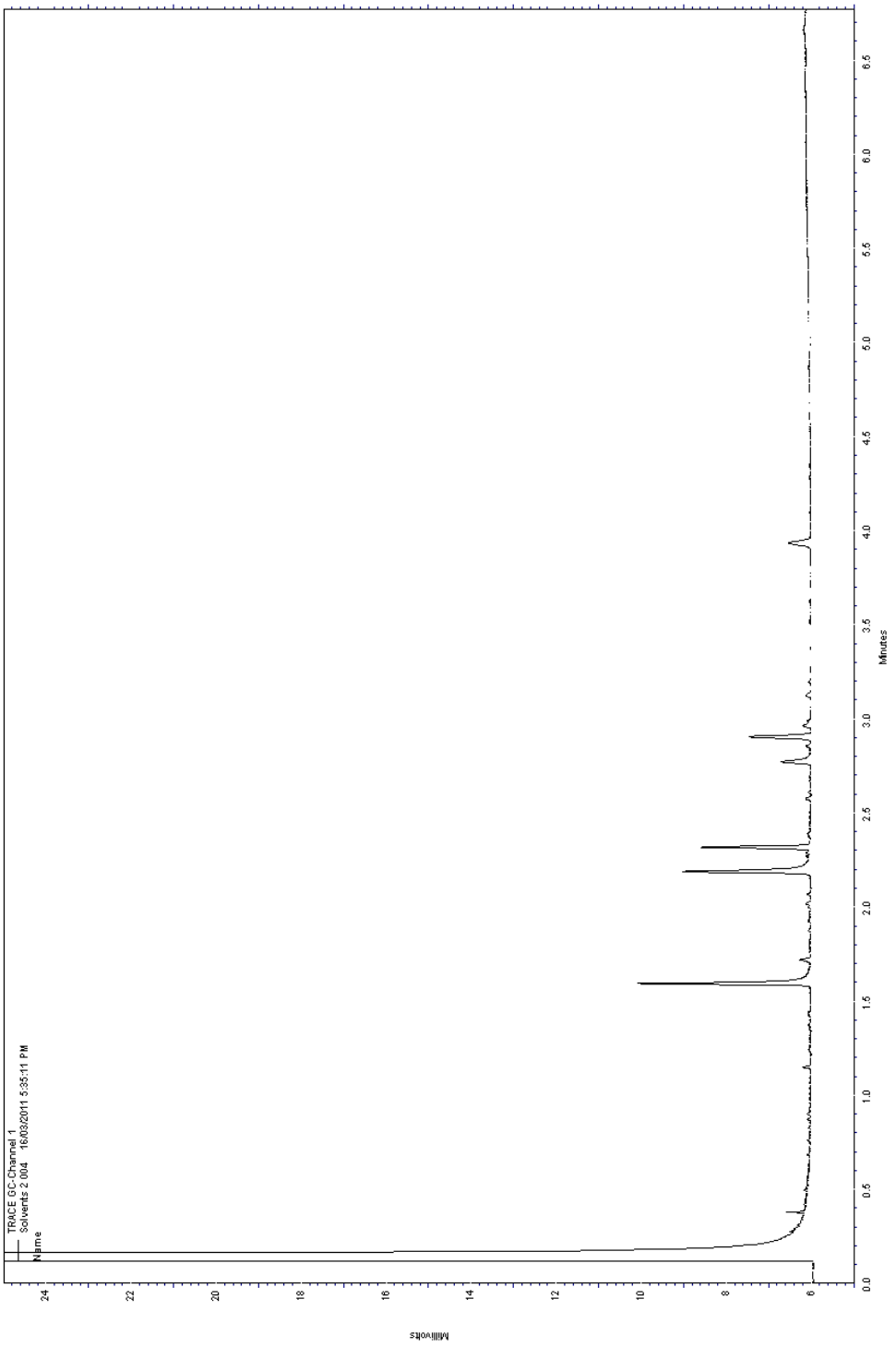


**Figure 2.24 B**. Gas chromatograph of methanol solvent.

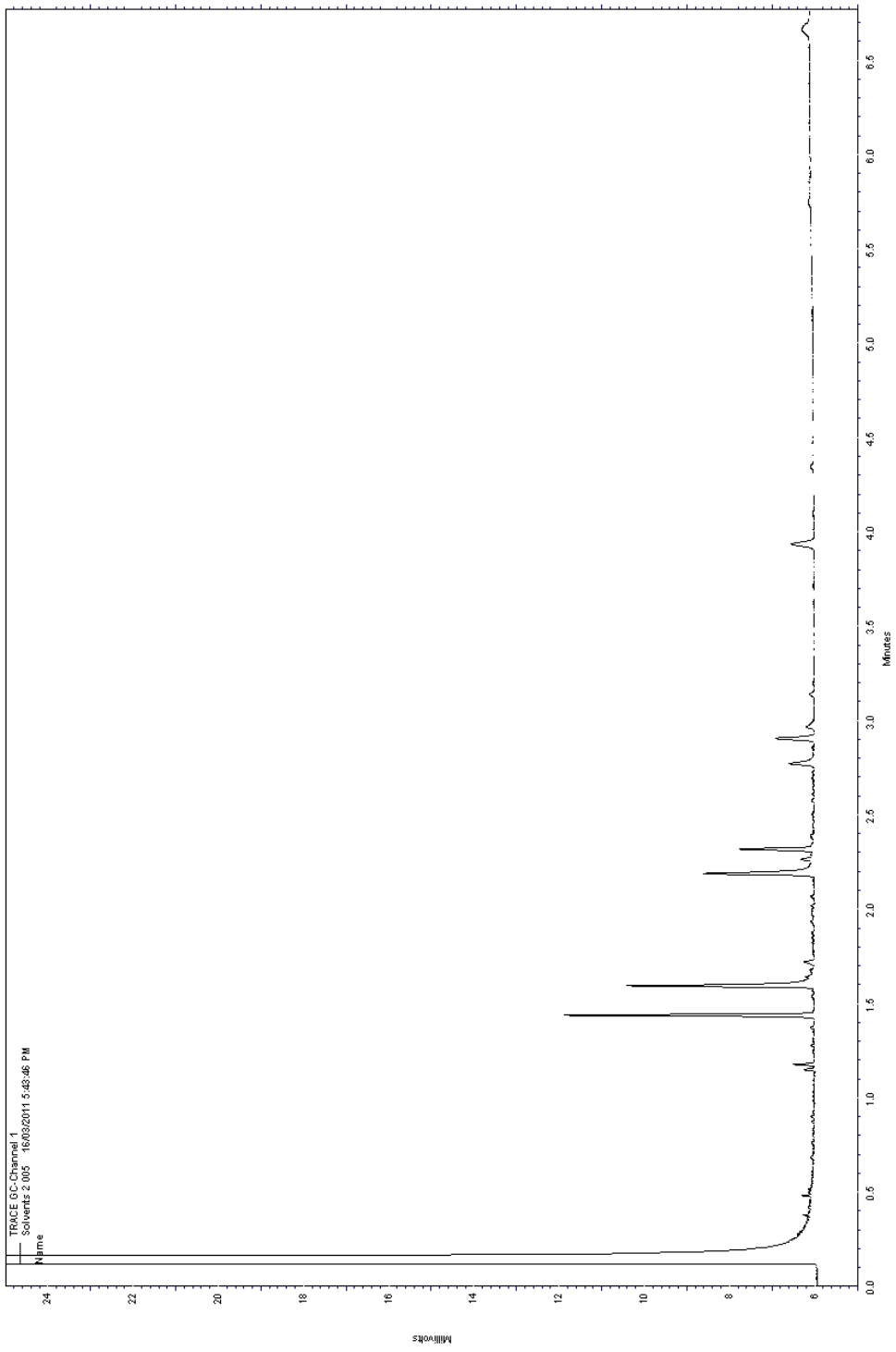


**Figure 2.24 C**. Gas chromatograph of diethyl ether solvent.

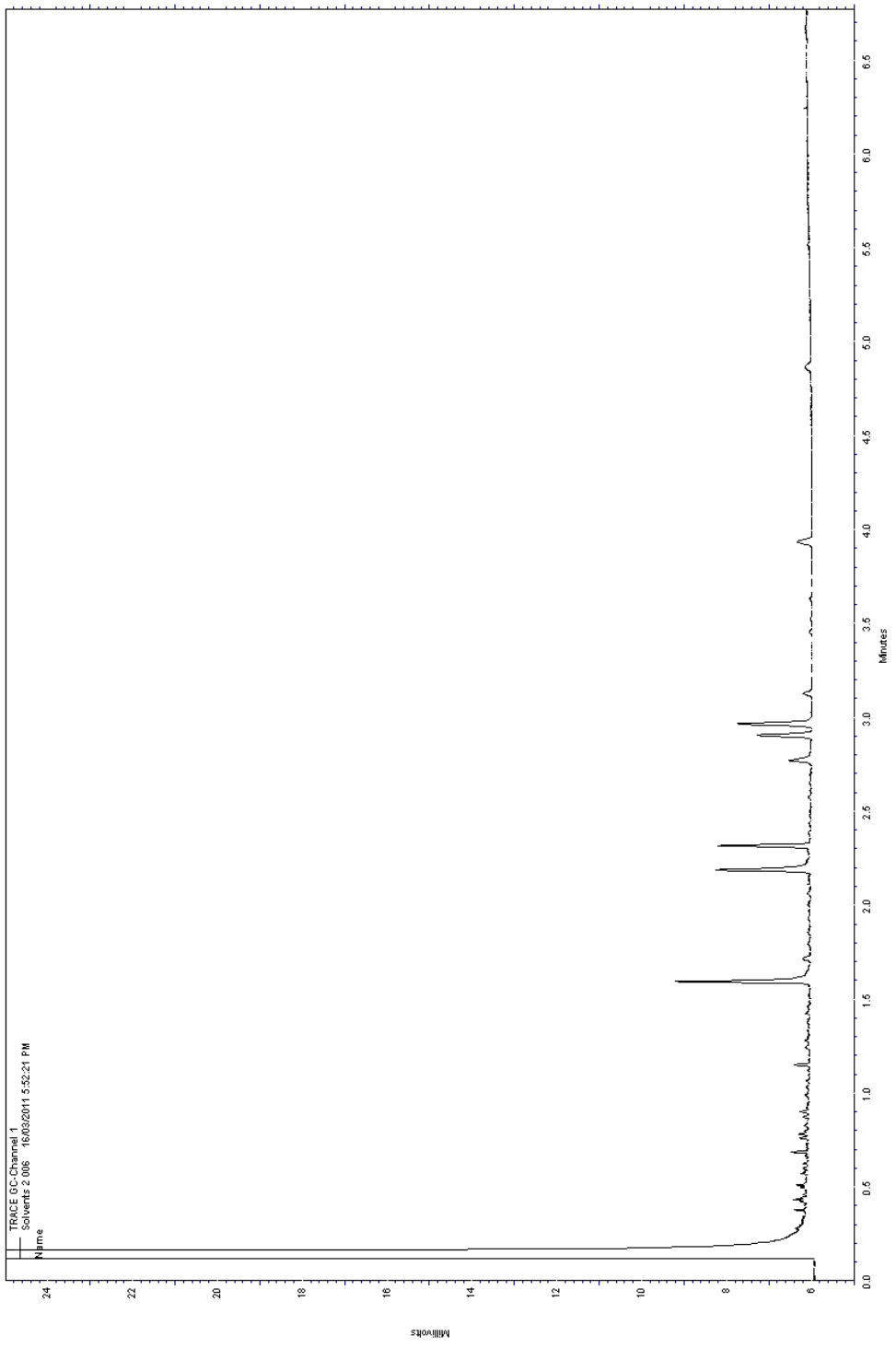


**Figure 2.24 D**. Gas chromatograph of ethanol solvent.

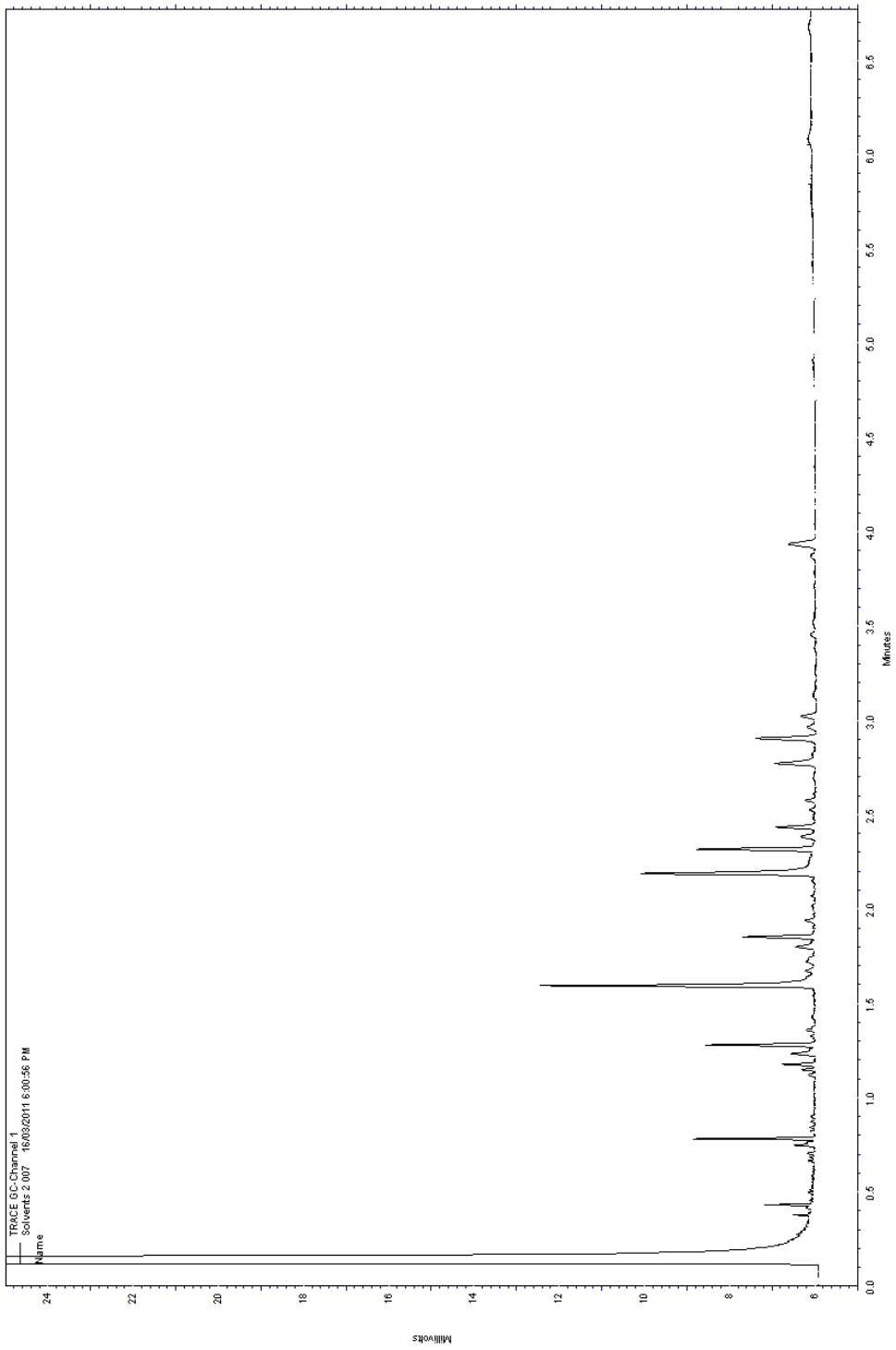


**Figure 2.24 E**. Gas chromatograph of isopropanol solvent.

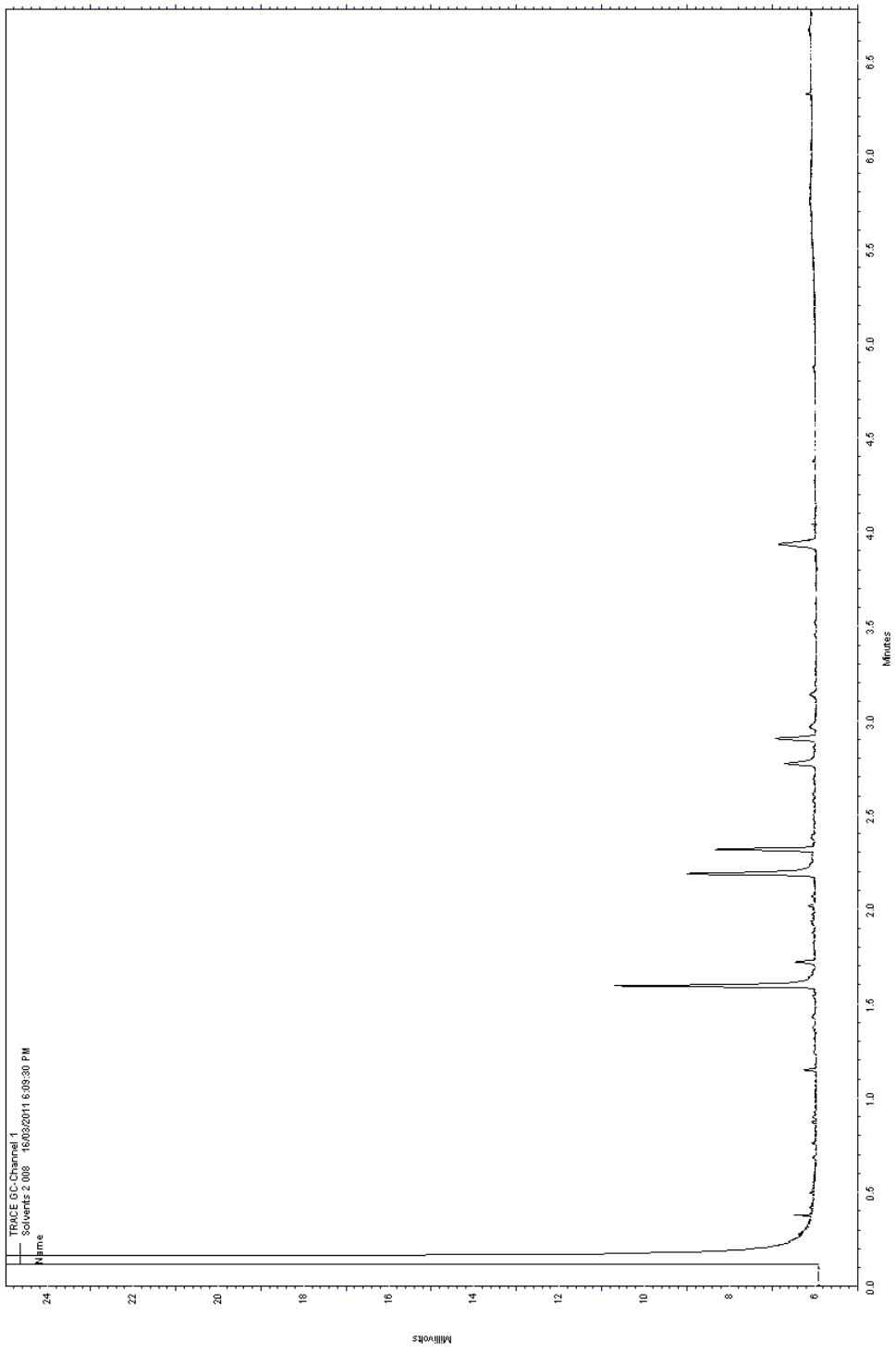


**Figure 2.24 F**. Gas chromatograph of ethyl acetate solvent.

Given the similar peaks seen across all solvents (Figure 2.24 A – F), it was thought that the contamination may be from the methylation protocol. More specifically, it was thought that the 6% $H_2SO_4$ in methanol solution was improperly made. To test for this a new acidic methanol solution was made. Despite these efforts, the contaminating peaks were still present (Figure 2.25).

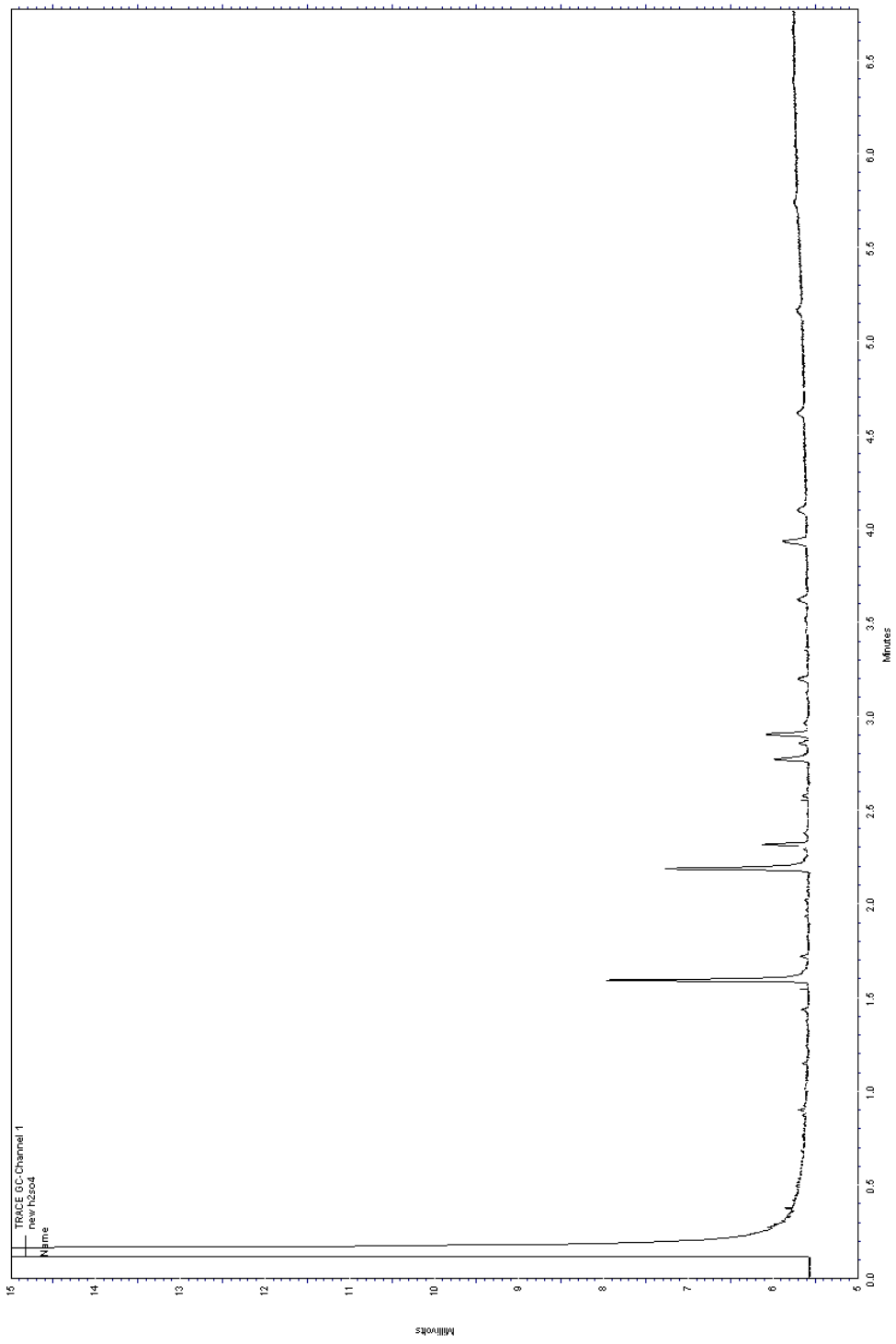


**Figure 2. 25**. Gas chromatograph of a blank sample with new 6% $H_2SO_4$ in methanol solution.

Given the chromatograph with new 6% $H_2SO_4$ in methanol solution (Figure 2.25), it was then thought the contamination was from the kimex tubes used for methylation. Thus, old and new tubes were tested against each other, only to reveal the same peak patterns (Figure A4.26A & B).

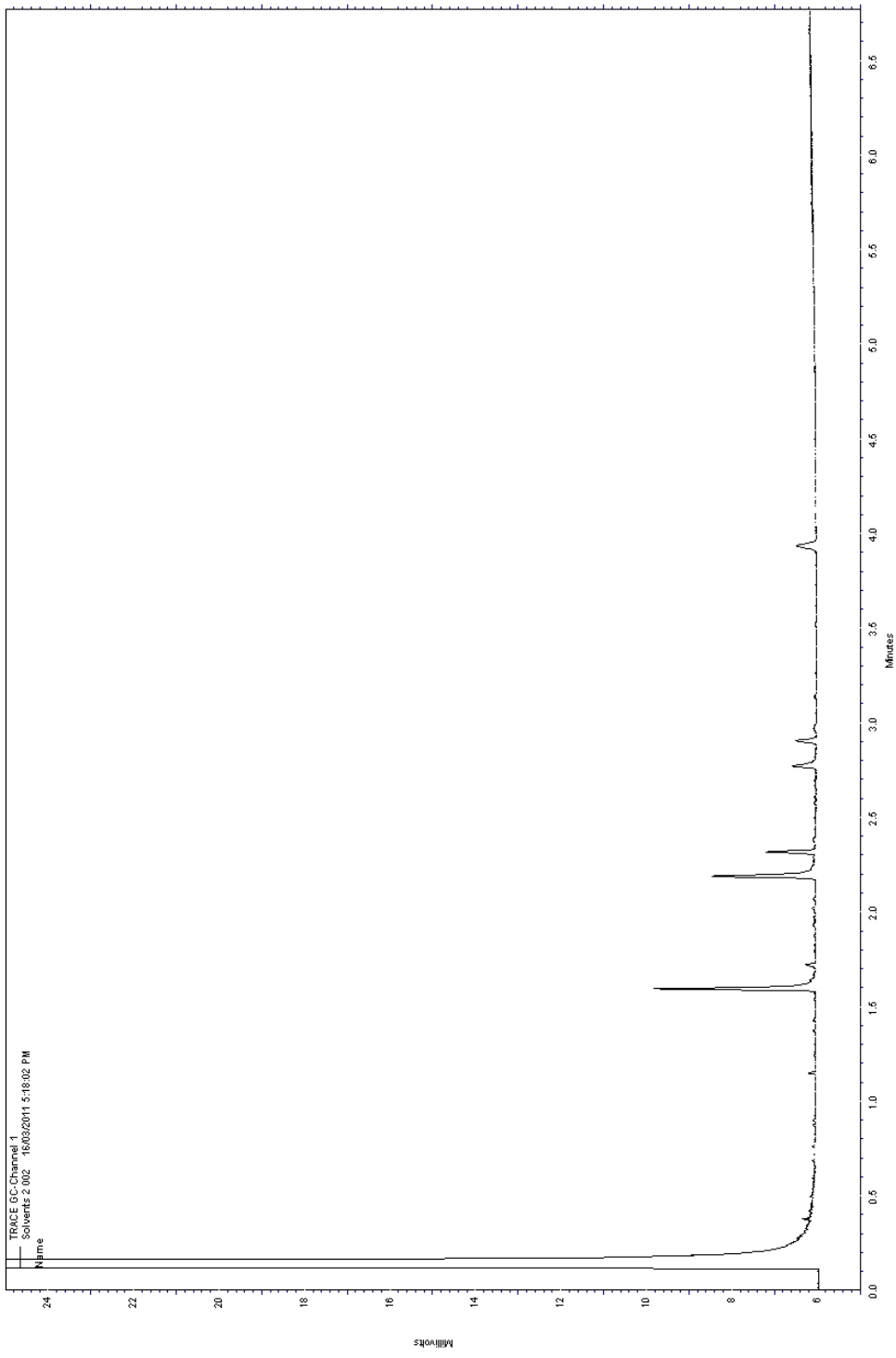


**Figure 2.26 A**. Gas chromatograph of a blank sample with an old kimex tube.

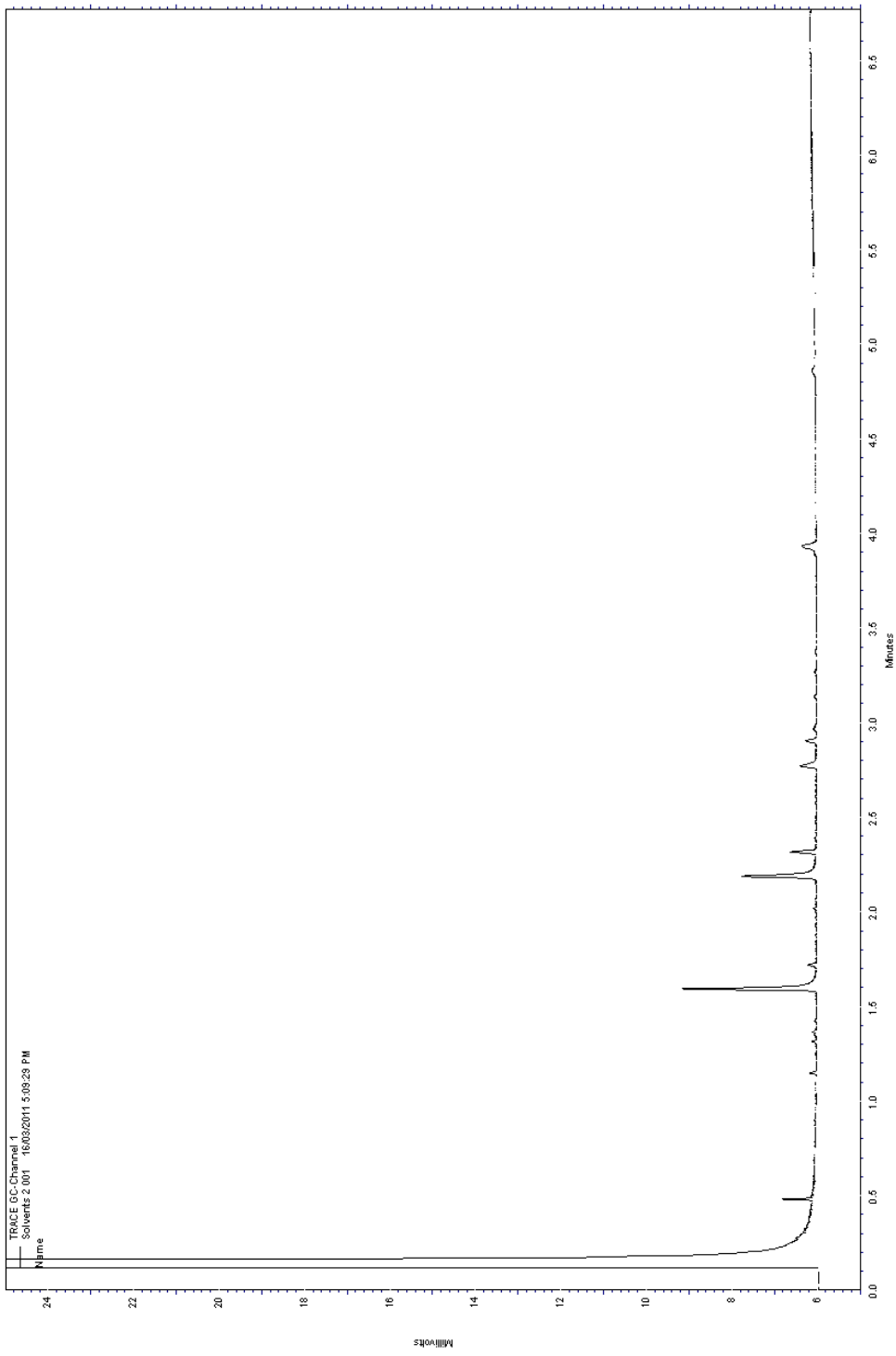


**Figure 2.26 B**. Gas chromatograph of a blank sample with a new kimex tube.

Since, the chromatographs in Figure 2.26 A & B indicate that the glassware was not the contaminating factor, new Teflon caps for the kimex tubes were tested. However, there was no alleviation of contaminating peaks (Figure 2.27). Furthermore, despite cleaning the GC septa and replacing purifier tube for the GC the peak patterns were still evident (data not shown). It was then considered that these peak patterns were unavoidable. Therefore, individual phospholipids and their corresponding blank lanes were scraped from HPTLC plates and were subtracted from each other (Figure 2.28).

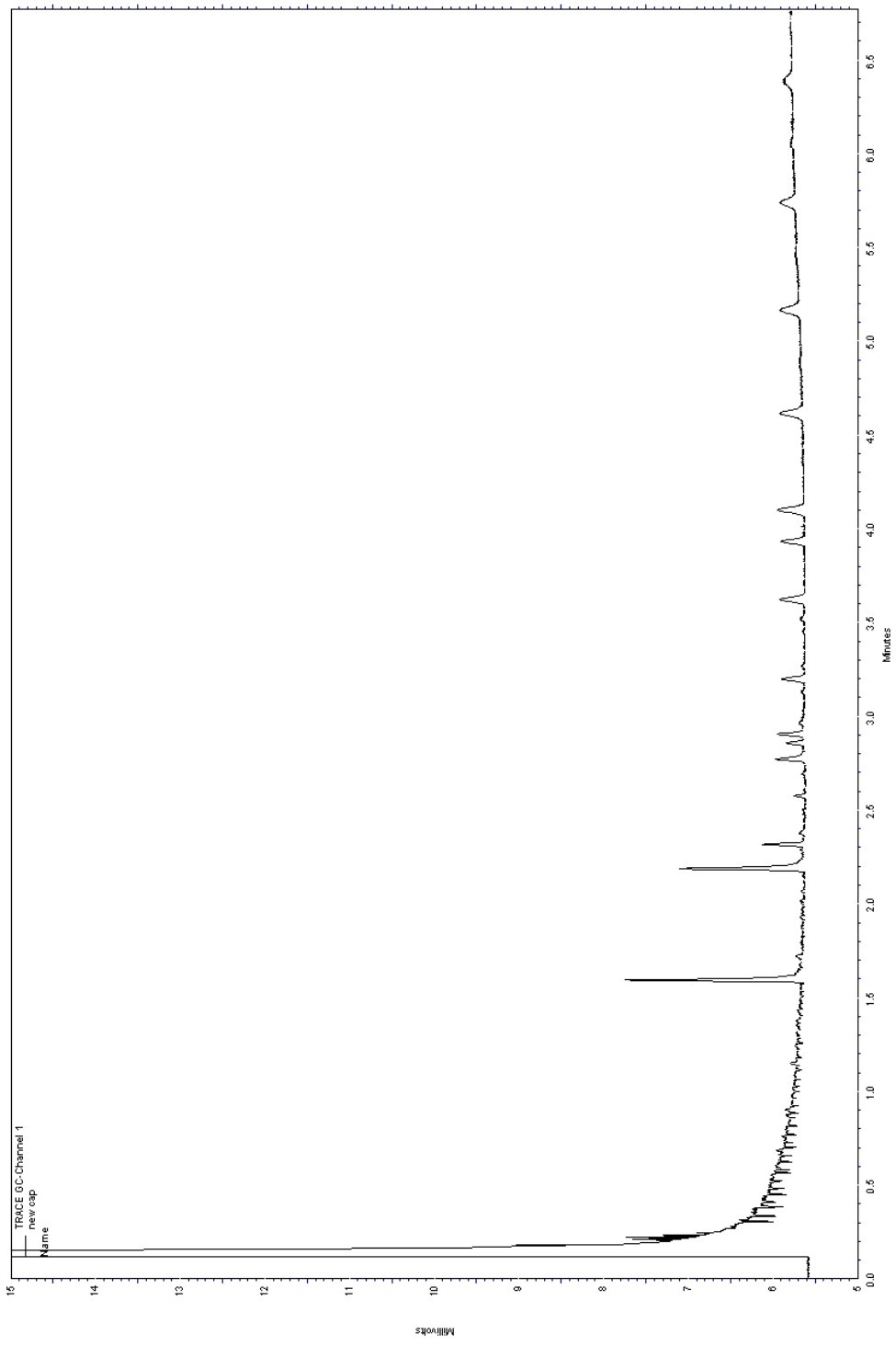


**Figure 2.27**. Gas chromatograph of a blank sample with new Teflon caps.

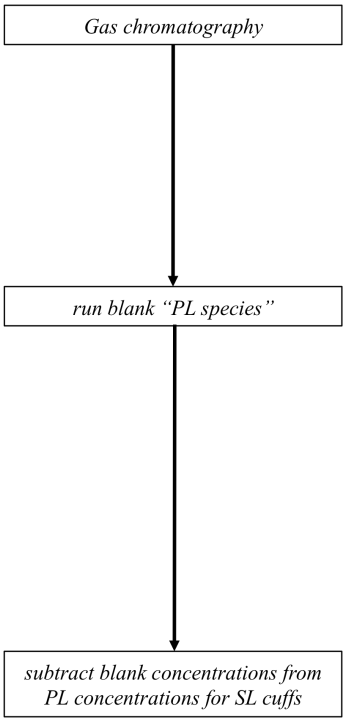


**Figure 2.28**. Diagrammatic flow-chart illustrating the steps for Gas chromatography.

Taken together, there were numerous considerations when developing the method for the lipid analysis of SL cuffs. These considerations were carried out with mini experiments to devise an appropriate protocol for Chapter 3. Figure 2.29 summarizes the included and excluded steps involved for all four areas in the lipid analysis of sarcolemmal cuffs.

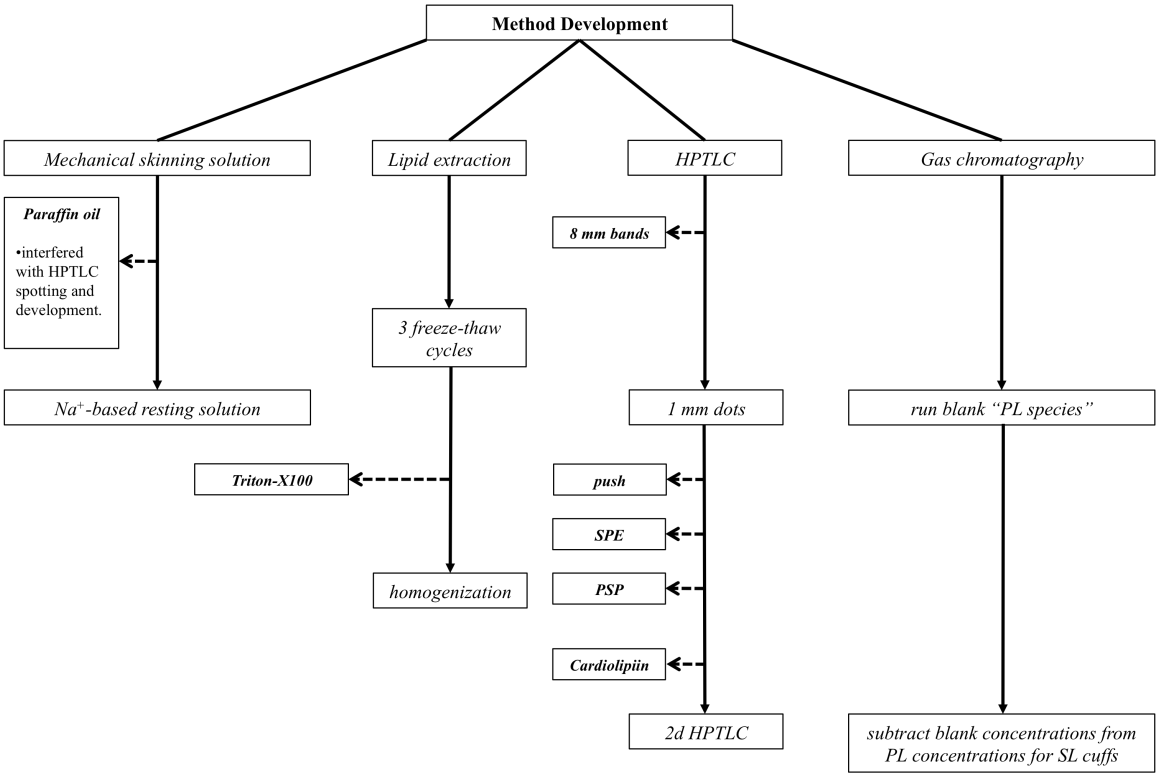


**Figure 2.29**. Diagrammatic flow-chart summarizing the included and excluded steps for all four areas of sarcolemmal cuff lipid analysis. Dashed arrows = excluded.

**References**

Dodds, E. D., McCoy, M. R., Rea, L. D., & Kennish, J. M. (2005). Gas chromatographic quantification of fatty acid methyl esters: flame ionization detection vs. electron impact mass spectrometry. *Lipids, 40*(4), 419-428.

Fiehn, W., Peter, J. B., Mead, J. F., & Gan-Elepano, M. (1971). Lipids and fatty acids of sarcolemma, sarcoplasmic reticulum, and mitochondria from rat skeletal muscle. *J Biol Chem, 246*(18), 5617-5620.

Kupke, I. R., & Zeugner, S. (1978). Quantitative high-performance thin-layer chromatography of lipids in plasma and liver homogenates after direct application of 0.5-microliter samples to the silica-gel layer. *J Chromatogr, 146*(2), 261-271.

Mollica, J. P., Oakhill, J. S., Lamb, G. D., & Murphy, R. M. (2009). Are genuine changes in protein expression being overlooked? Reassessing Western blotting. *Anal Biochem, 386*(2), 270-275.

Morgan, W. A., Nk, T., & Ding, Y. (2008). The use of High Performance Thin-Layer Chromatography to determine the role of membrane lipid composition in bile salt-induced kidney cell damage. *J Pharmacol Toxicol Methods, 57*(1), 70-73.

Murphy, R. M., Mollica, J. P., & Lamb, G. D. (2009). Plasma membrane removal in rat skeletal muscle fibers reveals caveolin-3 hot-spots at the necks of transverse tubules. *Experimental cell research, 315*(6), 1015-1028.

Murphy, R. M., Verburg, E., & Lamb, G. D. (2006). Ca2+ activation of diffusible and bound pools of mu-calpain in rat skeletal muscle. *The Journal of physiology, 576*(Pt 2), 595-612.

Oberkochen, C. Z. (1977). Potential and experience in quantitative "high performance thin-layer chromatography" HPTLC. In I. A. Zlatis, Kaiser, R. E. (Ed.), *HPTLC high performance thin-layer chromatography* (Vol. 9, pp. 147-167): Elseveir Scientific Publishing Company.

Pernet, F., Pelletier, C. J., & Milley, J. (2006). Comparison of three solid-phase extraction methods for fatty acid analysis of lipid fractions in tissues of marine bivalves. *J Chromatogr A, 1137*(2), 127-137.

Ponec, M., Weerheim, A., Lankhorst, P., & Wertz, P. (2003). New acylceramide in native and reconstructed epidermis. *J Invest Dermatol, 120*(4), 581-588.

Ramstedt, B., & Slotte, J. P. (2002). Membrane properties of sphingomyelins. *FEBS Lett, 531*(1), 33-37.

Rissmann, R., Groenink, H. W., Weerheim, A. M., Hoath, S. B., Ponec, M., & Bouwstra, J. A. (2006). New insights into ultrastructure, lipid composition and organization of vernix caseosa. *J Invest Dermatol, 126*(8), 1823-1833.

Stefanyk, L. E., Coverdale, N., Roy, B. D., Peters, S. J., & LeBlanc, P. J. (2010). Skeletal muscle type comparison of subsarcolemmal mitochondrial membrane phospholipid fatty acid composition in rat. *J Membr Biol, 234*(3), 207-215.

Voet, V. (2004). *Biochemistry* (3rd ed.). Pennsylvannia: John Wiley and Sons, Inc.

Weerheim, A. M., Kolb, A. M., Sturk, A., & Nieuwland, R. (2002). Phospholipid composition of cell-derived microparticles determined by one-dimensional high-performance thin-layer chromatography. *Anal Biochem, 302*(2), 191-198.

Yao, J. K., & Rastetter, G. M. (1985). Microanalysis of complex tissue lipids by high-performance thin-layer chromatography. *Anal Biochem, 150*(1), 111-116.

**Chapter 3: Lipid analysis of mechanically skinned sarcolemmal membranes in rodent EDL muscle.**

**Introduction**

The sarcolemma (SL) is generally defined as a three-layer surface membrane, which includes a plasma membrane, situated between a basement membrane and a submembranous cytoskeletal network (Ozawa, et al., 2001; Sanes, 1982). Importantly, membrane lipid composition can influence membrane structure and can correlate with membrane function. The SL membrane is intimately connected with many biological processes, including metabolism and muscle contraction through the action of membrane-spanning proteins, including insulin receptors, GLUT4, and ion channels (Kanzaki, 2006; Lamb, 2009; O. B. Nielsen & de Paoli, 2007). The role of SL in metabolism and contraction has been well established and has generated interest in the relationship between SL membrane structure and protein function.

Most studies examining the relationship between membrane lipid composition and protein function have been restricted to whole muscle (Abbott, et al., 2010; Andersson, et al., 1998; Blackard, et al., 1997; Pan, et al., 1995). A whole muscle perspective may indeed be inappropriate considering that the SL has biological functions unique from other skeletal muscle subcellular organelles and thus, may potentially have its own specific membrane lipid composition (Fiehn, et al., 1971; Lau, et al., 1979; Rosemblatt, et al., 1981; Stefanyk, et al., 2008). However, studies that have assessed SL lipid composition are limited because of two factors. Firstly, most studies assessing SL lipid composition are incomplete as they only provide data on PL specie distribution and neglect the FA composition of individual PL species (Lau, et al., 1979; Rosemblatt, et al., 1981; Smith & Appel, 1977; Sumnicht & Sabbadini, 1982). Secondly, their isolation protocols have shown to be contaminated with t-tubules, sarcoplasmic reticulum, and

nuclei (Dombrowski, et al., 1996; Fiehn, et al., 1971; Liu, et al., 1994; Ohlendieck, et al., 1991; Smith & Appel, 1977; Sumnicht & Sabbadini, 1982; Zorzano & Camps, 2006; Stefanyk, 2008). The latter limitation may be due to the utilization of aggressive isolation protocols high in mechanical and chemical manipulation.

It is evident that in order to possess a clear understanding of the effect of SL membrane lipid composition on membrane function and vice versa, a microscopic manipulative isolation protocol that minimizes subcellular contamination is needed. Mechanically skinning fibres of their SL has been used for decades leading to discoveries in skeletal muscle excitation-contraction coupling/uncoupling processes and SR properties (Lamb, et al., 1994; Lamb & Stephenson, 1990a, 1990b; Posterino, et al., 2000). Furthermore, studies using immunohistochemistry revealed that SL non membrane-spanning markers, dystrophin; localized to the submembranous cytoskeletal network and laminin; localized to the basal lamina, were only detected in the skinned sarcolemmal membranes (Rybakova, et al., 2000; Murphy, et al., 2009). Importantly, previous isolation protocols have failed to achieve this same result whereby dystrophin was detected by Western blotting in t-tubule membrane fractions and other intracellular membrane fractions (Ohlendieck, et al., 1991; Zorzano & Camps, 2006). And, because the mechanical skinning approach involves mechanically skinning single fibre segments, it may be considered more meticulous than previous protocols which process whole muscles through steps including homogenization, differential centrifugation and membrane purification. Herein lies the novelty of the present study, whereby to date; there have been no studies assessing the potential use of this preparation for subsequent lipid composition analysis. Thus, the purpose of this study was to assess the validity of

the mechanical skinning technique as an alternative method for SL lipid analysis inclusive of both PL and FA composition. It is hypothesized that SL membranes isolated with the mechanical skinning technique 1) will provide sufficient membranes for lipid compositional data inclusive of both PL and FA and 2) will have minimized subcellular contamination.

## Methods

### *Animals*

Eight male Long Evans rats (324.8 ± 25.4 g) used in this study were housed in an environment maintained at 22±1°C with a 12:12 hour light (6:00am to 6:00pm)-dark (6:00pm to 6:00am) cycle. Rats had free access to water and a generic rodent chow diet (27% protein, 11% fat, 63% carbohydrate; 5012 Rat Diet, Lab Diet, Oakville, Ontario) ad libitum.

### *Specimen Collection*

Rodents were anaesthetized through an intraperitoneal injection of sodium pentobarbital (6mg/100g body weight). Extensor digitorum longus (EDL; 4% type I, 20% type IIa, 38% type IId/x, 38% type IIb) (Delp & Duan, 1996) from one hind limb was removed and cleaned of any visible fat, nerves and fasciae and prepped for mechanically skinning fibre protocol. The animals were killed by excision of the heart.

#### *Mechanical skinning of fibres*

Sarcolemmal membranes were skinned from individual fibre segments (~ 2 - 5 mm long, 40 – 60 μm in diameter) as previously described by Murphy et al. (2006) using

a dissecting microscope (Nikon SMZ645 coupled with Nikon 3002752 objective and Nikon C-W10 x A/22 eyepiece) and forceps. In brief, EDL muscles were placed into a petri dish containing a Sylgard layer (Sylgard 184, DOW Corning) topped with a $Na^+$-based resting solution ( 90 mM HEPES, 50 mM EGTA, 10.3 mM MgO, 8 mM ATP, 10 mM creatine phosphate, pH 7.1 with 4 M NaOH, ~295 mOsmoles). Muscle fibre bundles either centrally or laterally localized were randomly chosen and pulled away from the muscle belly and ~1 – 4 single fibre segments per bundle were teased out from them, measured in length, and skinned under 20x magnification with the use of microdissecting forceps (Inox 5, Fine Science Tools, Canada). The diameters of single fibre segments were measured at 40X magnification with a Nikon Crossline reticle (25 mm scale: 10 mm/100 divisions). At the same magnification, SL cuff and skinned fibre were collected with black silk sutures (USP 4.0) and pools of 10 cuffs and 10 skinned fibres were stored separately in 20 μL Buffer A (10 mM $NaHCO_3$, 5 mM $NaN_3$, 100 μm PMSF and 0.25 M sucrose) at -80°C until further lipid or Western blot analysis. In general, 20 – 30 fibres were skinned per EDL muscle fibre per animal.

***Allocation of skinned fibres and cuffs***

In general, 20 – 30 fibres were skinned per EDL muscle fibre per animal. Of the total 8 male Long Evans used in this study, 4 were used for lipid analysis, 2 were used for Western blot analysis, and 2 were used for both lipid and Western blot analysis (Figure 3.1 A, B).

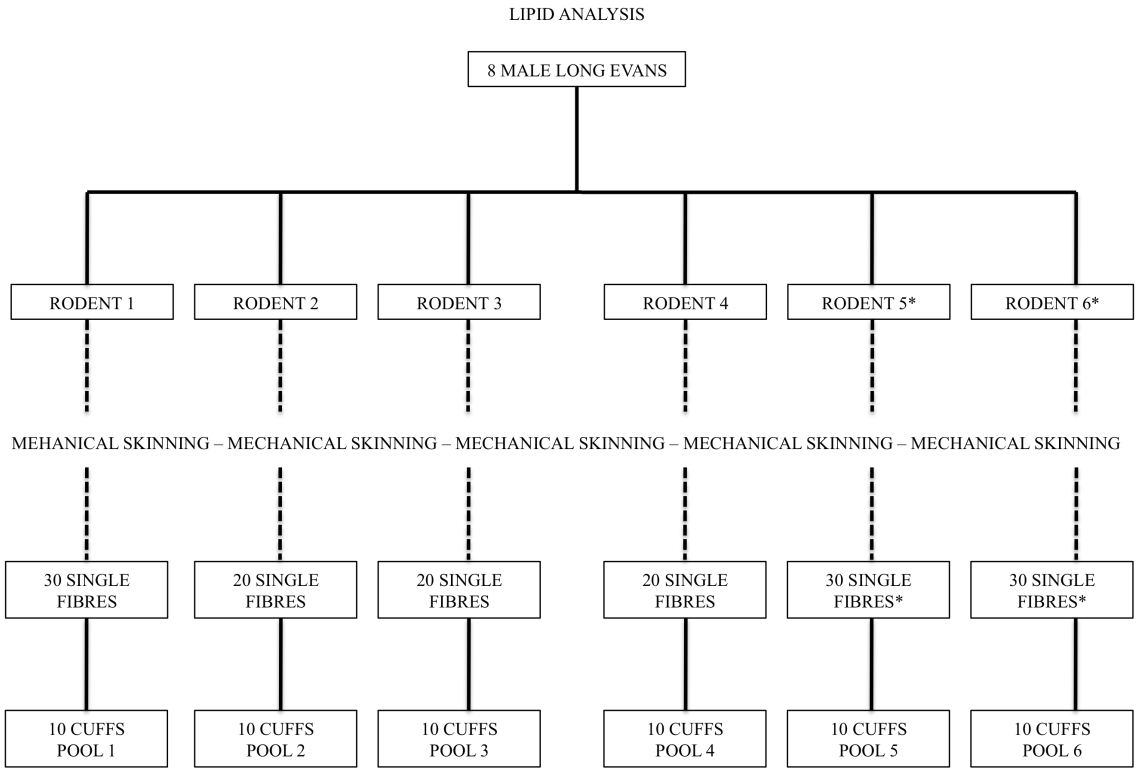


**Figure 3.1 A .** Flow-chart diagrammatic representation illustrating the collection of 10 cuff pools from 6 of total 8 rodents used for lipid analysis. *Used for both lipid and Western blot analysis.

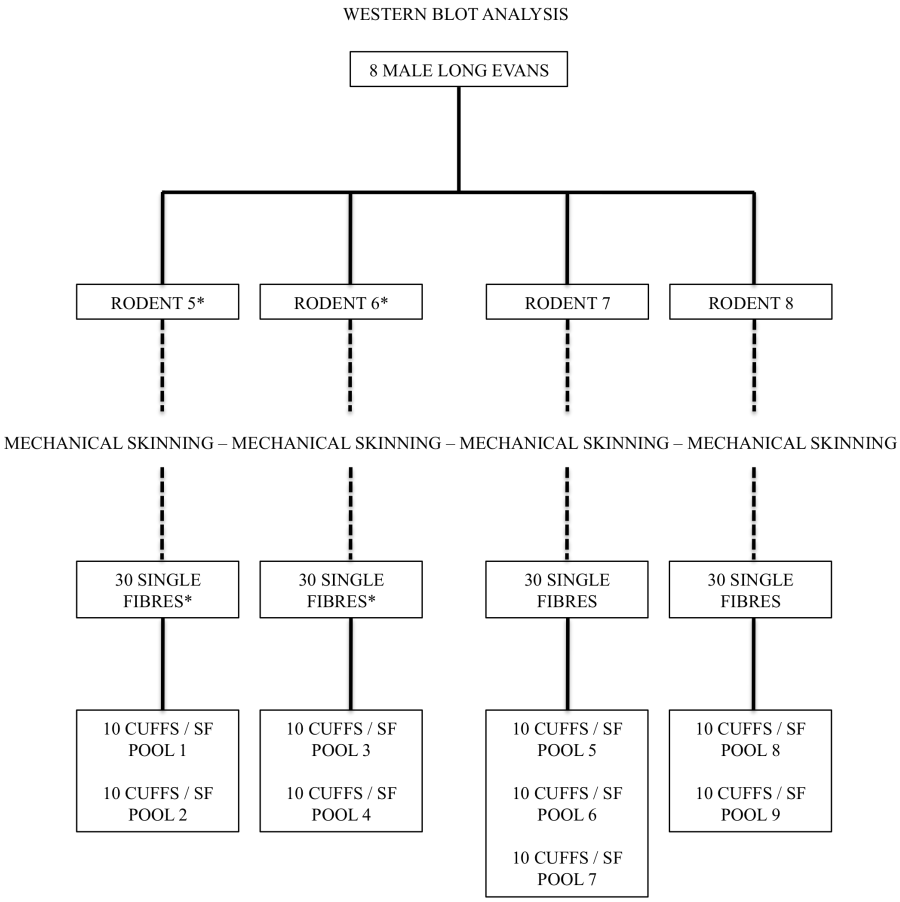


**Figure 3.1 B**. Flow-chart diagrammatic representation illustrating the collection of 10 cuff pools from 4 of total 8 rodents used for Western blot analysis. SF, skinned fibres. *Used for both Western blot and lipid analysis.

Excess single fibres that were not used for Western blot and lipid analysis, were used prior to data collection for method development.

### *High-sensitivity Western Blot Analysis*

*Contamination & SL presence*

High-sensitivity Western blot analysis (Murphy et al., 2009) was performed to determine t-tubule, sarcoplasmic reticulum, mitochondria (outer and inner membrane) and nuclear membrane contamination of SL. This was achieved through the use of

antibodies raised against membrane specific proteins dihydropyridine receptor (CaV 1.1; Abcam, ab2862) for t-tubule; sarco(endo)plasmic reticulum $Ca^{2+}$-ATPase 1 and 2 (SERCA1; Affinity BioReagents MA3-911 & SERCA 2; Abcam, ab2861 ) for sarcoplasmic reticulum; emerin (Abcam, ab40688) for nucleus; MitoNEET (Proteintech Group, 16006-1-AP) for outer mitochondrial membranes; and COX IV subunit 4 (MitoSciences, MS407) for inner mitochondrial membranes. All antibodies were probed with either mouse (CaV 1.1, SERCA 1, SERCA 2, COX IV) or rabbit (emerin, MitoNEET) secondaries conjugated to HRP, and were treated with Luminata™ Forte Western HRP Substrate (Millipore, MA, USA). Since SERCA 2 is only expected in type I rat muscle fibres (Germinario, et al., 2002; Wu & Lytton, 1993), 7.5 μg of soleus protein was loaded as a positive control when SERCA 2 was probed for EDL SL cuffs and skinned fibres.

Ten μl of 3x solubilising/loading buffer (1 M Tris base [pH 6.8], 6% [w/v] SDS, 30% glycerol [v/v], 15% [v/v] 2-mercaptoethanol, and 0.06% [w/v] bromophenol blue) was added to the separate pools of 10 isolated SL cuffs and their 10 respective skinned fibres, each of which were originally contained in 20 μl of Buffer A. This resulted in a total volume of 30 μl and a final concentration of either 1 cuff/ 3 μl or 1 skinned fibre/3 μl. The sample underwent 3 freeze-thaw cycles to release membrane proteins since preliminary data showed that without this protocol, proteins from SL cuffs were undetected (data not shown). Due to the low volume used to store the SL cuffs and skinned fibres (each in 20 μl Buffer A), there was no determination of protein concentration prior to Western blot analysis. Alternatively, protein was loaded as equivalents of 1 cuff or skinned fibre. For example, 1 cuff or skinned fibre equivalent, is

1 cuff or skinned fibre worth of protein. Through loading a gradient for both the skinned fibres and cuffs on the same gel (¼ cuff or skinned fibre (0.75 µl) to 4 cuffs or skinned fibres (12 µl) equivalents), contamination was assessed while also determining the lowest level of detection for the protein of interest. In similar manner, to confirm presence of sarcolemma in the SL cuffs, a common SL membrane-spanning marker was used, β-dystroglycan (Abcam, ab4951, mouse monoclonal) (Cluchague, et al., 2004; Sotgia, et al., 2003). Furthermore, due to the intricate nature of the mechanical skinning technique, a muscle specific caveolar region marker, caveolin-3 (BD Transduction Laboratories, 610420, mouse monoclonal) was probed in order to estimate and compare distributions between cuffs and skinned fibres with that of a previous study using the same mechanical skinning approach (Murphy, et al., 2009). Standard SDS-PAGE electrophoresis was performed as previously described (Leblanc, et al., 2007) with the use of a separating gel made with 2.5 mL of 14% overlayed with 1 mL of 10% and topped with 4% stacking gel. Alongside the samples, 10 µL of a molecular weight standard was present (BioRad Precision Plus Kaleidescope Molecular Weight Marker, CA, USA). Electrophoretically separated proteins were transferred onto polyvinylidene difluoride (PVDF) transfer membranes (Immobilon, Millipore, MA, USA) with transfer buffer (0.05% SDS, 25 mM glycine, 192 mM Tris base, 20% methanol). Membranes were treated with MemCode$^{TM}$ reversible protein stain, to confirm presence of proteins before being incubated in blocking solution (TBST buffer: 20mM Tris base, 137 mM NaCl, and 0.1% (v/v) tween 20, pH 7.5) with 5% (w/v) non-fat dry milk) for 1 hour to block all non-specific binding sites. To maximize data obtained from one set of cuffs and skinned fibres, membranes were cut into three strips consisting of proteins between 1) 75 – 250 kDa which were

probed for either DHPR, SERCA 1 or 2, 2) 25 – 75 kDa that were probed for either β-dystroglycan or emerin, and 3) 10 – 25 kDa which were probed for either caveolin-3, COX IV subunit 4 or MitoNEET. All primary antibodies were incubated overnight in blocking solution. The membranes were then washed (3 times for 5 minutes with TBST buffer) and set to incubate for 1 hour in blocking solution containing an HRP-conjugated secondary antibody. Membranes were washed (3 times for 5 minutes with TBST buffer), treated with Luminata™ Forte Western HRP Substrate (Millipore, MA, USA) for 2 minutes, developed using the FluroChem imaging system (Alpha-Innotec, CA, USA), and quantified using Image J software (National Institutes of Health, MD, USA) (Appendix I, Part iii).

*Laminin distribution in SL cuff and skinned fibres*

To assess the laminin distribution in SL cuffs and skinned fibre equivalents, one EDL from a Long Evans rat was used with approval of the La Trobe University Animal Ethics Committee, Melbourne,, Australia. Six single fibre segments were skinned and the resulting cuffs and skinned fibre segments were placed in separate tubes containing 30 µl of solubulising/loading buffer (0.125 M Tris-Cl [pH 6.8], 4% [w/v] SDS, 10% glycerol, 4M urea, 10% [v/v] mercaptoethanol, and 0.001% [v/v] bromophenol blue and stored at -20°C for Western blotting.

Western blotting of the cuffs and skinned fibre equivalents were done as adapted from Molica et al., (2009). Briefly, a gradient of cuff (2 – 4) and skinned fibre (3/32 – 3) equivalents were loaded and proteins were separated for 60 min at 200 V on a 10% SDS-PAGE gel. Proteins in the gel were transferred onto a PVDF membrane with transfer buffer (140 mM glycine, 37 mM Tris base, and 20% [v/v] methanol) for 60 min at 100 V. Membranes were then incubated in blocking solution (TBST buffer: 20 mM Tris base,

137 mM NaCl, and 0.1% [v/v] tween 20, pH 7.5 with 5% (w/v) non-fat dry milk) for 1 hour. The membrane was then probed for laminin overnight, and then incubated with rabbit secondary antibody conjugated with HRP for 1 hour. The membrane was then treated with SuperSignal West Femto HRP substrate (Thermo Scientific). Images were collected using a CCD camera attached to a ChemiDoc XRS (Bio-Rad, USA) and using Quantity One software (Bio-Rad) (Figure A2.9).

***Lipid Analysis***

*Lipid Extraction*

Lipids were extracted from SL cuffs as previously described (Bligh & Dyer, 1959). Briefly, a pool of 10 SL cuffs underwent 3 freeze-thaw cycles and was homogenized in eppendorf tubes. The 10 cuffs were then placed into a 15 ml kimex tube with 750µl of double distilled water (DDW). Samples were vortexed for 2 minutes with 3.75 ml of chloroform:methanol (1:2) supplemented with 0.1% antioxidant, butylated hydroxytoluene (BHT). Samples were then vortexed with an additional 1.25 ml of chloroform. Double distilled water was subsequently added (1.25 ml), and the sample mixture was spun at 720g for 6 minutes. Lipids were then extracted by collecting the chloroform phase, and stored at - 20°C until further analysis.

*High Performance Thin Layer Chromatography*

Two-dimensional HPTLC was used to move and prevent cholesterol, free fatty acid, triglyceride, and cholesterol ester interference in the separation of individual PL species (PC, PE, PA, PI, PS, and SM) from lipid extracts. The composition of cholesterol, free fatty acid, triglyceride, and cholesterol ester was not measured in this study. Prior to

spotting, lipid extracts were dried under nitrogen and then resuspended in 20 μl of chloroform:methanol (2:1). The sample was then spotted (~1mm dots) on pre-baked (10 min at 130°C) HPTLC plate (60 Å) and placed in a chamber containing a solvent system for separation of neutral lipids (hexane: diethyl ether: acetic acid, 80:20:1.5 (Kupke & Zeugner, 1978)) for 35 minutes. The plate was then removed and placed in an oven at 130°C to remove excess acetic acid. After, the plate was rotated 90°, and a blank lane of 20 μl of chloroform:methanol (2:1) and phospholipid standards were spotted and the plate was then placed in a solvent system for separation of phospholipid species (chloroform: ethyl acetate: isopropanol: acetone: ethanol: methanol: water: acetic acid, 60: 12: 12: 12: 32: 56: 12: 4 (Weerheim, et al., 2002)) for approximately 20 min (solvent front travel distance: 5.5 cm). After, the plate was removed and dried before spraying with dichlorofluoroscein (DCF) solution (methanol:water 1:1, and 2',7' –DCF filtered and washed with petroleum ether) and set in a chamber containing 25% ammonium hydroxide for ~5 minutes to develop. The plate was viewed under ultraviolet light and the bands marked (from solvent front, PE, PI, PS, PC, SM) and scraped into individual 15 ml kimex culture tubes. For each HPTLC plate, a set of blank phospholipids was collected using a lane without any sample loaded and the phospholipid standards as reference. CL was omitted from analysis due to difficulties in migration towards a potential contaminating artefact (see Chapter 2.0, Figure 2.20). Importantly, the separation of phospholipids using 2D HPTLC for the purposes of a representative image required the destruction of the lipid species via charring method, which prevented further FA analysis. Furthermore, the images obtained from the charred HPTLC plates were not visually sufficient (see Chapter 2.0, Figure 2.20). Since there were a limited number of SL cuffs

achieved per EDL muscle, lipid extract from red gastrocnemius whole homogenate underwent 2D HPTLC plate development strictly to clearly illustrate the two-dimensional process (Figure 3.2).

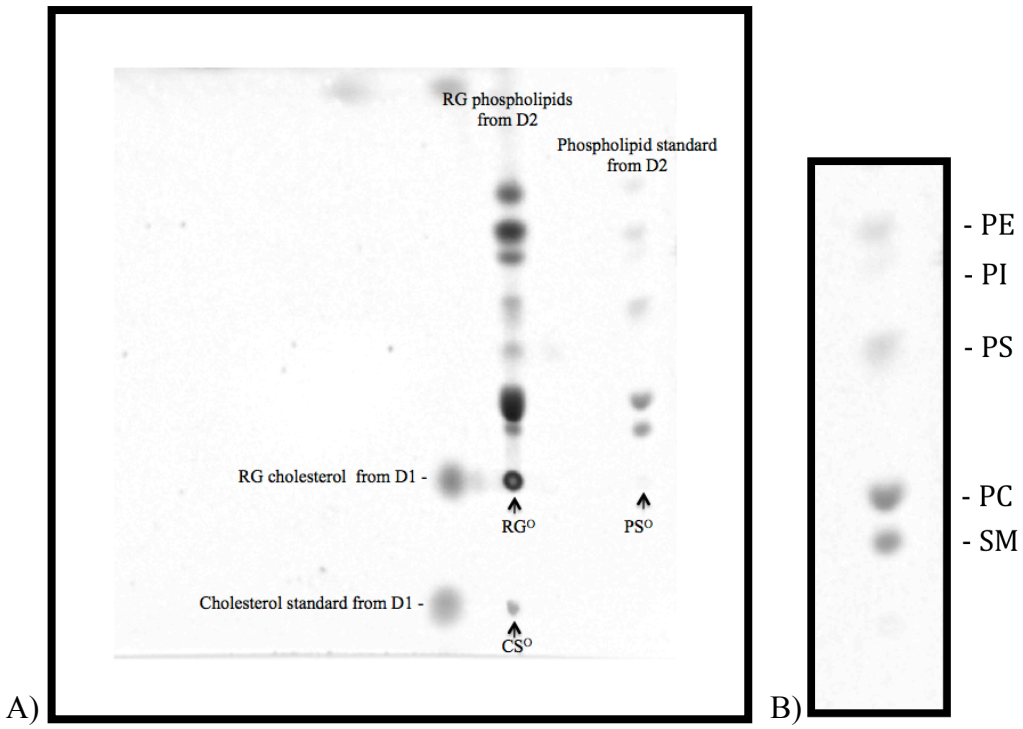


**Figure 3. 2**. Representative 2D HPTLC plate illustrating typical migration of lipids. A) Lipid extract from red gastrocnemius (RG) whole homogenate was spotted along with a cholesterol standard on an HPTLC plate and developed first in a tank saturated with hexane: diethyl ether: acetic acid (80:20:1.5) for 35 minutes (Kupke & Zeugner, 1978) (D1). After, the phospholipid standard was spotted, and the plate was rotated clockwise 90° and developed in a tank saturated with chloroform: ethyl acetate: isopropanol: acetone: ethanol: methanol: water: acetic acid (60: 12: 12: 12: 32: 56: 12: 4) until solvent front reached 5.5 cm migration (D2) (Weerheim, et al., 2002). B) Magnified inset illustrating typical migration of the phospholipid species in the phospholipid standard. $CS^{O}$, cholesterol standard spot of origin; $RG^{O}$, red gastrocnemius lipids spot of origin; $PS^{O}$, phospholipid standard spot of origin. PE, phosphatidylethanolamine; PI, phosphatidylinositol; PS, phosphatidylserine; PC, phosphatidylcholine; SM, sphingomyelin.

*Methylation*

The scrapings of the different PLs and their corresponding blanks were methylated as per Mahadevappa & Holub (1987). Briefly, 6% $H_2SO_4$ was added to each tube with 10 μg of internal standard (tridecanoic acid; 13:0) and incubated at 80°C for 2 hours. After cooling for 10 min and addition of 1mL of water and 2mL of petroleum ether, the samples were vortexed and centrifugation for 6 minutes at 720g. The top phase, consisting of newly formed fatty acid methyl esters (FAME) were extracted and put into microvials (Fisher Scientific, CA), dried down under nitrogen and resuspended in 12 μL hexane for analysis by gas chromatography.

*Gas Chromatography*

The FA composition of each PL were analyzed by gas chromatography (GC; (Bradley, et al., 2008) and FA subclasses (SFA, MUFA, PUFA) were subsequently analyzed. A 5.0 μl sample of methyl esters from each sample were injected into a GC (Trace GC Ultra, Thermo Electron Corp, Milan, Italy) fitted with a split/splitless injector, a fast flame ionization detector (FFID), and Triplus AS autosampler (Trace GC Ultra, Thermo Electron Corp, Milan, Italy). FA methyl esters were separated on an UFM RTX-WAX analytical column (Trace GC Ultra, Thermo Electron Corp, Milan, Italy) using helium as a carrier gas. FAs were identified by comparison of retention times with those of a known standard solution (Supelco 37 component FAME mix, Supelco, Bellefonte, PA, USA). The areas of each individual peak were converted to concentrations with the aid of the internal standard, tridecanoic acid (13:0). It has been previously established

that there are no endogenous 13:0 in samples previously analyzed (Stefanyk, 2008). FA composition was adjusted by subtracting their respective blanks.

*Statistics and calculations*

All values are expressed as the mean ± standard error (SE). The sum of the values for spot densitometry analysis for cuff and skinned fibre equivalents detected with Western blotting were considered as total as long as both were in linear range. For example, if 1 cuff equivalent and 1 skinned fibre equivalent were both in the linear range for a given protein of interest, the spot densitometric value of 1 cuff equivalent was added to spot densitometric value of 1 skinned fibre equivalent and was considered as total. Since this study involved extensive method development, it did not require any direct comparisons, and as such, no statistical tests were done.

**Results**

Sarcolemmal cuffs

*Single fibre characteristics*

Six sets of 10 single fibres skinned from each EDL (Figure 3.1 A) was used for lipid analysis. The single fibres skinned for lipid analysis were 2.89 ± 0.11 mm in length, and 52.80 ± 0.79 μm in diameter (Appendix 3 Table A3.1). For Western blot analysis, nine sets of 10 single fibres skinned from EDL muscle were used (Figure 3.1 B). The single fibres skinned for Western blot analysis were 2.61 ± 0.09 mm in length, and 50.75 ± 0.26 μm in diameter (Appendix 3 Table A3.2).

High-Sensitivity Western Blot analysis

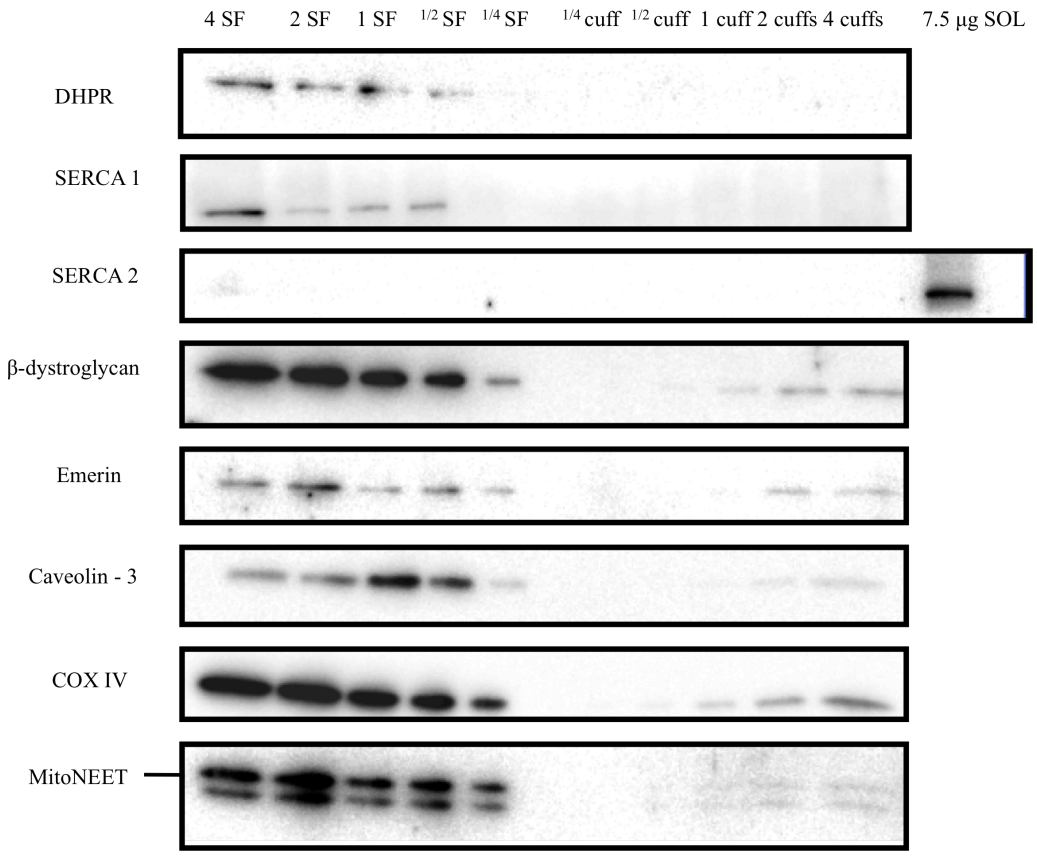


**Figure 3. 3**. Representative Western blots performed on skinned fibre equivalents and sarcolemmal cuffs probing for various subcellular membrane markers. Transverse-tubules, DHPR (n=3); sarcoplasmic reticulum, SERCA1 (n=3) & SERCA2 (n=3); sarcolemma, β-dystroglycan (n=3); nucleus, emerin (n=2); outer mitochondria, mitoNEET (n=3); inner mitochondria, COX IV (n=3); caveolar, caveolin-3 (n=3). SF, skinned fibre equivalent (worth of protein); cuff, sarcolemmal cuff equivalent; SOL, soleus muscle protein.

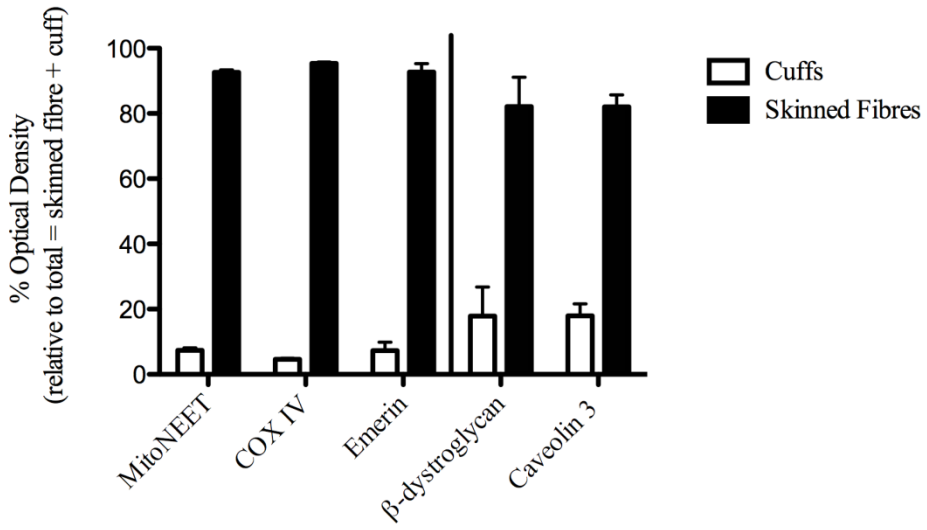


**Figure 3. 4**. Relative amounts of membrane specific markers (outer mitochondria - mitoNEET; inner mitochondria - COX IV; nuclear – emerin; sarcolemma – β-dystroglycan; caveolar – caveolin -3) in sarcolemmal cuffs and skinned fibres. Proteins expected to be found within sarcolemma are located on the right side of the x-axis (β-dystroglycan and caveolin-3).

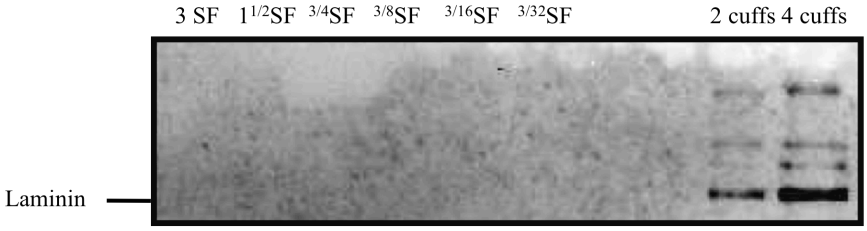


**Figure 3. 5**. Representative Western blot performed on skinned fibre equivalents and sarcolemmal cuffs probing for the non-membrane spanning sarcolemmal marker, laminin (n=1). SF, skinned fibre equivalent (worth of protein).

High-sensitivity Western blot analysis revealed that both the sarcolemmal marker β-dystroglycan and the caveolar marker caveolin-3 were both present in the cuffs (~20% of total for β-dystroglycan and caveolin-3). Interestingly, both proteins were also highly

detected in the skinned fibres (~80% of total for β-dystroglycan and caveolin-3; Figure 3.3, Figure 3.4). Sarcoplasmic reticulum marker SERCA 1 was detected in as low as ¼ skinned fibre equivalent but not detected in as high as 4 cuff equivalents. In contrast, SERCA 2, an isoform only present in rat type I fibres (Germinario, et al., 2002; Wu & Lytton, 1993), was not detected in either 4 equivalents of skinned fibres or cuffs despite positive detection in 7.5 μg of soleus protein (Figure 3.3). Similar to SERCA 1, t-tubule marker, DHPR, was detected in as low as ½ skinned fibre equivalent but not detected in as high as 4 cuff equivalents (Figure 3.3). However, nuclear membrane marker emerin was present in both skinned fibres and cuffs with detection as low as ¼ skinned fibre and 1 cuff equivalent, respectively. Relative to total, the sarcolemmal cuffs had ~7% of emerin (Figure 3.4). Mitochondrial membrane markers, COX IV and mitoNEET, were also detected in both skinned fibres and cuffs with detection as low as ¼ skinned fibre and ½ cuff equivalent, respectively for COX IV, and ¼ skinned fibre and 1 cuff equivalent, respectively for mitoNEET. Relative to total, the sarcolemmal cuffs had ~5% of COX IV and 7% of mitoNEET (Figure 3.4). Figure 3.5 reveals that laminin was only detected in the cuff equivalents, and was not detected in as high as 3 skinned fibre equivalents. Table 3.1 summarizes subcellular contamination seen in rat SL cuffs and rat SL membrane fractions obtained through traditional isolation methods.

**Table 3. 1**. Summary of subcellular contamination in rat sarcolemmal cuffs from the mechanical skinning approach and rat sarcolemmal membrane fractions obtained by homogenization + differential centrifugation.

| Subcellular membrane | Sarcolemmal cuff | Sarcolemmal fraction |
|---|---|---|
| t-tubules | not detected using DHPR | detected using DHPR[1,2,3] |
| sarcoplasmic reticulum | not detected using SERCA 1 & 2 | detected using SERCA[1] |
| outer mitochondria | detected using mitoNEET | not assessed |
| inner mitochondria | detected using COX IV | not detected using ANT[3] |
| nucleus | detected using emerin | detected using emerin[3] |

[1](Dombrowski et al., 1996), [2](Zorzano & Camps, 2006), [3](Stefanyk, 2008). DHPR, dihydropiridine receptors; SERCA, sarco(endo)plasmic $Ca^{2+}$-ATPase; COX IV, cytochrome c oxidase subunit 4; ANT, adenosine nucleotide translocase.

For the collection of SL membrane fractions one study started with 8-10 g of hindlimb musle from male Sprague-Dawley rats (300 – 350 g) (Dombrowski et al., 1996). Another study started with 12 g of skeletal muscle tissue from the gastrocnemius and quadriceps muscles of male Wistar rats (~250 g) (Zorzano & Camps, 2006). The last study started with 1.7 – 2.1 g of lower hind limb muscles from male Long Evans rats (337.5 ± 7.6g) (Stefanyk, 2008).

*Presentation of lipid data*

Studies analyzing SL membrane lipid composition have traditionally used percent mole fraction units. When converting the results from percent ng/mm$^2$ fraction units to percent mole fraction, the trends (phospholipid species and fatty acid composition) remained constant (Appendix 3 Figures A3.1 & A3.2, Table A3.2).

*Phospholipid species composition*

Five major phospholipids were identified (PC, SM, PE, PI, and PS). Lipid analysis from sarcolemmal cuffs indicated that the membrane is comprised of 26.5 ± 1.3 % PC, 23.8 ± 3.2 % SM, 21.9 ± 2.1 % PE, 15.5 ± 1.9 % PI, and 12.4 ± 1.6 % PS (Figure 3.6). These findings are similar to a previous study with the exception of higher SM (~10%) and lower PC (~5%) (Fiehn, et al., 1971; Stefanyk, et al., 2008).

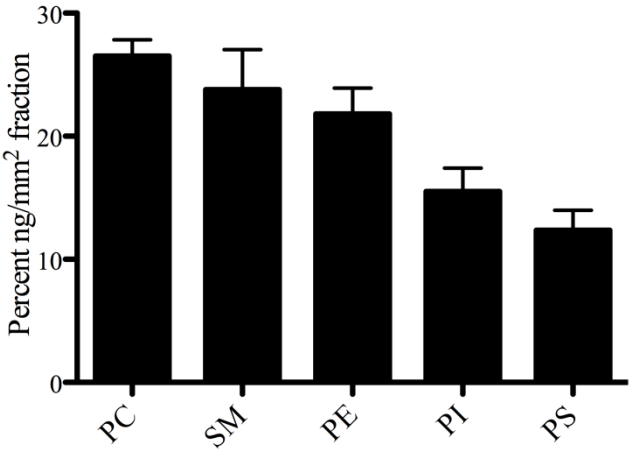


**Figure 3. 6**. Percent ng/mm$^2$ fraction of major phospholipid species of sarcolemmal membranes from extensor digitorum longus (EDL) skinned fibres. Values are represented as means ± standard error (n=6). PC, phosphatidylcholine; SM, sphingomyelin; PE, phosphatidylethanolamine; PI, phosphatidylinositol; PS, phosphatidylserine.

*Phospholipid fatty acid composition*

Four major FA subclasses were classified (SFA, MUFA, n3 PUFA, and n6 PUFA) and unsaturation index (UI) was calculated independent of individual phospholipid species (Figure 3.7). SFA was highest in proportion (58%) followed by

MUFA (26%) and n6 and n3 PUFA (11% and 5%, respectively). The UI was found to be 71 and along with the FA subclass hierarchy were both similar to findings from a previous study (Stefanyk, 2008).

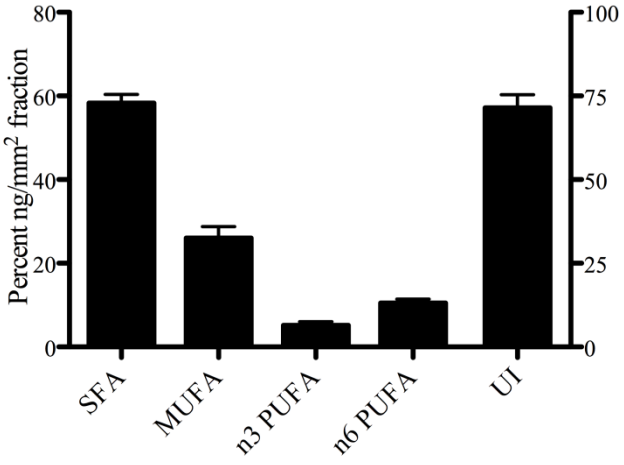


**Figure 3. 7**. Percent ng/mm$^2$ fraction of total fatty acid subclasses independent of phospholipid species of sarcolemmal membranes from EDL skinned fibres. Values are represented as means ± standard error with SFA, MUFA, n3, and n6 represented on the left *y*-axis and UI represented on the right (n=6). SFA, saturated fatty acids; MUFA, monounsaturated fatty acids; n3, n3 polyunsaturated fatty acids; n6, n6 polyunsaturated fatty acids; UI, unsaturation index = $\sum m_i$ x $n_i$, where $m_i$ is the ng/mm$^2$ fraction percentage and $n_i$ is the number of carbon–carbon double bonds of the fatty acid.

Fatty acid composition of individual phospholipid species revealed that the FA subclass hierarchy (SFA>MUFA>n6 PUFA>n3 PUFA) existed across all phospholipid species (Table 3.2, Figure 3.8). Furthermore, 16:0 and 18:0 were the major fatty acids for PC (27% and 15%, respectively), SM (26% and 23%, respectively), PE (20% and 15%, respectively) and PS (32% and 18%, respectively) (Table 3.2, Figure 3.8). In contrast, 18:0 was the primary major fatty acid for PI (38.3%) followed by 16:0 (18%) (Table 3.2). For the MUFA subclass 16:1 and 18:1 was the most dominant specie across all PL

species (Figure 3.8). The UI of the major phospholipid species in sarcolemmal cuffs were PE (100) > PC (74) > PS (59) > PI (57) and SM (51) (Table 3.2).

**Table 3. 2**. Percentage ng/mm$^2$ fraction of phospholipid species of sarcolemmal membranes from EDL skinned fibres (n=6).

| Fatty acid subclasses | Phosphatidylcholine | Sphingomyelin | Phosphatidylethanolamine | Phosphatidylinositol | Phosphatidylserine |
|---|---|---|---|---|---|
| 12:0 | 1.8 ± 0.7 | 2.4 ± 0.8 | 2.6 ± 1.3 | 1.8 ± 1.2 | 0.5 ± 0.3 |
| 14:0 | 1.6 ± 0.5 | 1.3 ± 0.7 | 1.7 ± 0.7 | 2.7 ± 1.6 | 1.6 ± 0.9 |
| 15:0 | 3.1 ± 1.0 | 5.8 ± 2.2 | 3.8 ± 0.8 | 0.5 ± 0.3 | 1.3 ± 1.0 |
| 16:0 | 27.2 ± 2.9 | 25.8 ± 3.7 | 19.2 ± 4.0 | 17.9 ± 4.9 | 31.9 ± 6.2 |
| 17:0 | 1.4 ± 0.7 | 2.3 ± 1.1 | 2.9 ± 0.7 | 0.8 ± 0.8 | 1.4 ± 1.1 |
| 18:0 | 14.5 ± 3.2 | 22.6 ± 6.3 | 14.9 ± 5.2 | 38.3 ± 10.1 | 17.5 ± 7.2 |
| 20:0 | 2.7 ± 0.5 | 4.6 ± 3.4 | 0.9 ± 0.6 | 0.5 ± 0.4 | 2.5 ± 2.4 |
| 22:0 | 0.4 ± 0.3 | 1.2 ± 0.5 | 1.4 ± 0.8 | 2.7 ± 1.3 | 1.2 ± 0.5 |
| 23:0 | 1.5 ± 0.9 | 0.1 ± 0.1 | 0.4 ± 0.3 | 1.3 ± 1.2 | 3.2 ± 1.5 |
| 14:1 | 3.3. ± 1.2 | 2.5 ± 1.4 | 2.2 ± 0.8 | 0.6 ± 0.4 | 0.5 ± 0.3 |
| 15:1 | 0.6 ± 0.5 | 1.2 ± 1.2 | 1.5 ± 0.6 | 3.2 ± 2.5 | nd |
| 16:1 | 4.4 ± 1.8 | 8.7 ± 4.6 | 7.3 ± 3.0 | 6.8 ± 2.4 | 7.1 ± 4.4 |
| 17:1 | 3.6 ± 0.6 | 1.8 ± 1.1 | 3.3 ± 1.3 | 1.9 ± 1.3 | 1.2 ± 0.8 |
| 18:1 | 15.3 ± 1.1 | 4.8 ± 3.3 | 10.8 ± 3.5 | 7.8 ± 3.3 | 10.9 ± 2.5 |
| 20:1 | 2.0 ± 1.3 | 2.7 ± 1.8 | 2.0 ± 2.0 | 0.9 ± 0.8 | 3.9 ± 2.4 |
| 22:1 | 1.3 ± 0.6 | 0.5 ± 0.4 | 0.4 ± 0.4 | 0.1 ± 0.1 | 0.8 ± 0.3 |
| 24:1 | 0.8 ± 0.8 | nd | 2.6 ± 1.7 | nd | 2.2 ± 1.5 |
| 18:3n3 | 1.6 ± 0.6 | 0.9 ± 0.4 | 1.0 ± 0.6 | 0.7 ± 0.6 | 1.2 ± 0.4 |
| 20:3n3 | nd | 1.6 ± 0.8 | 0.7 ± 0.3 | 0.8 ± 0.8 | 1.2 ± 1.2 |
| 20:5n3 | 2.1 ± 0.6 | 0.1 ± 0.1 | 4.0 ± 1.0 | 1.9 ± 0.9 | 0.8 ± 0.8 |
| 22:6n3 | 1.2 ± 0.9 | 1.3 ± 1.1 | 1.2 ± 0.7 | 1.0 ± 0.6 | 1.2 ± 0.8 |
| 18:2n6 | 3.5 ± 0.7 | 2.4 ± 1.1 | 3.3 ± 1.4 | 3.9 ± 1.4 | 5.6 ± 1.3 |
| 18:3n6 | 0.5 ± 0.2 | 0.5 ± 0.3 | 4.7 ± 1.2 | 1.8 ± 1.1 | 0.8 ± 0.5 |
| 20:2n6 | 1.2 ± 0.9 | 1.4 ± 0.9 | 0.5 ± 0.3 | 0.6 ± 0.4 | 0.1 ± 0.1 |
| 20:3n6 | 0.2 ± 0.1 | nd | 2.0 ± 0.1 | 0.2 ± 0.2 | 0.3 ± 0.3 |
| 20:4n6 | nd | 0.9 ± 0.6 | 0.9 ± 0.7 | 0.1 ± 0.1 | nd |
| 22:2n6 | 4.1 ± 1.4 | 2.8 ± 1.3 | 3.8 ± 1.9 | 1.3 ± 0.7 | 2.4 ± 1.7 |
| Total saturates | 54.4 ± 2.1 | 66.2 ± 2.9 | 47.8 ± 3.7 | 66.3 ± 7.2 | 61.0 ± 3.7 |
| Total monoenes | 31.2 ± 1.7 | 22.2 ± 4.2 | 30.0 ± 6.0 | 21.3 ± 7.5 | 26.7 ± 5.1 |
| n3 polyenes | 4.9 ± 1.0 | 3.9 ± 0.9 | 6.9 ± 1.8 | 4.4 ± 0.5 | 4.5 ± 1.7 |
| n6 polyenes | 9.5 ± 0.9 | 7.6 ± 2.5 | 15.3 ± 2.5 | 7.9 ± 1.7 | 7.8 ± 1.8 |
| n6/n3 | 2.6 ± 0.6 | 3.4 ± 1.6 | 2.1 ± 0.5 | 1.9 ± 0.3 | 2.9 ± 0.8 |
| U/S | 0.8 ± 0.1 | 0.5 ± 0.1 | 1.2 ± 0.2 | 0.6 ± 0.2 | 0.7 ± 0.1 |
| UI | 73.8 ± 6.3 | 50.9 ± 3.5 | 99.6 ± 6.1 | 57.1 ± 7.4 | 58.6 ± 3.6 |
| Chain length | 17.5 ± 0.1 | 17.2 ± 0.2 | 17.6 ± 0.3 | 17.5 ± 0.2 | 17.7 ± 0.3 |

Values are represented as means ± standard error (n=6). SFA, saturated fatty acids; MUFA, monounsaturated fatty acids; n3, n3 polyunsaturated fatty acids; n6, n6 polyunsaturated fatty acids; UI, unsaturation index = $\sum m_i$ x $n_i$, where $m_i$ is the mole percentage and $n_i$ is the number of carbon–carbon double bonds of the fatty acid.

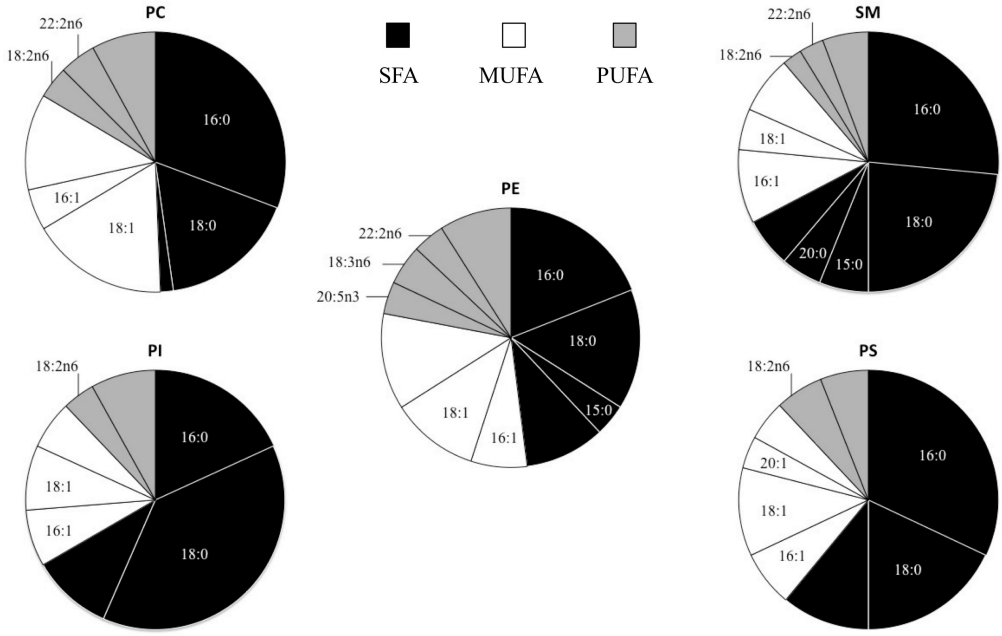


**Figure 3. 8**. Pie chart representations summarizing major FA subclass distribution and their dominant FAs of each PL specie.

**Discussion**

The major findings of this study were 1) sarcolemmal lipid composition can be obtained with the mechanical skinning approach, 2) the mechanical skinning method revealed a SL membrane higher in SM and lower in PC content than that seen in previous studies and 3) the mechanical skinning approach reveals a SL membrane devoid of contamination from sarcoplasmic reticulum and t-tubule membranes but not of nuclear and mitochondrial membranes. Membrane lipid composition can alter various aspects of membrane structure such as membrane fluidity and thickness. In turn, these alterations in membrane structure may play an important role in the overall function of the proteins embedded within the membrane. The sarcolemmal membrane is a critical component to the overall health of skeletal muscle, by playing roles in ECC, metabolism and prevention of unnecessary muscle damage. The lipid composition of skeletal muscle has been studied extensively. One specific limitation in the literature is with regards to the lack of analysis of purified subcellular organelles, including the sarcolemma. Furthermore, studies that have assessed sarcolemmal lipid composition are limited in lipid analysis because they presented only PL specie distribution and not FA composition, and also relied on aggressive isolation protocols revealing t-tubule and sarcoplasmic reticular contamination while disregarding the assessment of other potential contaminants including the nuclear and mitochondrial membranes. To overcome these limitations, the present study assessed a method of mechanically skinning skeletal muscle fibres as an alternative to analyze lipid composition of sarcolemmal membranes inclusive of both PL and FA composition.

*Single fibre characteristics*

This is the first study to analyze lipid composition from sarcolemmal membranes obtained from individually skinned skeletal muscle fibres. It should be highlighted that the single fibres were < 5mm in length and 40 – 60 μm wide. Indeed, there are three primary assumptions when interpreting the results from this analysis: 1) the single fibre segments are good representations of the whole fibre length, 2) the SL membranes are of relatively high purity and 3) the length of SL cuff is equivalent to the length of the single fibre from which it was obtained. However, with regards to representation, when utilizing the mechanical skinning technique one can specify the quantity of sarcolemma obtained using dimensions such as total surface area in the pool (Appendix 3 Table **A3.1**). Thus, the lipid analysis results here are assumed to be a specific amount of pure sarcolemma in each pool.

*Western blot analysis*

When isolating subcellular membranes from any tissue, arguments towards recovery and contamination can be made. The first traditionally involves procuring a protein specific to the isolated membrane, and the latter involves proteins specific to potential contaminating membranes. With these two subsets of proteins, one can determine the recovery of the membrane of interest whilst estimating any existing contamination from other subcellular membranes via Western blotting (Dombrowski, et al., 1996; Zorzano & Camps, 2006).

Recovery

β-dystroglycan is a sarcolemmal membrane-spanning protein belonging to the complex of proteins interacting with dystrophin and laminin that has been commonly used as a sarcolemmal marker (Cluchague, et al., 2004; Frigeri, et al., 2004; Mulvey, et al., 2005; Sotgia, et al., 2003). The results presented here indicate that β-dystroglycan was indeed detected in the SL cuffs but was mostly found in the skinned fibre equivalents (80% of total, Figure 3.4). It may be argued that the lipid composition data presented here represents only 20% of the whole SL membrane. However, utilizing a similar mechanical skinning approach and immunohistochemistry, it has been shown that sarcolemmal markers, laminin, of the basal lamina, and dystrophin, of the submembranous cytoskeletal network, are detected solely in the SL cuffs and not in the skinned fibres (Robyn M. Murphy, et al., 2009; Rybakova, et al., 2000). In conjunction with the immunohistochemical data, laminin was shown to be exclusive to the SL cuffs via Western blotting (n=1, Figure 3.5). Importantly, laminin and dystrophin are connected to the sarcolemmal membrane via linkages to dystroglycan. Specifically, laminin is bound to α-dystroglycan extracellularly, and dystrophin is bound to β-dystroglycan intracellularly (Draviam, et al., 2006; Ozawa, et al., 2001; Sotgia, et al., 2000). Moreover, α-dystroglycan is an extracellular subunit bound to the membrane-spanning β-dystroglycan subunit (Draviam, et al., 2006; Ozawa, et al., 2001; Sotgia, et al., 2000). Due to the sole detection of laminin (Figure 3.5) and dystrophin in the mechanically skinned sarcolemmas and not their respective skinned fibres from previous studies using immunohistochemistry (Murphy, et al., 2009; Rybakova, et al., 2000), and their known linkages to β-dystroglycan (indirectly and directly), it may be posed that the non-exclusive detection of β-dystroglycan in the SL cuffs, may be an example which

showcases the difficulty of finding a SL membrane-spanning specific marker rather than an incomplete recovery of SL membranes.

It is possible that the continuous nature between the SL and t-tubule membranes make it difficult for certain proteins to be found only in SL and not in the t-tubule. Caveolin-3 was believed to be exclusive to the sarcolemmal membrane until shown to be only 25% in the sarcolemma and mainly localized in the t-tubule necks using the same mechanical skinning approach utilized in this study (Murphy, et al., 2009). As eluded previously, the results presented here are similar to that seen in Murphy et al., 2009, revealing localizations of 25% of caveolin-3 to the SL cuffs and the remaining ~75% to the skinned fibre portions. Interestingly, caveolin-3 has been shown to co-localize and co-immunoprecipitate with β-dystroglycan via a direct interaction at the C-terminus of β-dystroglycan (Sotgia, et al., 2000). Furthermore, β-dystroglycan has been suggested to be associated with caveolae microdomains (Sotgia, et al., 2003). In support of this notion, the percent distribution found for both caveolin-3 and β-dystroglycan in the skinned fibre equivalents in this study was both ~80% (Figure 3.4). One other possibility explaining the abundant detection of β-dystroglycan to skinned fibre portions involves the compartmentalization of this protein into internal vesicles (Sotgia, et al., 2003). However, internalization to these vesicles requires phosphorylation of β-dystroglycan at the tyrosine 492 residue to which the physiological stimuli is still currently unknown (Sotgia, et al., 2003). Another possible consideration is that the β-dystroglycan in the skinned fibre segments, are those that remained bound to dystrophin and the submebranous cytoskeletal network. However, this is not likely because of the exclusive immunohistochemical detection of dystrophin to mechanically skinned SL membranes

seen in a previous study (Rybakova, et al., 2000). Along with the sole detection of laminin in the Western blot analysis presented in this study (Figure 3.5) and immunohistochemical analysis by Murphy et al., (2009), this allows for the assumption that there was full recovery of β-dystroglycan belonging to an SL membrane situated between the submembranous cytoskeletal network and basement membrane. Nonetheless, the presence of the β-dystroglycan in the skinned fibre segments and not solely in the SL cuffs, questions it use as a membrane-spanning SL marker. Due to the lack of an exclusive membrane-spanning SL marker, the recovery of sarcolemma plasma membrane in the cuffs could not be calculated.

Contamination

When isolating cellular membranes from tissue there lies the potential for contamination from other surrounding cellular membranes. Previous protocols for isolation of sarcolemmal membranes from rat skeletal muscles have shown to be contaminated with subcellular membranes including t-tubules; indicated by presence of DHPR, sarcoplasmic reticulum; indicated by presence of SERCA, and nuclei; indicated by presence of emerin (Table 3.1). Furthermore, these contaminations are present despite protocols whereby muscle homogenates undergo initial sedimentation to remove myofibrillar and nuclear debris (Dombrowski et al., 1996) and purified sarcolemmal membrane fractions undergo further chemical processing including immunoprecipitation (Olhendiek et al., 1991) and $Ca^{2+}$-loading to remove the sarcoplasmic reticulum (Zorzano & Camps, 2006). In an attempt to minimize contamination from other subcellular membranes, this study utilized the mechanical skinning method for lipid analysis from rat

EDL muscle fibres. With the use of exclusive specific membrane markers: sarcoplasmic reticulum (SERCA 1 & 2), t-tubules (DHPR), nuclear (emerin), mitochondria (outer: mitoNEET, inner: COX IV), Western blot analysis revealed no detectable contamination of sarcoplasmic reticulum and t-tubules in the SL cuffs (Figure 3.3). It may be argued that since t-tubules are deep invaginations of the sarcolemma that communicate with the SR deep within the myofibrils, DHPR may only be localized in the deeper regions of the t-tubules. Therefore, the negative detection of DHPR in the SL cuffs may only indicate no contamination from deep portions of t-tubules and may still be contaminated with the shallow portions. However, this would fail to recognize that the caveolin-3 distributions within the cuffs and skinned fibres are similar to the study that also revealed caveolin-3 was localized mainly at the t-tubule necks (Murphy, et al., 2009). Because the relative distribution of caveolin-3 in the cuffs and skinned fibres are similar to Murphy et al., 2009, it is likely that the t-tubule necks stayed in the skinned fibre equivalents, and therefore, it is not likely that the SL cuffs have shallow t-tubule contamination. However, there was minimal contamination from nuclear (represented with ~7% of total emerin in the cuffs) and mitochondrial (outer: ~7% of total mitoNEET in the SL cuffs, inner: ~5% of total COX IV in the SL cuffs) membranes (Figure 3.4). To the author's knowledge, there is one other study assessing nuclear and mitochondrial contamination within SL membranes (Table 3.1; Stefanyk, 2008). Western blot analysis on the SL membranes isolated in this study revealed nuclear contamination as indicated by emerin, but no inner mitochondrial contamination as indicated by the absence of adenine nucleotide translocase. However, the sensitivity of the Western blotting techniques in the study done

by Stefanyk (2008) was unknown and cannot rule out the possibility of contamination from the outer mitochondrial membrane.

Taken together, because our caveolin-3 distributions were similar to that of Murphy et al., 2009, 3 plausible assumptions could be made. Firstly, there is no contamination from the shallow regions of the t-tubules. Secondly, along with data indicating a direct connection between β-dystroglycan and caveolin-3, the high detection of β-dystroglycan in the skinned fibre equivalents may be bound to caveolin-3 at the t-tubule necks. Thirdly, and most importantly, because Murphy et al., 2009, showed laminin solely in the skinned cuffs using immunohistochemistry, it is likely that the laminin distributions would also be similar. In agreeance with the last assumption, laminin was shown to be exclusive to SL cuffs via Western blotting (Figure 3.5, n=1). Since, laminin and dystrophin surround the sarcolemma plasma membrane, and they have been detected solely in the SL with a similar mechanical skinning approach, it can be further assumed that the lipid analysis performed in this study, was of a SL plasma membrane situated between the basement membrane and submembranous cytoskeletal network. Indeed, there was minimal nuclear and mitochondrial contamination, however, the lipid analysis performed in this study was of a SL membrane devoid of t-tubule and SR contamination, which is novel compared to previous isolation protocols (Dombrowski, et al., 1996; Ohlendieck, et al., 1991; Zorzano & Camps, 2006).

*Phospholipid species composition*

The amounts of the predominant phospholipids (PC, PE, SM, PI and PS) relative to total are similar to those previously seen (Fiehn, et al., 1971; Stefanyk, 2008) with the

exception of high SM and low PC percent contribution. This finding may indicate that the mechanical skinning technique may reveal more lipid raft/caveolae rich regions known to be high in SM and low in PC (Koumanov, et al., 2005). Previous protocols isolating sarcolemmal membranes have relied on membrane disruption (often with non-ionic detergents) followed by a gradient centrifugation. It is well known that non-ionic detergents at cold temperatures segregate membranes into two fractions: 1) detergent soluble and 2) detergent insoluble (enriched in cholesterol and SM) (Koumanov, et al., 2005; Sot, et al., 2006). By avoiding these protocols, the mechanical skinning technique may include more of the detergent insoluble fractions, which could account for the high SM and lower PC. Indeed, this theory is limited since cholesterol was not measured in this study. Nonetheless, plasma membranes, in general, have high SM relative to PC content (Alberts, et al., 2002), thus the SL membrane obtained from the mechanical skinning technique may be a more accurate depiction of the sarcolemmal plasma membrane.

*Phospholipid fatty acid composition*

Within the literature, most studies assessing SL lipid composition have been limited to a PL species distribution level and have neglected the FA composition (Lau, et al., 1979; Rosemblatt, et al., 1981; Smith & Appel, 1977; Sumnicht & Sabbadini, 1982). Previous work comparing FA composition of individual PL species at both a mitochondrial and whole muscle level, revealed significant differences across the PL species and membrane preparations (Tsalouhidou, et al., 2006). Furthermore, specific PL species and their FA profile may impact specific membrane functions, for example, PC unsaturation correlating with insulin sensitivity but not PE (Clore, et al., 1998),

meanwhile CL and PE unsaturation from mitochondrial membranes are known to correlate with palmitate oxidation (LeBlanc, et al., 2010). Taken together, these studies emphasizes the limitation of neglecting FA analysis of individual PL species. To address the limitations, GC analysis was performed on individual PL species to assess both total and individual PL FA compositions. The relative abundance of the major FA subclasses (SFA > MUFA > n6 PUFA and > n3 PUFA) from total phospholipids was found to be similar to a previous study (Stefanyk, 2008). When assessing individual phospholipid species FA composition, the relative abundance of the hierarchy of major FA subclasses did not change. The results from individual phospholipid FA composition were similar to that previously seen with 16:0 and 18:0 as the dominant FA species (Fiehn, et al., 1971; Stefanyk, 2008). All PL species with the exception of PI had higher levels of 16:0 compared to 18:0 which was not surprising since 18:0 is considered a major FA for PI (Voet, 2004). In addition, unsaturation index of individual phospholipid species and the hierarchy between them (PE > PC > PS > PI > SM) were similar to that previously seen (Stefanyk, 2008). Specifically, the high unsaturation of PE was mainly due to an abundance of MUFAs 16:1 and 18:1, and PUFAs; 20:5n3, 18:2n6, 18:3n6, 22:2n6 comprising 70-75% of total PUFA. Similarly, PC's unsaturation was mostly contributed to by MUFA 18:1 and PUFAs; 18:2n6, 22:2n6 representings 65-70% of total PUFA. Both PI and PS unsaturation levels were mainly due to 16:1, 18:1, and 18:2n6 FAs. Similar to previous studies, SM had the lowest unsaturation (Fiehn, et al., 1971; Stefanyk, 2008), with 16:1 and 18:1 as its most abundant unsaturated FAs. Overall, the similarities with phospholipid FA composition suggest further that the mechanical skinning technique may be a viable method for SL lipid analysis.

*Practical advantages of the mechanical skinning approach*

By utilizing the mechanical skinning approach a few practical advantages may be considered when compared to the traditional SL isolation methods. Firstly, the isolation of membrane fractions has required high amounts of initial tissue (2 - 12 g of muscle) that often results in using mixed muscle approaches (Dombrowski, et al., 1996; Zorzano & Camps, 2006; Stefanyk, 2008). This mixing of muscles may mask differences that might occur at the fibre type level. Secondly, membrane fractionation protocols are 2-day tasks subject to technical difficulties throughout the protocol steps, including differential centrifugation. Specifically, differential centrifugation can result in problems including leakage from ultracentrifuge tubes and gradient collapse, leading to loss of sample and time. In contrast, the mechanical skinning technique can be considered more simple than the traditional methods. Indeed, developing the mechanical skinning skill requires patience and manual dexterity, but once developed, the isolation protocol can range between 4 – 6 hours. Furthermore, since the mechanical skinning involves single muscle fibre segments, less muscle tissue is required, enabling for studies on fibre type differences. And since, the mechanical skinning technique eliminates the need for differential centrifugation, the technical difficulties in isolating SL membranes are eliminated. Given that the mechanical skinning technique decreases the amount of: tissue, time, and technical difficulties while isolating SL membranes, it can be viewed as advancement in the isolation of SL membranes.

**Conclusion**

In summary, this was the first study to utilize the mechanical skinning technique for complete sarcolemmal phospholipid analysis (inclusive of PL and FA composition).

This membrane preparation may be a more accurate depiction of the SL membrane when compared to traditional methods that may have lost detergent-resistant fractions since SM% was higher and PC% was lower. However, estimating recovery of the SL membrane proved difficult due to the lack of an exclusive membrane-spanning SL marker. Nonetheless, with similar distributions of caveolin-3 to that of another study (Murphy, et al., 2009), it could be assumed that 1) there was no contamination from the shallow portions of the t-tubules, 2) along with data from Sotgia et al., 2003, the high levels of β-dystroglycan in the skinned fibres is likely to be associated with high levels of caveolin-3 at the necks of t-tubules, and 3) laminin is also solely in the SL cuffs used in this study. The latter assumption is supported by Western blot data indicating sole detection of laminin in the SL cuffs (Figure 3.5, n=1). Moreover, since laminin and dystrophin were detected only in SL membranes in previous studies (Murphy, et al., 2009; Rybakova, et al., 2000) via immunohistochemistry using a similar mechanical skinning approach, it can be assumed that the lipid analysis of this study was of a SL membrane sandwiched between the submembranous cytoskeletal network and basement membrane. Future experiments could assess the validity of this sandwich theory by using both extracellular matrix and submembranous cytoskeletal network probes under confocal immunomicroscopy similar to that done by Murphy et al., (2009). Western blot analysis revealed that the mechanical skinning method was slightly contaminated with nuclear (marked by emerin) and mitochondrial membranes (marked by COX IV and mitoNEET) to 5-7% of total fibre equivalent. A previous study also indicated nuclear contamination without inner mitochondrial contamination, but the sensitivity of Western blotting techniques and the potential for outer mitochondrial contamination are unknown.

Unlike previous studies, this study used an SL membrane void of t-tubule and sarcoplasmic reticulum contamination (absence of DHPR and SERCA1/2, respectively) without involving processes including, differential centrifugation, immunoprecipitation and $Ca^{2+}$ loading. Therefore, the mechanical skinning approach represents a SL isolation technique, which proves useful for complete (PL and FA) lipid analysis. This is advancement in SL membrane lipid analysis and future studies could use this technique to analyse the SL membrane lipid composition and its relationship to cellular function in normal and disease/disorder states.

**References**

Abbott, S. K., Else, P. L., & Hulbert, A. J. (2010). Membrane fatty acid composition of rat skeletal muscle is most responsive to the balance of dietary n-3 and n-6 PUFA. *The British journal of nutrition*, 1-8.

Alberts, B., Johnson, A., Lewis, J., Raff, M., Roberts, K., & Walter, P. (2002). *Molecular Biology of the Cell* (4 ed.): Garland Science.

Andersson, A., Sjodin, A., Olsson, R., & Vessby, B. (1998). Effects of physical exercise on phospholipid fatty acid composition in skeletal muscle. *Am J Physiol, 274*(3 Pt 1), E432-438.

Blackard, W. G., Li, J., Clore, J. N., & Rizzo, W. B. (1997). Phospholipid fatty acid composition in type I and type II rat muscle. *Lipids, 32*(2), 193-198.

Bligh, E. G., & Dyer, W. J. (1959). A rapid method of total lipid extraction and purification. *Can J Biochem Physiol, 37*(8), 911-917.

Bradley, N. S., Heigenhauser, G. J., Roy, B. D., Staples, E. M., Inglis, J. G., LeBlanc, P. J., et al. (2008). The acute effects of differential dietary fatty acids on human skeletal muscle pyruvate dehydrogenase activity. *J Appl Physiol, 104*(1), 1-9.

Cluchague, N., Moreau, C., Rocher, C., Pottier, S., Leray, G., Cherel, Y., et al. (2004). beta-Dystroglycan can be revealed in microsomes from mdx mouse muscle by detergent treatment. *FEBS Lett, 572*(1-3), 216-220.

Delp, M. D., & Duan, C. (1996). Composition and size of type I, IIA, IID/X, and IIB fibers and citrate synthase activity of rat muscle. *J Appl Physiol, 80*(1), 261-270.

Dombrowski, L., Roy, D., Marcotte, B., & Marette, A. (1996). A new procedure for the isolation of plasma membranes, T tubules, and internal membranes from skeletal muscle. *The American Journal of Physiology, 270*(4 Pt 1), E667-676.

Draviam, R. A., Wang, B., Shand, S. H., Xiao, X., & Watkins, S. C. (2006). Alpha-sarcoglycan is recycled from the plasma membrane in the absence of sarcoglycan complex assembly. *Traffic, 7*(7), 793-810.

Fiehn, W., Peter, J. B., Mead, J. F., & Gan-Elepano, M. (1971). Lipids and fatty acids of sarcolemma, sarcoplasmic reticulum, and mitochondria from rat skeletal muscle. *J Biol Chem, 246*(18), 5617-5620.

Frigeri, A., Nicchia, G. P., Balena, R., Nico, B., & Svelto, M. (2004). Aquaporins in skeletal muscle: reassessment of the functional role of aquaporin-4. *FASEB J, 18*(7), 905-907.

Germinario, E., Esposito, A., Midrio, M., Betto, R., & Danieli-Betto, D. (2002). Expression of sarco(endo)plasmic reticulum Ca(2+)-ATPase slow (SERCA2) isoform in regenerating rat soleus skeletal muscle depends on nerve impulses. *Exp Physiol, 87*(5), 575-583.

Kanzaki, M. (2006). Insulin receptor signals regulating GLUT4 translocation and actin dynamics. *Endocrine journal, 53*(3), 267-293.

Koumanov, K. S., Tessier, C., Momchilova, A. B., Rainteau, D., Wolf, C., & Quinn, P. J. (2005). Comparative lipid analysis and structure of detergent-resistant membrane raft fractions isolated from human and ruminant erythrocytes. *Arch Biochem Biophys, 434*(1), 150-158.

Kupke, I. R., & Zeugner, S. (1978). Quantitative high-performance thin-layer chromatography of lipids in plasma and liver homogenates after direct application of 0.5-microliter samples to the silica-gel layer. *J Chromatogr, 146*(2), 261-271.

Lamb, G. D. (2009). Mechanisms of excitation-contraction uncoupling relevant to activity-induced muscle fatigue. *Appl Physiol Nutr Metab, 34*(3), 368-372.

Lamb, G. D., Posterino, G. S., & Stephenson, D. G. (1994). Effects of heparin on excitation-contraction coupling in skeletal muscle toad and rat. *J Physiol, 474*(2), 319-329.

Lamb, G. D., & Stephenson, D. G. (Writer) (1990a). Calcium release in skinned muscle fibres of the toad by transverse tubule depolarization or by direct stimulation, *The Journal of physiology*. ENGLAND.

Lamb, G. D., & Stephenson, D. G. (Writer) (1990b). Control of calcium release and the effect of ryanodine in skinned muscle fibres of the toad, *The Journal of physiology*. ENGLAND.

Lau, Y. H., Caswell, A. H., Brunschwig, J. P., Baerwald, R., & Garcia, M. (1979). Lipid analysis and freeze-fracture studies on isolated transverse tubules and sarcoplasmic reticulum subfractions of skeletal muscle. *J Biol Chem, 254*(2), 540-546.

Leblanc, P. J., Harris, R. A., & Peters, S. J. (2007). Skeletal muscle fiber type comparison of pyruvate dehydrogenase phosphatase activity and isoform expression in fed and food-deprived rats. *Am J Physiol Endocrinol Metab, 292*(2), E571-576.

Liu, S., Baracos, V. E., Quinney, H. A., & Clandinin, M. T. (1994). Dietary omega-3 and polyunsaturated fatty acids modify fatty acyl composition and insulin binding in skeletal-muscle sarcolemma. *Biochem J, 299 ( Pt 3)*, 831-837.

Mulvey, C., Harno, E., Keenan, A., & Ohlendieck, K. (2005). Expression of the skeletal muscle dystrophin-dystroglycan complex and syntrophin-nitric oxide synthase complex is severely affected in the type 2 diabetic Goto-Kakizaki rat. *Eur J Cell Biol, 84*(11), 867-883.

Murphy, R. M., Mollica, J. P., & Lamb, G. D. (2009). Plasma membrane removal in rat skeletal muscle fibers reveals caveolin-3 hot-spots at the necks of transverse tubules. *Experimental cell research, 315*(6), 1015-1028.

Nielsen, O. B., & de Paoli, F. V. (2007). Regulation of Na+-K+ homeostasis and excitability in contracting muscles: implications for fatigue. *Appl Physiol Nutr Metab, 32*(5), 974-984.

Ohlendieck, K., Ervasti, J. M., Snook, J. B., & Campbell, K. P. (1991). Dystrophin-glycoprotein complex is highly enriched in isolated skeletal muscle sarcolemma. *The Journal of cell biology, 112*(1), 135-148.

Ozawa, E., Nishino, I., & Nonaka, I. (2001). Sarcolemmopathy: muscular dystrophies with cell membrane defects. *Brain Pathol, 11*(2), 218-230.

Pan, D. A., Lillioja, S., Milner, M. R., Kriketos, A. D., Baur, L. A., Bogardus, C., et al. (1995). Skeletal muscle membrane lipid composition is related to adiposity and insulin action. *J Clin Invest, 96*(6), 2802-2808.

Posterino, G. S., Lamb, G. D., & Stephenson, D. G. (2000). Twitch and tetanic force responses and longitudinal propagation of action potentials in skinned skeletal muscle fibres of the rat. *The Journal of physiology, 527 Pt 1*, 131-137.

Rosemblatt, M., Hidalgo, C., Vergara, C., & Ikemoto, N. (1981). Immunological and biochemical properties of transverse tubule membranes isolated from rabbit skeletal muscle. *J Biol Chem, 256*(15), 8140-8148.

Rybakova, I. N., Patel, J. R., & Ervasti, J. M. (2000). The dystrophin complex forms a mechanically strong link between the sarcolemma and costameric actin. *J Cell Biol, 150*(5), 1209-1214.

Sanes, J. R. (1982). Laminin, fibronectin, and collagen in synaptic and extrasynaptic portions of muscle fiber basement membrane. *J Cell Biol, 93*(2), 442-451.

Smith, P. B., & Appel, S. H. (1977). Isolation and characterization of the surface membranes of fast and slow mammalian skeletal muscle. *Biochim Biophys Acta, 466*(1), 109-122.

Sotgia, F., Bonuccelli, G., Bedford, M., Brancaccio, A., Mayer, U., Wilson, M. T., et al. (2003). Localization of phospho-beta-dystroglycan (pY892) to an intracellular vesicular compartment in cultured cells and skeletal muscle fibers in vivo. *Biochemistry, 42*(23), 7110-7123.

Sotgia, F., Lee, J. K., Das, K., Bedford, M., Petrucci, T. C., Macioce, P., et al. (2000). Caveolin-3 directly interacts with the C-terminal tail of beta -dystroglycan. Identification of a central WW-like domain within caveolin family members. *J Biol Chem, 275*(48), 38048-38058.

Stefanyk, L.E. (2008). *Skeletal Muscle Fibre-Type Comparison of Whole tissue and Subcellular Phospholipids and Fatty Acids.* Brock University, St. Catharines.

Stefanyk, L. E., Hajna, S., Roy, B. D., Peters, S. J., & LeBlanc, P. J. (2008). Phospholipid fatty acid composition of skeletal muscle sarcolemmal and T-tubule membranes. *Appl Physiol Nutr Metab*, S95.

Sumnicht, G. E., & Sabbadini, R. A. (1982). Lipid composition of transverse tubular membranes from normal and dystrophic skeletal muscle. *Arch Biochem Biophys, 215*(2), 628-637.

Voet, V. (2004). *Biochemistry* (3rd ed.). Pennsylvannia: John Wiley and Sons, Inc.

Weerheim, A. M., Kolb, A. M., Sturk, A., & Nieuwland, R. (2002). Phospholipid composition of cell-derived microparticles determined by one-dimensional high-performance thin-layer chromatography. *Anal Biochem, 302*(2), 191-198.

Wu, K. D., & Lytton, J. (1993). Molecular cloning and quantification of sarcoplasmic reticulum Ca(2+)-ATPase isoforms in rat muscles. *Am J Physiol, 264*(2 Pt 1), C333-341.

Zorzano, A., & Camps, M. (2006). Isolation of T-tubules from skeletal muscle. *Current protocols in cell biology / editorial board, Juan S.Bonifacino ...[et al.], Chapter 3*, Unit 3.24.

## Chapter 3: General Conclusions

This thesis was successful in addressing limitations with regards to sarcolemmal membrane lipid composition analysis. The novelty of these experiments was the 1) analysis of lipids (inclusive of PL and FA composition) in SL membranes obtained by mechanically skinning individual muscle fibre segments and 2) the identification and quantification of contamination from other subcellular membranes, namely, t-tubule, sarcoplasmic reticulum, nucleus and mitochondria. The changes in sarcolemmal membrane lipid composition with various disease states, including; muscular dystrophy and insulin resistance, has been previously assessed (de Kretser & Livett, 1977; Liu, et al., 1994; Ohlendieck, et al., 1991) but have used aggressive SL membrane preparations known to be contaminated with t-tubule, sarcoplasmic reticulum, and nuclear membranes. By assessing the potential use of SL membranes obtained from skinned fibres for complete lipid analysis, this thesis provides the methodological framework for improving our understanding of the relationship between SL membrane composition and cellular function under both normal and disease states.

The most significant component to this study was with regards to the isolation of sarcolemmal membranes. Traditional methods are often less meticulous whereby, whole muscles are processed through homogenization, differential centrifugation and membrane purification (Dombrowski, et al., 1996; Liu, et al., 1994; Ohlendieck, et al., 1991; Zorzano & Camps, 2006). In contrast, this study isolated sarcolemmal membranes by mechanically skinning individual muscle fibre segments. Furthermore, this research has shown that the mechanical skinning approach provides sufficient membranes for complete analysis of lipids, which have resulted in similarities and slight differences

when compared to previous literature. Specifically, the differences were between PL species distribution, whereby there were higher SM and lower PC levels detected in comparison to previous work (Fiehn, et al., 1971; Rosemblat et al., 1981; Saido, et al., 1992; Stefanyk, 2008). These trends may indicate that the mechanical skinning technique is more inclusive of detergent resistant membrane domains that are indeed high in SM and low in PC.

Another important component to this study was identifying contamination from other subcellular organelles. High-sensitivity Western blotting was successful in detecting specific proteins in as low as ¼ cuff and fibre equivalents respectively. Traditional isolation protocols demonstrate contamination from t-tubules (defined as presence of DHPR), sarcoplasmic reticulum (defined as presence of SERCA), and nuclei (defined as presence of emerin) (Dombrowski, et al., 1996; Liu, et al., 1994; Ohlendieck, et al., 1991; Zorzano & Camps, 2006). Importantly, the SL membranes obtained using the mechanical skinning approach in this study had no detectable levels of DHPR and SERCA, indicating unlikely t-tubule and sarcoplasmic reticulum contamination. This study has shown minimal contamination from both nuclear and mitochondrial membranes. In contrast, one study was able to avoid mitochondrial contamination, although the sensitivity of Western blot techniques was unknown (Stefanyk, 2008).

This study also proves that determining an SL membrane exclusive protein marker is a difficult task. This theory is based on the fact that the SL membrane is continuous with the t-tubule membrane in a way that makes it unlikely that there is an SL membrane-spanning protein that is not shared with the t-tubule domain. The commonly used SL marker, β-dystroglycan was initially thought to be exclusive to the SL

membrane, but the results in this study may indicate that it is not exclusively on the sarcolemma whereby there was positive detection within the skinned fibre equivalents. This event is similar to caveolin-3, which was once thought to be a skeletal muscle specific caveolin isoform strictly located at the sarcolemma, until biochemical analysis revealed a more dominant localization at the t-tubule necks (Robyn M. Murphy, et al., 2009). Moreover, there is evidence that β-dystroglycan interacts with caveolin-3 and is targeted to caveolar domains (Sotgia, et al., 2003; Sotgia, et al., 2000), which may explain the presence of β-dystroglycan in the skinned fibre equivalents. Nonetheless, since laminin and dystrophin were both detected solely in the SL cuffs via immunohistochemistry, and both are two proteins known to interact with β-dystroglycan extra- and intracellularly, it was assumed that SL lipid analysis was performed on an SL membrane situated between the basement membrane and cytoskeletal network. Indeed, the sarcolemma can be generally defined as a three layer surface membrane whereby a plasma membrane is surrounded by an extracellular basement membrane and an intracellular cytoskeletal network.

Indeed some practical advantages can be considered when comparing the mechanical skinning technique and the traditional SL isolation methods. It is known that the isolation of membrane fractions has a specific requirement for the amount of initial tissue used (2 - 12 g of muscle) that often results in using mixed muscle approaches (Dombrowski, et al., 1996; Zorzano & Camps, 2006; Stefanyk, 2008). This therefore, eliminates the possibility of detecting differences in SL membrane lipid composition across specific muscle fibre types. Furthermore, most membrane fractionation protocols are 2 day tasks, that are subject to technical difficulties throughout the protocol steps,

specifically differential centrifugation. Specifically, differential centrifugation can result in problems such as leakage from ultracentrifuge tubes and gradient collapse, which both lead to loss of sample and time. In contrast, the mechanical skinning technique can be considered more simple than the traditional methods. Indeed, developing the mechanical skinning technique requires patience and skill, but once developed, the isolation protocol can range between 4 – 6 hrs. Furthermore, since the mechanical skinning involves single muscle fibre segments, less muscle tissue is required, enabling for studies on fibre type differences. And since, the mechanical skinning technique eliminates the need for differential centrifugation, the technical difficulties in isolating SL membranes are thus eliminated. Given that the mechanical skinning technique decreases the amount of: tissue, time, and technical steps for isolating SL membranes, it can be viewed as advancement in the isolation of SL membranes.

*Future Directions*

The sarcolemma membrane is vital for skeletal muscle with roles in metabolism, excitation-contraction coupling and protection of muscle integrity. Importantly, the sarcolemma relies on many membrane integral proteins in order to contribute to these aforementioned processes. The membrane structure-protein function relationship outlines a potential influence of membrane lipids on the function of membrane proteins. Because this thesis was successful in utilizing the mechanical skinning approach for a complete lipid analysis of SL membranes, future studies can now assess SL lipid composition in disease/disorder states such as muscular dystrophy and insulin resistance in attempt to add insights on the sarcolemmal membrane structure-protein function relationship. Furthermore, biological membranes and their lipid composition can be influenced by

external perturbations such as diet and exercise {Abbott, 2010 #2;Andersson, 2000 #281;Andersson, 1998 #352;Hulbert, 2005 #33}. Therefore, it would be of interest to assess the SL lipid composition after dietary and training interventions.

**References**

Abbott, S. K., Else, P. L., & Hulbert, A. J. (2010). Membrane fatty acid composition of rat skeletal muscle is most responsive to the balance of dietary n-3 and n-6 PUFA. *The British journal of nutrition*, 1-8.

Andersson, A., Sjodin, A., Hedman, A., Olsson, R., & Vessby, B. (2000). Fatty acid profile of skeletal muscle phospholipids in trained and untrained young men. *Am J Physiol Endocrinol Metab, 279*(4), E744-751.

Andersson, A., Sjodin, A., Olsson, R., & Vessby, B. (1998). Effects of physical exercise on phospholipid fatty acid composition in skeletal muscle. *Am J Physiol, 274*(3 Pt 1), E432-438.

de Kretser, T. A., & Livett, B. G. (1977). Skeletal-muscle sarcolemma from normal and dystrophic mice. Isolation, characterization and lipid composition. *The Biochemical journal, 168*(2), 229-237.

Dombrowski, L., Roy, D., Marcotte, B., & Marette, A. (1996). A new procedure for the isolation of plasma membranes, T tubules, and internal membranes from skeletal muscle. *The American Journal of Physiology, 270*(4 Pt 1), E667-676.

Fiehn, W., Peter, J. B., Mead, J. F., & Gan-Elepano, M. (1971). Lipids and fatty acids of sarcolemma, sarcoplasmic reticulum, and mitochondria from rat skeletal muscle. *J Biol Chem, 246*(18), 5617-5620.

Hulbert, A. J., Turner, N., Storlien, L. H., & Else, P. L. (2005). Dietary fats and membrane function: implications for metabolism and disease. *Biological reviews of the Cambridge Philosophical Society, 80*(1), 155-169.

Liu, S., Baracos, V. E., Quinney, H. A., & Clandinin, M. T. (1994). Dietary omega-3 and polyunsaturated fatty acids modify fatty acyl composition and insulin binding in skeletal-muscle sarcolemma. *Biochem J, 299 ( Pt 3)*, 831-837.

Murphy, R. M., Mollica, J. P., & Lamb, G. D. (2009). Plasma membrane removal in rat skeletal muscle fibers reveals caveolin-3 hot-spots at the necks of transverse tubules. *Experimental cell research, 315*(6), 1015-1028.

Ohlendieck, K., Ervasti, J. M., Snook, J. B., & Campbell, K. P. (1991). Dystrophin-glycoprotein complex is highly enriched in isolated skeletal muscle sarcolemma. *The Journal of cell biology, 112*(1), 135-148.

Saido, T. C., Shibata, M., Takenawa, T., Murofushi, H., & Suzuki, K. (1992). Positive regulation of mu-calpain action by polyphosphoinositides. *J Biol Chem, 267*(34), 24585-24590.

Sotgia, F., Bonuccelli, G., Bedford, M., Brancaccio, A., Mayer, U., Wilson, M. T., et al. (2003). Localization of phospho-beta-dystroglycan (pY892) to an intracellular vesicular compartment in cultured cells and skeletal muscle fibers in vivo. *Biochemistry, 42*(23), 7110-7123.

Sotgia, F., Lee, J. K., Das, K., Bedford, M., Petrucci, T. C., Macioce, P., et al. (2000). Caveolin-3 directly interacts with the C-terminal tail of beta -dystroglycan. Identification of a central WW-like domain within caveolin family members. *J Biol Chem, 275*(48), 38048-38058.

Stefanyk (2008). *Skeletal Muscle Fibre-Type Comparison of Whole tissue and Subcellular Phospholipids and Fatty Acids.* Brock University, St. Catharines.

Zorzano, A., & Camps, M. (2006). Isolation of T-tubules from skeletal muscle. *Current protocols in cell biology / editorial board, Juan S.Bonifacino ...[et al.], Chapter 3*, Unit 3.24.

## APPENDIX 1: Laboratory Procedures

*Part I. Single fibre mechanical skinning and cuff collection*

REAGENTS

| | | |
|---|---|---|
| 1. Na-based skinning solution | HEPES | 90mM |
| | EGTA | 50mM |
| | MgO | 10.3mM |
| | *Heat and stir for at least 30 mins at 50°C. Cool to room Temperature* | |
| | NaOH (4M) | ~pH 7.0 |
| | $Na_2ATP$ | 8mM |
| | $Na_2CP$ | 10mM |
| | NaOH (4M) | ~pH 7.1 |
| 2. Buffer A | 10 mM $NaHCO_3$ (sodium bicarbonate) | |
| | 5 mM $NaN_3$ (sodium azide) | |
| | 100 µM phenylmethylsulfonylfloride (PMSF) | |
| | *Just before use, add* | |
| | 0.25M Sucrose | |

APPARATUS & MATERIALS

1. Petri dish with Sylgard layer (0.8 – 1 cm thick)
2. Two pairs of Dumont Inox Forceps (5)
3. Cabinet points (0.5 – 1.0 cm)

Protocol

1. Place ~15 – 20 ml of skinning solution into petri dish and keep on ice.
2. Pin muscle on each tendon to the sylgard layer.
3. Split the muscle to expose single fibres.
4. Tease out a bundle of fibres. Then work this bundle to tease out a single fibre.

5. Once a single fibre is isolated, pinch one end of the fibre with forceps (~1/3 of diameter) and pinch the other third of the fibre with the other forcep and pull forceps away from each other.
6. The cuff will form towards the attached muscle belly.
7. With microscissors cut the skinned fibre from the muscle belly.
8. Pull the fibrils completely off from each other and then collect the cuff with a piece (~0.5 – 1 cm) of suture.
9. Place the suture along with the cuff into 250 ul of Buffer A. Repeat 9x for a pool of 10 in the same 250 ul of Buffer A. If running Western blots only pool into 20 ul of Buffer A (so that 10 ul of 3x Laemmli buffer can be added).
10. Store at -80°C for future analysis.

*Part II. Lipid Analysis From Sarcolemmal Cuffs*

Methods used: Lipid Extraction, 2-dimensional High Performance Thin Layer Chromatography and Gas Chromatography

This is a multi-day protocol, but there are various freeze points. Essentially, this outlines in order what methods need to be done for complete lipid analysis of membranes for mechanically skinned single fibres.

---

**Lipid Extraction (Bligh & Dyer, 1959) + freeze thaw cycle to disrupt the membranes.**

1. Pool 10 cuffs from mechanically skinned single fibre segments (record the length of each segment) in 250 ul of Buffer A in eppendorf tubes.
2. Perform 3 freeze thaw cycles
3. Use eppendorf plunger to homogenize the cuffs with sutures in the tubes.
4. Transfer the membranes into kimex tubes and add 750 ul of double distilled water
5. Add 3.75 ml of Chloroform:Methanol (1:2) with 0.1% BHT and vortex well for 2 min.
6. Add 1.25 ml of chloroform and vortex for 10 seconds.
7. Add 1.25 ml of double distilled water and vortex until white colour change (~2 sec).
8. Centrifuge at 2000 RPM for 6 min.
9. Collect the chloroform phase (bottom phase) carefully, not collecting any of the aqueous layer.
10. Either freeze at - 20 or prepare for solid phase extraction.

---

**HPTLC – 2-dimensional HPTLC.**

After performing lipid extraction the sample will undergo 2-dimensional HPTLC to be able to clean the sample from neutral lipids (cholesterol, free fatty acids, triglycerides) and other artefacts interfering with phospholipid separation (without dealing with lipid extractions from silica). The first development is for neutral lipids. This development will not move the phospholipids and glycolipids, and as such they remain at the spot of (**Figure A1.1**).

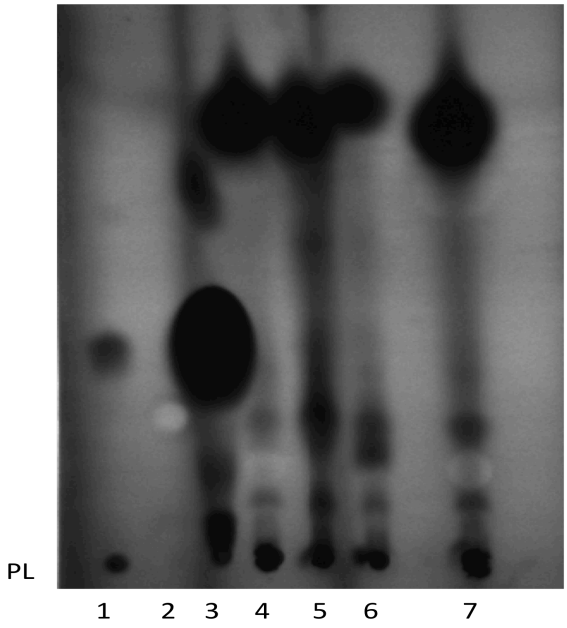


**Figure A1. 1**. Neutral lipid development with immobile Phospholipids NL, GL, PL and non SPE are 4,5,6 and 7 respectively

**Protocol**

1. Saturate development tank with Hexane: Diethyl Ether: Acetic Acid (80:20:1.5) (Kupke et al., 1978).
2. Bake HPLC plates at 130°C for 10 min to activate the plate.
3. Take lipid extract and dry down under nitrogen and reconstitute in 20 µl of C:M (2:1).
4. Spot sample 2 cm from the bottom, and 2 cm from the left of the plate. (This will ensure that when the plate is turned 90 degrees for development 2 that we know where to spot the PL standard).
5. Spot cholesterol standard.
6. Place the plate in the developing tank and allow for 35 min.
7. Let the plate dry and then place in oven at 130°C for 5 min (get rid of acetic acid).

**HPTLC – 2nd development Phospholipid Separation**

This second HPTLC is for phospholipid separation. To do this we just turn the plate 90 degrees and run the plate in another tank.

1. Saturate development tank with Chloroform: Ethyl Acetate: Acetone: Isopropanol: Ethanol: Methanol: Water: Acetic Acid (60:12:12:12: 32: 56: 12: 4). (Hint: get this tank ready when the neutral lipids are being separated)
2. Turn plate 90 degrees and spot the PL standard ≤ 1 µg of lipid (so get proper separation when spotting dots not bands) beside the previously spotted sample

(Hint: you will be able to see where you spotted it, by lifting the plate directed towards a light source).
3. Place the plate in the developing tank and allow to run up 5.5 cm from the spot of origin.
4. Let the plate dry and then place in oven at 130°C for 5 min.
5. Spray with DCF and then place in a tank saturated with ammonia hydroxide vapours (25% in water).
6. Scrape phospholipid lanes and place into kimex tubes. *Most expected phospholipids to be present on the plate PC, PE and SM. But still scrape the 'ghost lanes' of the other phospholipids, PI and PS.*
7. Scrape blank PL lanes also to be able to subtract in GC analysis.
8. Freeze at – 20°C for future methylation ad gas chromatography analysis.

---

**Methylation – Fatty Acid Methyl Esters**

Methylation of fatty acids is a crucial step before gas chromatography. Without prior methylation the fatty acids are not volatile substances, and thus will not enter gaseous state easily (which is imperative for gas chromatography). By the addition of the methyl group with an ester linkage the fatty acids are easily put into gaseous state, when heated at high temperatures.

1. To each kimex tube with silica scrapings, add 2mL of 6% H2SO4 in methanol.
2. As accurately as possible, add 10uL of 13:0 (External Standard; 1mg/mL hexane)→ rinse syringe in hexane
3. Close tightly, and incubate for 2hrs at 80°C
4. Cool for 10 min, then break seal
5. Add 1mL DDW
6. Add 2mL petroleum ether→ vortex
7. Centrifuge for 6min at 2000 RPM
8. Extract petroleum ether phase (top) into mini vial
9. Seal cap with parafilm and store at -20°C for future Gas chromatography analysis.

---

**Gas Chromatography**

Gas chromatography, like any other chromatography involves a stationary phase and a mobile phase. The stationary phase, that we deal with at Brock University, is via a column packed with diamataceous earth. The mobile phase is helium gas. So basically, when the fatty acid methyl esters enter into gaseous state (depending on what temperature is needed for them to do this), they will be dissolved into the helium gas. Depending on size of the fatty acid and stability into gaseous state, they may be held by the solid phase, whereby they must wait for higher temperatures to enter into gaseous state. Then a flame ionizing detector, will blow up the fatty acids into ions that is read by the detector, and we are then left with peaks, where the concentration is related to the area under the curve.

1. Transfer FAMEs to GC vials.
2. Dry down under gaseous nitrogen.
3. Reconstitute in 10uL of hexane or dichloromethane
4. Seal cap very well (otherwise the samples will evaporate). Use 5 μl injection method.
5. Calibrate the standard. This calibration involves having the 13:0 matching the 13:0 of the samples in terms of retention time.
6. Inject only 0.1 ul of FAME mix (or any volume to make sure that the peak heights will be as close to the heights of the sample peak heights).

***Because only adding 10 ul of DCM samples will have to be watched. Dry down and reconstitute samples in 10 ul of DCM 1 samples at a time. This will prevent problems with evaporation. Also since we are detecting such low levels of lipid, and contamination from previous runs (standards or unknown samples) can have a big impact. Thus, a DCM clean is necessary after each sample and standard.***

***** Run PL blanks also to be able to subtract concentrations.***

*Part III. Western blotting*

REAGENTS

1. Sample Buffer 3.0x

1.875 mL 1 M Tris base solution (1 M Tris Base Solution = 1.2114g of Tris in 10 mL DDW) (pH 6.8)

3.625 mL DDW

0.6 g SDS

3 mL glycerol

1.5 mL of 2-ME

0.006 g B-Blue

2. Ammonium Persulfate

0.06 g ammonium persulfate (APS)

600 μL DDW

* Make fresh daily

3. Resolving Gel Buffer. pH 8.8

1.5 M Tris-HCl

0.4% SDS

4. Stacking Gel Buffer. pH 6.8

0.5 M Tris-HCl

0.4% SDS

5. 10x electrode (running) Buffer

250 mM Tris base
1.92 M glycine
1% SDS
* Store at 4°C. If precipitation occurs, warm to room temp before use.
* Dilute 50 mL of 10X electrode buffer per 450 ml of DDW before use.

6. 10 x TBS. pH 7.5

200 mM Tris base

1.37 M NaCl

38mL of 1M HCl/L of TBS made

7. TBST

Dilute 10x TBS to 1x with DDW.

25% Tween needed (mL) = Volume of TBS (mL) x 0.004

8. Blocking Solution

Add 5g of skim milk powder per 100ml TBST.

9. Transfer Buffer

0.05% SDS

192 mM glycine

25 mM Tris Base

Methanol 20% (add day of)

10. Coomaisse Blue Gel stain

40 mL methanol

10 mL acetic Acid

0.25g Coomassie Blue

50 mL DDW

11. Membrane stain

MemCode™ reversible PVDF stain (Pierce, Thermo Scientific)

PROTOCOL

Cuff and Skinned fibre preparation

a) Pool 10 cuffs and their respective skinned fibres into separate Eppendorf tubes with 20 µl of Buffer A (see Part I).
b) Add 10 µl of 3x sample buffer to each tube.
c) Freeze-thaw the cuffs and skinned fibres 3x.
d) With an Eppendorf tube homogenizer, plunge 3x into to both tubes to help disrupt the membranes.
e) If needed, spin the samples to ensure all the volume is at the bottom of the Eppendorf tubes.

Gel Electrophoresis and membrane transfer

Assembly of Mini-PROTEAN 3 module:

a) Clean glass plates with soap and water, rinse well with DDW. Before use, wipe plates carefully with methanol on a kimwipe and allow to dry.

b) Assemble the glass plates and place into casting frame keeping the short plate facing front. Insure both plate bottoms are flush on a level surface and lock the pressure cams to secure plates in place. Secure the casting frame in the casting stand (don't forget to place the gray rubber gasket down before inserting the casting frame).

Cast Gel

Preparation of gel (running or stacking, 10mL for 2x0.75mm mini gels):

a) Prepare the monomer solution by mixing all reagents except TEMED and 10% AP.

For 2 Gels

| Separating 14% | | Separating 10% | | Stacking 4% | |
|---|---|---|---|---|---|
| ProtoGel | 4.66 mL | ProtoGel | 3.33 mL | ProtoGel | 1.3 mL |
| 4x Resolving buffer | 2.5 mL | 4x Resolving buffer | 2.5 mL | 4x Stacking buffer | 2.5 mL |
| DDW | 2.83 mL | DDW | 3.96 mL | DDW | 6.1mL |
| AP | 100 µL | AP | 100 µL | AP | 100 µL |
| TEMED | 10 µL | TEMED | 10 µL | TEMED | 20 µL |

** Do not add AP and Temed until immediately before casting the gel

** Do this step in the fume hood

b) Immediately prior to pouring the 14% running gel, add AP and Temed, swirl gently to initiate polymerization and pipette 2.5 mL into gel cast.
c) Add methanol to the top of the 14% separating gel before it sets, to eliminate any bubbles and to straighten the gel.
d) After the 14% separating gel polymerizes, drain all methanol, using the corners of a kim wipe to ensure it is emptied.
e) Prepare the 10% running gel by adding AP and Temed, swirl gently to initiate polymerization and pipette 1.0 mL into gel cast above the 14% running gel (total volume pipetted so far = 3.5 mL).
f) After the 10% separating gel polymerizes, drain all methanol, using the corners of a kim wipe to ensure it is emptied.
g) Pour the stacking solution between glass plates until the top of the short plate is reached. Insert the comb and allow gel to polymerize.
h) Gently remove the comb and rinse the wells thoroughly with DDW or electrode buffer.

Assembly of electrophoresis module and sample loading:

a) Remove casting frame from stand and place gel cassettes into electrode assembly (be sure the short plate faces inward toward the notches of the gasket). If you are only using one gel, be sure to use a buffer dam.

b) Slide the gel cassettes and electrode assembly into the clamping frame. Press down on the electrode assembly while closing the two cam levers of the clamping frame. Place whole assembly into the mini-tank.
c) Fill the inner chamber with running buffer (half way between the tops of the tall and short glass plates, DO NOT overfill). Fill the outer chamber with ~300 mL of running buffer.
d) Place the loading guide between the two gels and load samples slowly into each well.
e) Load the skinned fibres and their respective cuffs in a gradient fashion:

| Sample: | Concentration: | Volume loaded | Description |
|---|---|---|---|
| **Skinned Fibres** | 1skinned fibre/ 3 µL | 12 µL | Protein equivalent to 4 skinned fibres |
| | 1skinned fibre/ 3 µL | 6 µL | Protein equivalent to 2 skinned fibres |
| | 1skinned fibre/ 3 µL | 3 µL | Protein equivalent to 1 skinned fibre |
| | 1skinned fibre/ 3 µL | 1.5 µL | Protein equivalent to ½ skinned fibre |
| | 1skinned fibre/ 3 µL | 0.75 µL | Protein equivalent to ¼ skinned fibre |
| **Cuffs** | 1cuff / 3 µL | 12 µL | Protein equivalent to 4 cuffs |
| | 1cuff / 3 µL | 6 µL | Protein equivalent to 2 cuffs |
| | 1cuff / 3 µL | 3 µL | Protein equivalent to 1 cuff |
| | 1cuff / 3 µL | 1.5 µL | Protein equivalent to ½ cuffs |
| | 1cuff / 3 µL | 0.75 µL | Protein equivalent to ¼ cuffs |

f) Connect the apparatus to the power pack and run at 120 V for 90 min. or until the blue dye front travels to the bottom edge of the plate.
g) Remove the gels carefully, discarding the stacking gel, and transfer to plastic trays to equilibrate in transfer buffer.

Transfer Blotting

a) Prior to use, the PVDF membrane (Immobilon-P, Millipore, Bedford, MA, USA) must be cut to the dimensions of the gel and immersed in methanol for 10 seconds.
b) Equilibrate the gel and soak the membrane, filter paper, and fibre pads in transfer buffer (5 min. to 1 hour depending on gel thickness).
c) Prepare the gel sandwich.
    a. Place the cassette, with the clear side down, in a container (shallow tupperware) containing transfer buffer.
    b. Place one pre-wetted fibre pad on the clear side of the cassette.
    c. Place a sheet of filter paper on the fibre pad.
    d. Place the pre-wetted membrane on the filter paper.
    e. Place the equilibrated gel on the membrane.
    f. Place a filter paper on the gel.
    g. Complete the sandwich by placing the fibre pad on the filter paper.
        * Remove any air bubbles which may have formed with a glass tube, gently roll the tube over the sandwich in one direction.

   h. Close the cassette firmly, being careful not to move the gel and filter paper sandwich.
   i. Lock the cassette with the white latch.
   j. Place cassette in module 'black at back'. Repeat with other cassettes.

d) Add the frozen Bio-Ice cooling unit. Fill the tank with buffer.
e) Add a standard stir bar to help maintain even buffer temperature and ion distribution in the tank. Set the speed for as fast as possible.
f) Put on lid, plug the cables into the power supply, and run the blot. (1 hour at 100V).
g) Upon completion of the run, dissemble the blotting sandwich and remove the membrane for development. Clean and save the fibre pads and cassettes with detergent and DDW and dispose of the gel and filter pads.

MemCode™ Reversible staining (Thermo Scientific 24585):

a) Once transfer is complete, remove the membrane from the sandwich and place it protein side up in a square Petri dish.
b) Add 5 mL of DDW and rock three times and then quickly decant.
c) Add 5 mL of MemCode™ sensitizer and place on rocker for 2 min, then decant.
d) Add 5 mL of MemCode™ reversible stain and place on rocker for 1 min, then decant.
e) Add 5 mL of MemCode™ destain and rock three times and then quickly decant. Repeat this step an additional two times.
f) Add 2.5 mL of MemCode™ destain with 2.5 mL of methanol and place on rocker for 5 min, then decant.
g) Add 5 ml of DDW and rock three times and then quickly decant. Repeat this step and additional four times.
h) If proteins are not seen in the cuffs, then it may not be worth wasting antibodies and blotting (see Figure below).
i) Once satisfied with the membrane, reverse the satin by adding 2.5 mL MemCode™ destain with 2.5 mL of methanol and place on rocker for 10 min then decant.
j) Add 5 ml of DDW and rock three times and then quickly decant. Repeat this step and additional four times.
k) The membrane is now ready for blocking.

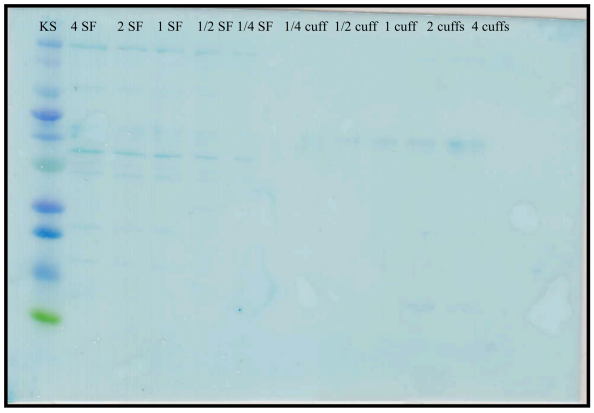


**Figure A1. 2**. Representative Memcode™ reversible stain applied onto PVDF membrane that was loaded with skinned fibre equivalents and sarcolemmal cuff equivalents. KS, kaleidescope standard; SF, skinned fibre equivalent.

Membrane Blocking

a) Once transfer or MemCode™ reversible staining is complete, place the membrane *protein side up* in square Petri dishes.
b) Block membrane with TBST with 5% skim milk for at least one hour at room temperature with gentle agitation (can be left overnight in blocking solution). Use ~5 mL per gel.

Incubations and Membrane Exposure

Antibodies

a) Dispose of blocking solution and cut the membrane into three strips: 1) 75 – 250 kDa, 2) 25 – 75 kDa and 3) 10 – 25 kDa. This maximizes the amount of data obtained from one set of cuffs and fibres, and since there was both 10% and 14% separating gel there should be efficient separation of all bands using the Kaleidescope ladder.
b) Add 1° Antibody in TBST with 5% skim milk as follows to each strip in correspondence with molecular weight:

| Antibody | Size (kDa) | Dilution | µL in 5 mL |
|---|---|---|---|
| β-dystroglycan | 43-50 | 1:500 | 10 |
| Caveolin-3 | 17 | 1:1000 | 5 |
| DHPR | 170 | 1:500 | 5 |
| SERCA1 ATPase | 110 | 1:1000 | 5 |
| SERCA2 ATPase | 100 | 1:2000 | 5 |
| GM130 | 130 | 1:2000 | 5 |
| Emerin | 37 | 1:3000 | 1.67 |
| COX IV subunit 4 | 15 | 1:3000 | 1.67 |
| MitoNEET | 17 | 1:3000 | 1.67 |

c) Incubate with gentle agitation at room temp for the time specified for the specific antibody/protein (See MSDS ~1-2 hours).
d) Wash 3x5 min with TBST
e) Add 2° Antibody (dependent on 1°) in TBST with 5% skim milk as follows:

| Antibody | anti- | Dilution | µL in 10 mL |
|---|---|---|---|
| β-dystroglycan | mouse | 1:10 000 | 1 |
| Caveolin-3 | mouse | 1:20 000 | 0.5 |
| DHPR | mouse | 1:20 000 | 0.5 |
| SERCA1 ATPase | mouse | 1:20 000 | 0.5 |
| SERCA2 ATPase | mouse | 1:20 000 | 0.5 |
| GM130 | rabbit | 1:20 000 | 0.5 |
| Emerin | rabbit | 1:10 000 | 1 |
| COX IV subunit 4 | mouse | 1:20 000 | 0.5 |
| MitoNEET | rabbit | 1:10 000 | 0.5 |

f) Incubate (shaking/rocking) at room temp for the time specified for the specific antibody/protein (See MSDS ~1-2 hours).
g) Wash 3x5 min with TBST

Luminata™ Forte Western HRP Substrate (Millipore) detection

a) Pour out all TBST from the Petri dish.
b) Pipette 2 mL of Luminata™ forte pre-mix solution over membrane and incubate for 5 minutes with agitation.
c) Blot edge of membrane with paper towel while holding vertically (don't touch protein side of membrane) to remove excess substrate solution.
d) Place membrane between two transparencies.
e) Place the enclosed membrane, protein side up, in the Gel Dock and run the 'auto Expose' function.
f) If quantifying use Image J.

REFERENCES

Bligh, E. G., & Dyer, W. J. (1959). A rapid method of total lipid extraction and purification. *Can J Biochem Physiol, 37*(8), 911-917.

Kupke, I. R., & Zeugner, S. (1978). Quantitative high-performance thin-layer chromatography of lipids in plasma and liver homogenates after direct application

Peters SJ, Harris RA, Wu P, Pehleman TL, Heigenhauser GJ, & Spriet LL (2001). Human skeletal muscle PDH kinase activity and isoform expression during a 3-day high-fat/low-carbohydrate diet. *Am J Physiol Endocrinol Metab* **281**, E1151-E1158.

Weerheim, A. M., Kolb, A. M., Sturk, A., & Nieuwland, R. (2002). Phospholipid composition of cell-derived microparticles determined by one-dimensional high-performance thin-layer chromatography. *Anal Biochem, 302*(2), 191-198.

*Part iv Solid Phase Extraction of Phospholipids from Sarcolemmal Cuffs*

(http://www.cyberlipid.org/fraction/frac0010.htm)

(Pernet, et al., 2006)

**Apparatus**

Glass columns (inside diameter: 8-10 mm, length: 20 cm) with a stopcock (glass or Teflon) at the bottom to control the solvent flow.

**Reagents**

Silica gel 60 A, 230-400 mesh

Chloroform, methanol and acetone, analytical grade.

**Procedure**

1. Soak enough silica gel (corresponding to amount of lipid) in water 6% (w/w). Study shows that recovery of phospholipids was significantly increased (approaching 100%) when the silica gel was first solvated with water (Pernet, et al., 2006).

*Indeed the use of water onto silica is generally thought to reduce adsorption of polar lipids on HPTLC and TLC plates due to partition effects between water and the lipids; leading to leakage of phospholipids into neutral lipid fraction. However Pernet et al., (2006) showed that when the neutral lipid:polar lipid ratio was similar (~ 40:60) the leakage of polar lipids into neutral lipid fraction was significantly reduced to a suggested zero level.*

***Another consideration is the amount of silica gel used. It has been previously shown that by increasing the amount of sorbent relative to the amount of lipid drastically reduces the recovery of phospholipids (namely, PC, since its choline group has high affinity for silica, corresponding to its low migration in HPTLC and TLC plates, for this reason Sphingomyelin may also be affected). It has been shown that a range of 1 – 2.5% ratio of sorbent:lipid for ~100% recovery (Pernet, et al., 2006). That is for 5 mg of lipid there can be 500 mg of silica or for 2.5 mg of lipid there can be 100 mg of silica for optimal recovery. At a ratio of 0.02% the recovery of PC drastically dropped to ~25% (theory of course if 100% of PC is recovered than the other PL species should be 100% recovered).* ***If we consider my calculations of 40 ng of lipid in a Sarcolemmal Cuff (Thesis Proposal Document) then a 1% ratio would require 0.04 mg of silica gel. But if we pool 5 cuffs, we get 200 ng of lipid requiring 0.2 mg of silica gel.***

2. After draining the water from the silica gel, precondition the column with 1 ml of methanol (3x) then 1 ml of chloroform (3x) (Pernet, et al., 2006).

> ***It is important to make sure the silica gel is solvated in order for the organization of binding moieties (http://lipidlibrary.aocs.org/topics/spe_alm/index.htm).*

3. On the last conditioning with chloroform, allow the solvent level to drop to the top of the silica gel.

4. Transfer lipid sample in chloroform (~1mL; may need to be dried down prior to this to get the correct volume).

5. After complete elution of the solvent, add carefully 2 ml of chloroform. This will elute **neutral lipids** (hydrocarbons, pigments, sterols, triglycerides, waxes, fatty acids).

> ***Cyberlipid.com suggest 10 ml of chloroform not 2 ml, but considering the small amount of lipid in cuffs we need to drastically reduce this amount to prevent overlap and possible leakage of Phospholipids into the neutral fraction (Pernet, et al., 2006).*

6. After draining the first solvent, add on the column 3 ml of acetone/methanol (9/1). This will elute **glycolipids** (cerebrosides, sulfatides, mono- and digalactosyl diglycerides, sterol glycosides) and **ceramides**.

7. After draining the second solvent, add on the column 2 ml methanol. This will elute all the **phospholipids**.

8. Take the phospholipid fraction and then dry down and reconstitute in 1 ml of chlorofom:methanol (2:1) for future analysis, including, phosphate assay, HPTLC and subsequent GC analysis.

> **Other considerations**
>
> * Study showed that at lower amounts of lipid levels compared to sorbent homemade columns increase percent recovery of phospholipid (Pernet, et al., 2006).
>
> * Need to make sure ~ 100 % recovery of phospholipids, because if some species are selectively retained on the silica gel then this will throw off FA composition data. **This specific retention is more of a problem on NH2 columns not silica gel columns, whereby NH2 columns retain acidic phospholipids (Pernet, et al., 2006).*

* Cross contamination of neutral lipids such as plasmalogens that give off dimethyl acetals is not of particular concern here because, after SPE the phospholipids will be placed onto HPTLC to separate out the phospholipid species.

* Flow rate of solvent should be controlled as much as possible (1 ml / min; http://www.cyberlipid.org/fraction/frac0010.htm)

## APPENDIX 2: Representative Western Blots

*Part I Determination of optimal primary and secondary antibody dilutions*

To determine the optimal primary and secondary antibody dilutions, plantaris muscle was homogenized and a gradient of protein weight was loaded (1.25 µg, 2.5 µg, 7.5 µg, 12.5 µg, and 17.5 µg). These primary and secondary dilutions were then used for Western blot analysis on SL cuffs and skinned fibre segments. Due to the low volume that the SL cuffs and skinned fibre segments were stored in, protein concentration could not be determined.

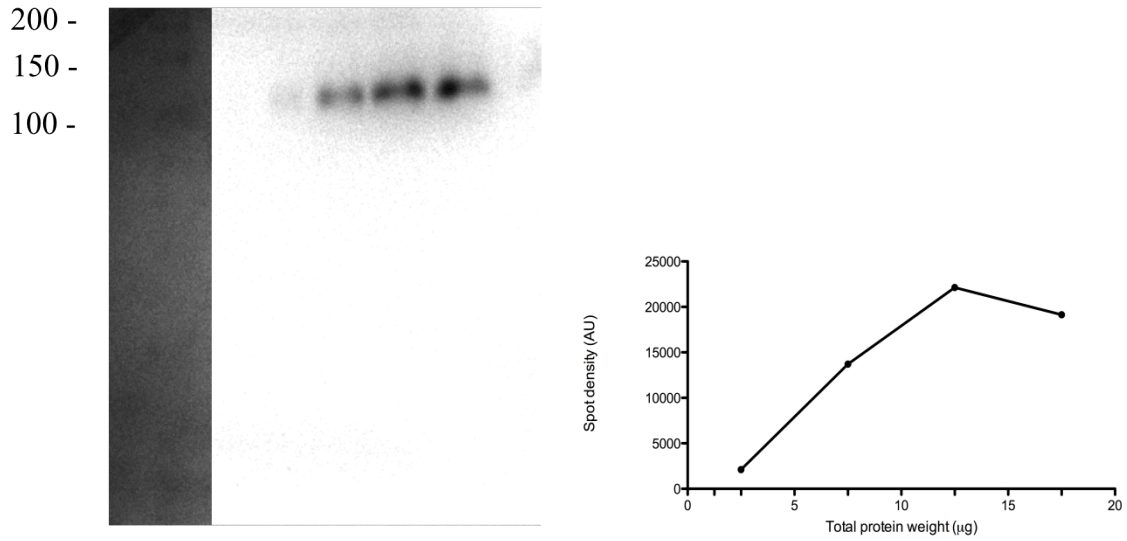


**Figure A2. 1.** Representative Western blots of a gradient of increasing protein concentration of whole muscle homogenate probed for the t-tubule specific protein DHPR (170-200 kDa protein; 1° = 1/500, 2° = 1/20 000).

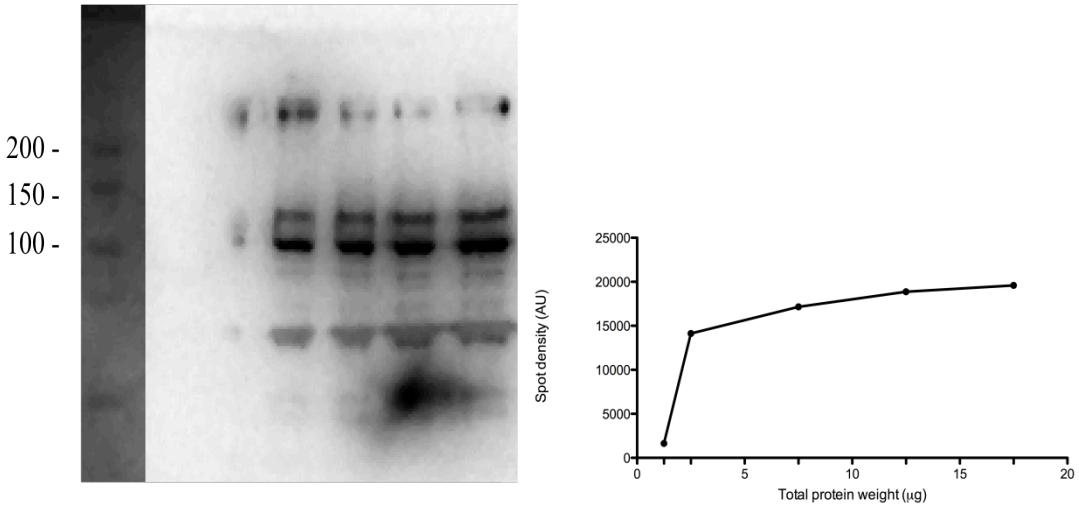


**Figure A2. 2.** Representative Western blots of a gradient of increasing protein concentration of whole muscle homogenate probed for sarco(endo)plasmic reticulum $Ca^{2+}$-ATPase 1 (SERCA 1), a marker for the sarcoplasmic reticulum (110 kDa protein; 1° = 1/1000, 2° = 1/20 000).

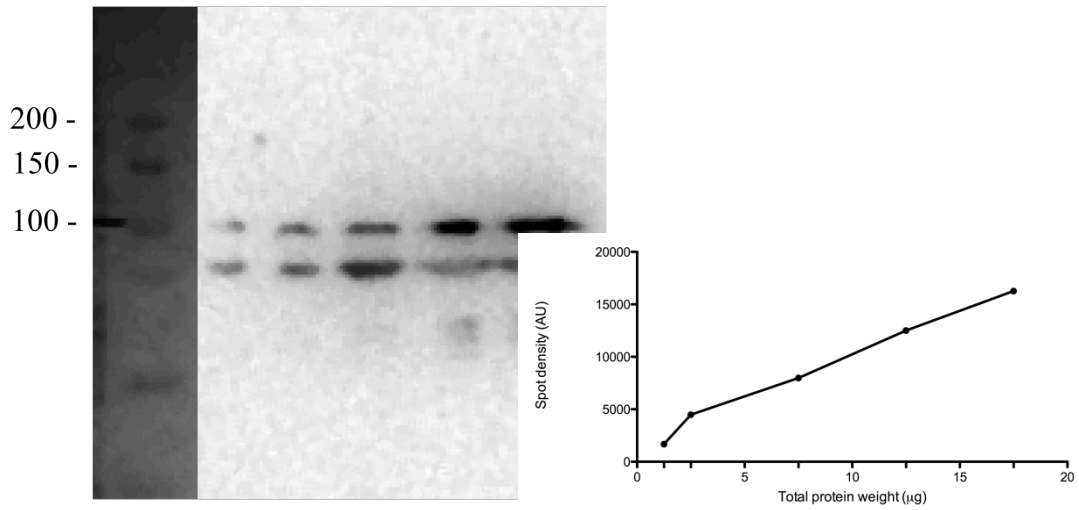


**Figure A2. 3.** Representative Western blots of a gradient of increasing protein concentration of whole muscle homogenate probed for sarco(endo)plasmic reticulum $Ca^{2+}$-ATPase 2 (SERCA 2), a marker for the sarcoplasmic reticulum (100 kDa protein; 1° = 1/2000, 2° = 1/20 000).

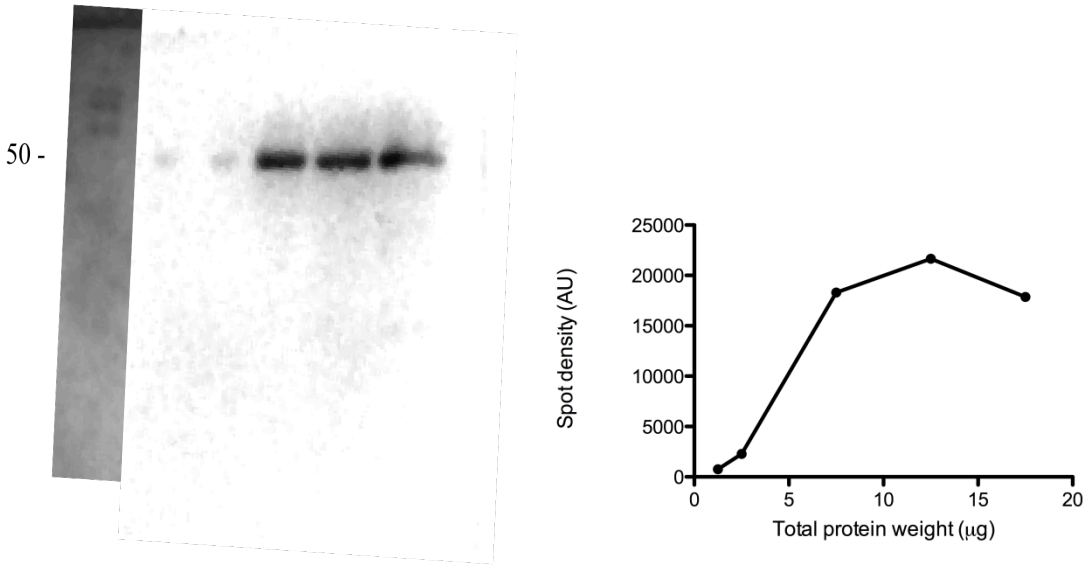


**Figure A2. 4**. Representative Western blots of a gradient of increasing protein concentration of whole muscle homogenate probed for β-dystroglycan, a marker for the sarcolemma (43-50 kDa protein; 1° = 1/500, 2° = 1/10 000).

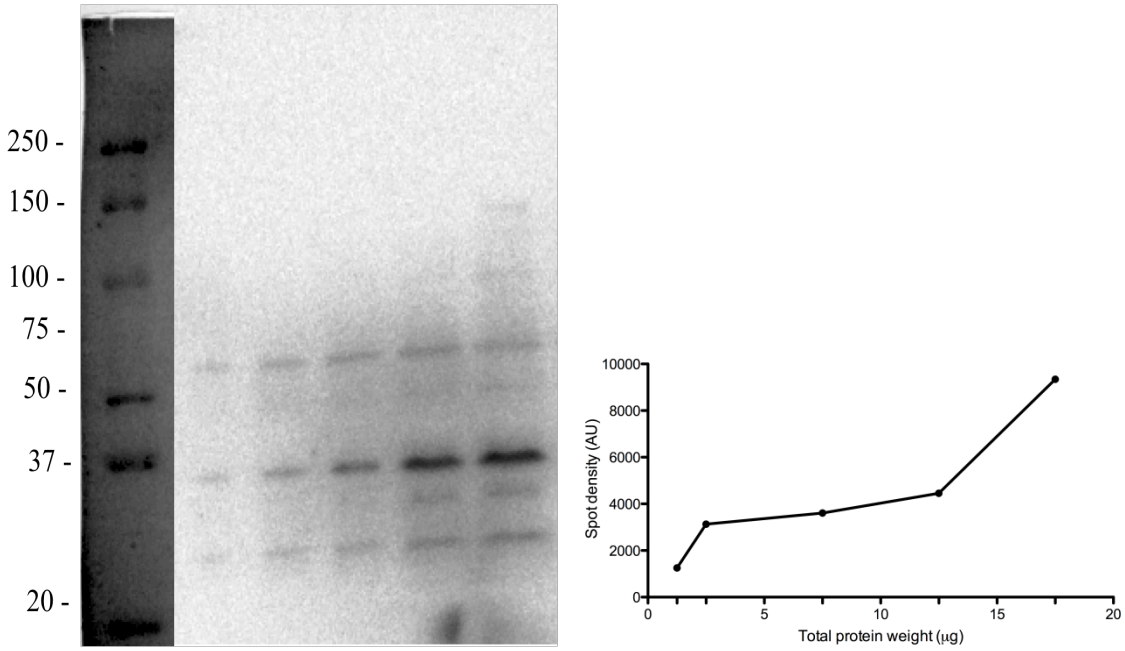


**Figure A2. 5.** Representative Western blots of a gradient of increasing protein concentration of whole muscle homogenate probed for emerin, a marker for the nucleus (37 kDa protein; 1° = 1/2000, 2° = 1/10 000).

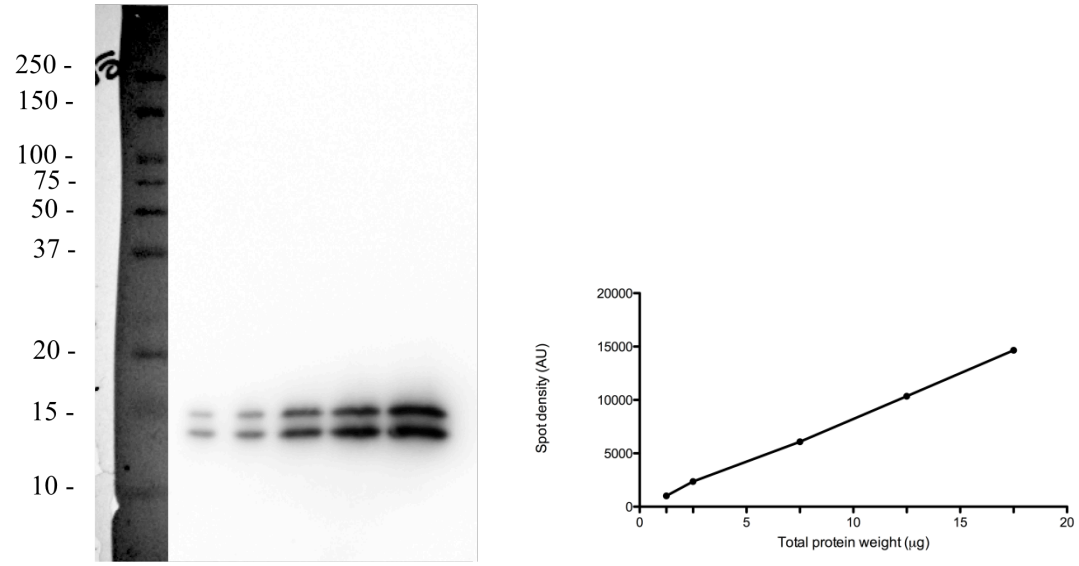


**Figure A2. 6**. Representative Western blots of a gradient of increasing protein concentration of whole muscle homogenate probed for MitoNEET, a marker for the outer mitochondrial membrane (17 kDa protein; 1° = 1/3000, 2° = 1/10 000).

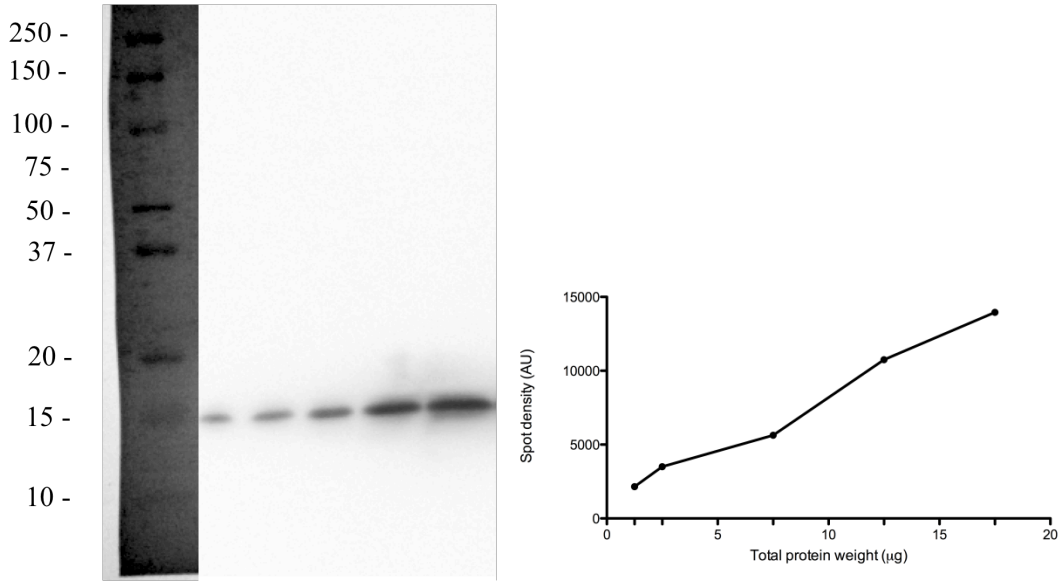


**Figure A2. 7.** Representative Western blots of a gradient of increasing protein concentration of whole muscle homogenate probed for COX IV subunit 4, a marker for the inner mitochondrial membrane (15 kDa protein; 1° = 1/3000, 2° = 1/20 000).

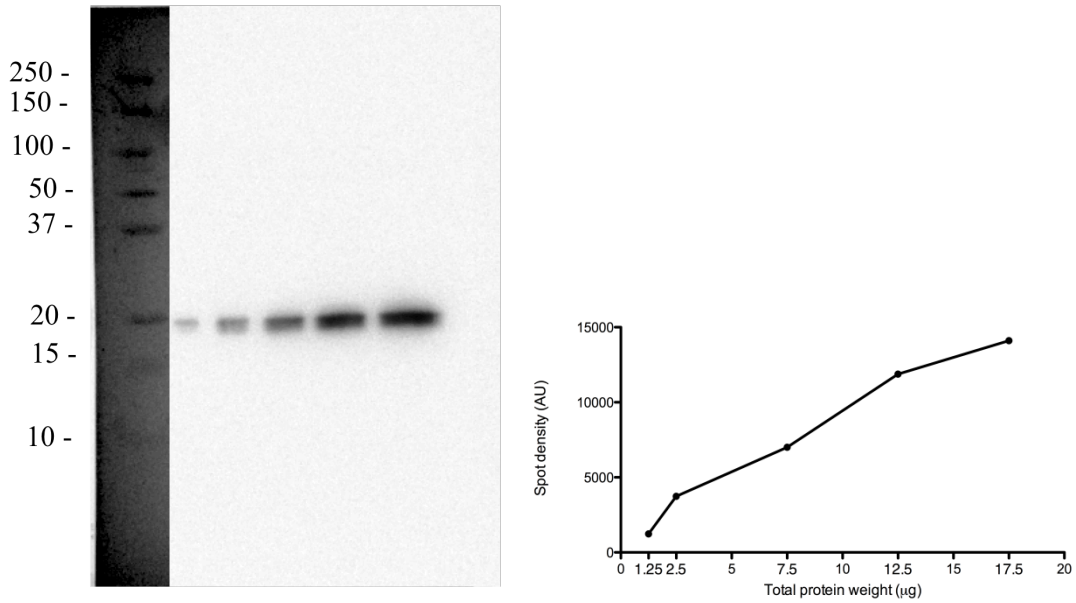


**Figure A2. 8.** Representative Western blots of a gradient of increasing protein concentration of whole muscle homogenate probed for caveolin-3, a muscle specific marker for caveolar regions (17 kDa protein; 1° = 1/1000, 2° = 1/20 000).

**APPENDIX 3: Complete Data Tables & Figures & Representation of Data**

**Table A3. 1.** Single fibre characteristics from each pool of 10 utilized for lipid analysis (n=6).

| | Fibre Length (mm) | Fibre Diameter (µm) | Surface area ($mm^1$) | | Fibre Length (mm) | Fibre Diameter (µm) | Surface area ($mm^1$) |
|---|---|---|---|---|---|---|---|
| **Pool** 1 | | | | **Pool** 4 | | | |
| 1 | 3.16 | 50.00 | 0.50 | 1 | 3.68 | 47.50 | 0.55 |
| 2 | 2.63 | 55.00 | 0.45 | 2 | 2.89 | 50.00 | 0.45 |
| 3 | 3.37 | 47.50 | 0.50 | 3 | 2.74 | 50.00 | 0.43 |
| 4 | 2.53 | 57.50 | 0.46 | 4 | 2.79 | 50.00 | 0.44 |
| 5 | 3.79 | 52.50 | 0.62 | 5 | 3.26 | 52.50 | 0.54 |
| 6 | 2.74 | 55.00 | 0.47 | 6 | 1.68 | 52.50 | 0.28 |
| 7 | 1.84 | 60.00 | 0.35 | 7 | 1.84 | 50.00 | 0.29 |
| 8 | 1.47 | 42.50 | 0.20 | 8 | 2.95 | 55.00 | 0.51 |
| 9 | 1.68 | 57.50 | 0.30 | 9 | 1.58 | 50.00 | 0.25 |
| 10 | 2.53 | 55.00 | 0.44 | 10 | 2.11 | 50.00 | 0.33 |
| Sum | 25.74 | | 4.29 | Sum | 25.53 | | 4.06 |
| **Pool 2** | | | | **Pool 5** | | | |
| 1 | 2.63 | 45.00 | 0.37 | 1 | 2.63 | 62.50 | 0.52 |
| 2 | 2.84 | 42.50 | 0.38 | 2 | 4.21 | 50.00 | 0.66 |
| 3 | 2.26 | 42.50 | 0.30 | 3 | 4.11 | 52.50 | 0.68 |
| 4 | 2.21 | 45.00 | 0.31 | 4 | 2.89 | 50.00 | 0.45 |
| 5 | 2.00 | 50.00 | 0.31 | 5 | 2.95 | 50.00 | 0.46 |
| 6 | 2.11 | 57.50 | 0.38 | 6 | 2.11 | 50.00 | 0.33 |
| 7 | 2.74 | 60.00 | 0.52 | 7 | 2.74 | 47.50 | 0.41 |
| 8 | 2.68 | 55.00 | 0.46 | 8 | 3.68 | 50.00 | 0.58 |
| 9 | 2.89 | 55.00 | 0.50 | 9 | 4.21 | 50.00 | 0.66 |
| 10 | 1.68 | 65.00 | 0.34 | 10 | 4.32 | 50.00 | 0.68 |
| Sum | 24.05 | | 3.88 | Sum | 33.84 | | 5.43 |
| **Pool 3** | | | | **Pool 6** | | | |
| 1 | 4.47 | 50.00 | 0.70 | 1 | 3.16 | 62.50 | 0.62 |
| 2 | 3.16 | 55.00 | 0.55 | 2 | 4.47 | 75.00 | 1.05 |
| 3 | 4.63 | 60.00 | 0.87 | 3 | 2.63 | 50.00 | 0.41 |
| 4 | 4.74 | 67.50 | 1.00 | 4 | 2.32 | 55.00 | 0.40 |
| 5 | 3.95 | 47.50 | 0.59 | 5 | 3.21 | 50.00 | 0.50 |
| 6 | 2.63 | 57.50 | 0.48 | 6 | 2.68 | 52.50 | 0.44 |
| 7 | 2.53 | 60.00 | 0.48 | 7 | 2.00 | 50.00 | 0.31 |
| 8 | 2.37 | 55.00 | 0.41 | 8 | 2.89 | 47.50 | 0.43 |
| 9 | 2.63 | 55.00 | 0.45 | 9 | 2.37 | 45.00 | 0.33 |
| 10 | 4.74 | 52.50 | 0.78 | 10 | 2.42 | 50.00 | 0.38 |
| Sum | 35.84 | | 6.31 | Sum | 28.16 | | 4.89 |
| | | | | Total average | | | |
| | | | | | 2.9 ± 0.1 | 52.8 ±0.8 | 0.5 ± 0.0 |

**Table A3. 2.** Single fibre characteristics from each pool of 10 utilized for Western blot analysis (n=9).

| | Fibre Length (mm) | Fibre Diameter (μm) | Surface area ($mm^{1}$) | | Fibre Length (mm) | Fibre Diameter (μm) | Surface area ($mm^{1}$) |
|---|---|---|---|---|---|---|---|
| **Pool** 1 | | | | **Pool** 4 | | | |
| 1 | 2.37 | 52.50 | 0.39 | 1 | 3.42 | 52.50 | 0.56 |
| 2 | 1.58 | 50.00 | 0.25 | 2 | 5.26 | 50.00 | 0.83 |
| 3 | 3.95 | 55.00 | 0.68 | 3 | 5.37 | 55.00 | 0.93 |
| 4 | 3.68 | 50.00 | 0.58 | 4 | 4.11 | 50.00 | 0.64 |
| 5 | 3.26 | 50.00 | 0.51 | 5 | 1.68 | 50.00 | 0.26 |
| 6 | 2.26 | 50.00 | 0.36 | 6 | 4.84 | 50.00 | 0.76 |
| 7 | 3.16 | 47.50 | 0.47 | 7 | 1.89 | 47.50 | 0.28 |
| 8 | 1.84 | 55.00 | 0.32 | 8 | 2.11 | 55.00 | 0.36 |
| 9 | 1.68 | 50.00 | 0.26 | 9 | 1.68 | 50.00 | 0.26 |
| 10 | 2.32 | 47.50 | 0.35 | 10 | 2.16 | 47.50 | 0.32 |
| Sum | 26.11 | | 4.17 | Sum | 32.53 | | 5.22 |
| **Pool 2** | | | | **Pool 5** | | | |
| 1 | 2.63 | 52.50 | 0.43 | 1 | 3.16 | 52.50 | 0.52 |
| 2 | 2.63 | 50.00 | 0.41 | 2 | 3.16 | 50.00 | 0.50 |
| 3 | 2.47 | 55.00 | 0.43 | 3 | 2.21 | 55.00 | 0.38 |
| 4 | 2.11 | 50.00 | 0.33 | 4 | 2.68 | 50.00 | 0.42 |
| 5 | 2.11 | 50.00 | 0.33 | 5 | 2.89 | 50.00 | 0.45 |
| 6 | 3.32 | 50.00 | 0.52 | 6 | 3.42 | 50.00 | 0.54 |
| 7 | 2.84 | 47.50 | 0.42 | 7 | 2.74 | 47.50 | 0.41 |
| 8 | 2.42 | 55.00 | 0.42 | 8 | 3.32 | 55.00 | 0.57 |
| 9 | 1.58 | 50.00 | 0.25 | 9 | 2.79 | 50.00 | 0.44 |
| 10 | 2.11 | 47.50 | 0.31 | 10 | 2.21 | 47.50 | 0.33 |
| Sum | 24.21 | | 3.86 | Sum | 28.58 | | 4.56 |
| **Pool 3** | | | | **Pool 6** | | | |
| 1 | 3.68 | 52.50 | 0.61 | 1 | 3.95 | 52.50 | 0.65 |
| 2 | 2.74 | 50.00 | 0.43 | 2 | 2.21 | 50.00 | 0.35 |
| 3 | 4.84 | 55.00 | 0.84 | 3 | 2.63 | 55.00 | 0.45 |
| 4 | 2.37 | 50.00 | 0.37 | 4 | 2.26 | 50.00 | 0.36 |
| 5 | 2.21 | 50.00 | 0.35 | 5 | 1.58 | 50.00 | 0.25 |
| 6 | 3.00 | 50.00 | 0.47 | 6 | 2.53 | 50.00 | 0.40 |
| 7 | 3.16 | 47.50 | 0.47 | 7 | 2.79 | 47.50 | 0.42 |
| 8 | 2.11 | 55.00 | 0.36 | 8 | 1.89 | 55.00 | 0.33 |
| 9 | 2.21 | 50.00 | 0.35 | 9 | 2.37 | 50.00 | 0.37 |
| 10 | 2.11 | 47.50 | 0.31 | 10 | 2.11 | 47.50 | 0.31 |
| Sum | 28.42 | | 4.56 | Sum | 24.32 | | 3.88 |

**Table A3. 2**. Single fibre characteristics from each pool of 10 utilized for Western blot analysis continued (n=9).

| | Fibre Length (mm) | Fibre Diameter (μm) | Surface area ($mm^{1}$) | | Fibre Length (mm) | Fibre Diameter (μm) | Surface area ($mm^{1}$) |
|---|---|---|---|---|---|---|---|
| **Pool** 7 | | | | **Pool** 9 | | | |
| 1 | 3.58 | 52.50 | 0.59 | 1 | 2.11 | 52.50 | 0.35 |
| 2 | 2.89 | 50.00 | 0.45 | 2 | 3.16 | 50.00 | 0.50 |
| 3 | 2.47 | 55.00 | 0.43 | 3 | 3.21 | 55.00 | 0.55 |
| 4 | 2.21 | 50.00 | 0.35 | 4 | 2.21 | 50.00 | 0.35 |
| 5 | 2.63 | 50.00 | 0.41 | 5 | 1.84 | 50.00 | 0.29 |
| 6 | 2.74 | 50.00 | 0.43 | 6 | 2.11 | 50.00 | 0.33 |
| 7 | 1.89 | 47.50 | 0.28 | 7 | 1.58 | 47.50 | 0.24 |
| 8 | 2.89 | 55.00 | 0.50 | 8 | 1.32 | 55.00 | 0.23 |
| 9 | 2.21 | 50.00 | 0.35 | 9 | 2.68 | 50.00 | 0.42 |
| 10 | 2.00 | 47.50 | 0.30 | 10 | 2.89 | 47.50 | 0.43 |
| Sum | 25.53 | | 4.09 | Sum | 23.11 | | 3.68 |
| **Pool 8** | | | | Total average | 2.6 ± 0.1 | 50.8 ± 0.3 | 0.4 ± 0.0 |
| 1 | 2.42 | 52.50 | 0.40 | | | | |
| 2 | 2.00 | 50.00 | 0.31 | | | | |
| 3 | 2.11 | 55.00 | 0.36 | | | | |
| 4 | 1.58 | 50.00 | 0.25 | | | | |
| 5 | 3.42 | 50.00 | 0.54 | | | | |
| 6 | 1.68 | 50.00 | 0.26 | | | | |
| 7 | 1.58 | 47.50 | 0.24 | | | | |
| 8 | 1.74 | 55.00 | 0.30 | | | | |
| 9 | 1.58 | 50.00 | 0.25 | | | | |
| 10 | 4.00 | 47.50 | 0.60 | | | | |
| Sum | 22.11 | | 3.51 | | | | |

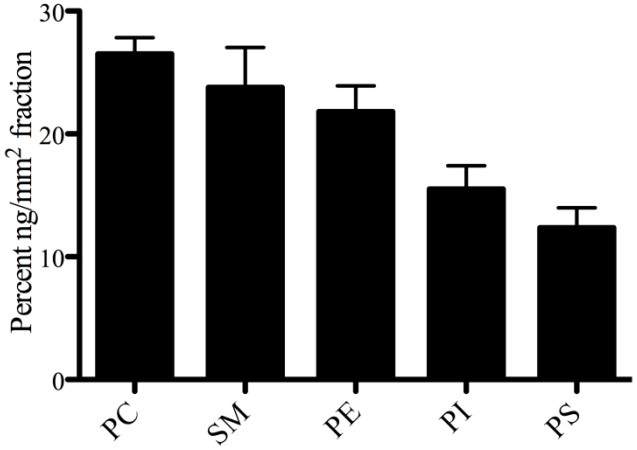


**Figure A3. 1.** Percent mole fraction of major phospholipid species of sarcolemmal membranes from extensor digitorum longus (EDL) skinned fibres. Values are represented as means ± standard error (n=6). PC, phosphatidylcholine; SM, sphingomyelin; PE, phosphatidylethanolamine; PI, phosphatidylinositol; PS, phosphatidylserine.

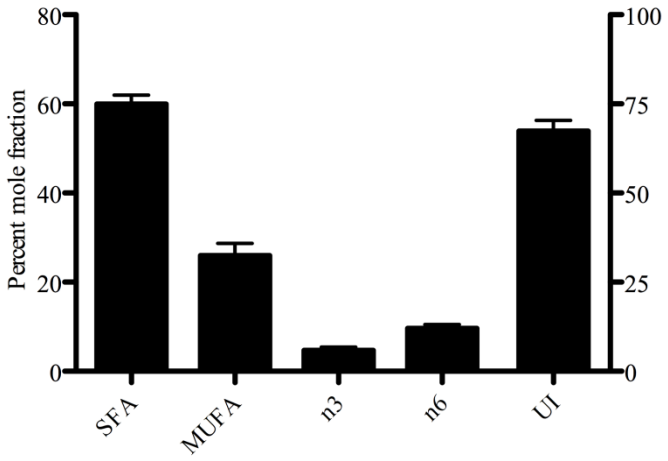


**Figure A3. 2**. Percent mole fraction of total fatty acid subclasses independent of phospholipid species of sarcolemmal membranes from EDL skinned fibres. Values are represented as means ± standard error with SFA, MUFA, n3, and n6 represented on the left *y*-axis and UI represented on the right (n=6). SFA, saturated fatty acids; MUFA, monounsaturated fatty acids; n3, n3 polyunsaturated fatty acids; n6, n6 polyunsaturated fatty acids; UI, unsaturation index = $\sum m_i$ x $n_i$, where $m_i$ is the mole percentage and $n_i$ is the number of carbon–carbon double bonds of the fatty acid.

**Table A3. 3**. Percentage mole fraction of phospholipid species of sarcolemmal membranes from EDL skinned fibres (n=6).

| Fatty acid subclasses | Phosphatidylcholine | Sphingomyelin | Phosphatidylethanolamine | Phosphatidylinositol | Phosphatidylserine |
|---|---|---|---|---|---|
| 12:0 | 2.4 ± 1.0 | 3.2 ± 1.1 | 3.6 ± 1.7 | 2.3 ± 1.6 | 0.6 ± 0.4 |
| 14:0 | 1.9 ± 0.6 | 1.6 ± 0.9 | 2.0 ± 0.8 | 3.1 ± 1.8 | 2.0 ± 1.1 |
| 15:0 | 3.5 ± 1.1 | 6.4 ± 2.4 | 4.3 ± 1.0 | 0.6 ± 0.3 | 1.4 ± 1.1 |
| 16:0 | 28.9 ± 3.1 | 27.1 ± 3.8 | 20.4 ± 4.3 | 19.0 ± 5.1 | 34.1 ± 6.3 |
| 17:0 | 1.4 ± 0.7 | 2.3 ± 1.1 | 2.9 ± 0.7 | 0.7 ± 0.7 | 1.4 ± 1.1 |
| 18:0 | 14.0 ± 3.2 | 21.7 ± 6.1 | 14.6 ± 5.2 | 37.4 ± 10.1 | 17.3 ± 7.1 |
| 20:0 | 2.4 ± 0.5 | 4.1 ± 3.0 | 0.8 ± 0.5 | 0.4 ± 0.4 | 2.3 ± 2.2 |
| 22:0 | 0.3 ± 0.2 | 1.1 ± 0.5 | 1.3 ± 0.7 | 2.3 ± 1.2 | 1.0 ± 0.5 |
| 23:0 | 1.0 ± 0.5 | 0.1 ± 0.1 | 0.3 ± 0.2 | 1.1 ± 1.0 | 2.6 ± 1.2 |
| 14:1 | 3.9 ± 1.5 | 3.0 ± 1.6 | 2.6 ± 1.0 | 0.7 ± 0.4 | 0.6 ± 0.4 |
| 15:1 | 0.6 ± 0.6 | 1.4 ± 1.4 | 1.7 ± 0.7 | 3.5 ± 2.7 | nd |
| 16:1 | 4.7 ± 1.9 | 9.1 ± 4.8 | 7.6 ± 3.1 | 7.3 ± 2.5 | 7.5 ± 4.6 |
| 17:1 | 3.7 ± 0.6 | 1.7 ± 1.1 | 3.2 ± 1.3 | 1.8 ± 1.2 | 1.2 ± 0.8 |
| 18:1 | 14.7 ± 1.1 | 4.6 ± 3.2 | 10.4 ± 3.4 | 7.4 ± 3.1 | 10.6 ± 2.3 |
| 20:1 | 1.8 ± 1.2 | 2.4 ± 1.6 | 1.6 ± 1.6 | 0.8 ± 0.8 | 3.5 ± 2.1 |
| 22:1 | 1.0 ± 0.5 | 0.4 ± 0.4 | 0.3 ± 0.4 | 0.1 ± 0.1 | 0.7 ± 0.2 |
| 24:1 | 0.6 ± 0.6 | nd | 2.0 ± 1.3 | nd | 1.8 ± 1.2 |
| 18:3n3 | 1.6 ± 0.5 | 0.9 ± 0.4 | 1.0 ± 0.6 | 0.6 ± 0.5 | 1.2 ± 0.4 |
| 20:3n3 | nd | 1.3 ± 0.7 | 0.6 ± 0.3 | 0.7 ± 0.7 | 1.1 ± 1.1 |
| 20:5n3 | 1.9 ± 0.6 | 0.1 ± 0.1 | 3.6 ± 0.9 | 1.7 ± 0.9 | 0.7 ± 0.7 |
| 22:6n3 | 1.0 ± 0.7 | 1.1 ± 1.0 | 1.0 ± 0.6 | 0.9 ± 0.5 | 1.1 ± 0.7 |
| 18:2n6 | 1.9 ± 1.0 | 3.4 ± 0.6 | 4.1 ± 1.5 | 3.9 ± 1.4 | 3.3 ± 1.4 |
| 18:3n6 | 0.5 ± 0.2 | 0.5 ± 0.3 | 4.6 ± 1.2 | 1.8 ± 1.1 | 0.8 ± 0.5 |
| 20:2n6 | 1.1 ± 0.8 | 1.3 ± 0.8 | 0.5 ± 0.3 | 0.5 ± 0.3 | 0.1 ± 0.1 |
| 20:3n6 | 0.2 ± 0.1 | nd | 1.8 ± 0.9 | 0.1 ± 0.1 | 0.3 ± 0.2 |
| 20:4n6 | nd | 0.8 ± 0.5 | 0.8 ± 0.5 | 0.1 ± 0.1 | nd |
| 22:2n6 | 3.2 ± 1.1 | 2.2 ± 1.1 | 3.1 ± 1.6 | 1.1 ± 0.6 | 2.0 ± 1.4 |
| Total saturates | 56.1 ± 2.1 | 67.4 ± 3.0 | 50.1 ± 3.8 | 67.0 ± 7.1 | 62.8 ± 3.8 |
| Total monoenes | 31.0 ± 1.8 | 22.6 ± 4.2 | 29.6 ± 6.0 | 21.6 ± 7.4 | 25.8 ± 5.1 |
| n3 polyenes | 4.4 ± 0.9 | 3.4 ± 0.8 | 6.2 ± 1.5 | 3.9 ± 0.5 | 4.1 ± 1.5 |
| n6 polyenes | 8.5 ± 0.7 | 6.6 ± 2.2 | 14.0 ± 2.3 | 7.6 ± 1.8 | 7.3 ± 1.7 |
| n6/n3 | 2.4 ± 0.5 | 3.3 ± 1.5 | 2.2 ± 0.5 | 2.0 ± 0.4 | 3.0 ± 0.8 |
| U/S | 0.8 ± 0.1 | 0.5 ± 0.1 | 1.1 ± 0.2 | 0.6 ± 0.2 | 0.6 ± 0.1 |
| UI | 69.0 ± 5.5 | 47.7 ± 2.7 | 93.1 ± 5.4 | 54.4 ± 7.5 | 55.2 ± 3.5 |
| Chain length | 17.2 ± 0.2 | 17.0 ± 0.2 | 17.4 ± 0.3 | 17.4 ± 0.3 | 17.5 ± 0.3 |

Values are represented as means ± standard error (n=6). SFA, saturated fatty acids; MUFA, monounsaturated fatty acids; n3, n3 polyunsaturated fatty acids; n6, n6 polyunsaturated fatty acids; UI, unsaturation index = $\sum m_i \times n_i$, where $m_i$ is the mole percentage and $n_i$ is the number of carbon–carbon double bonds of the fatty acid.

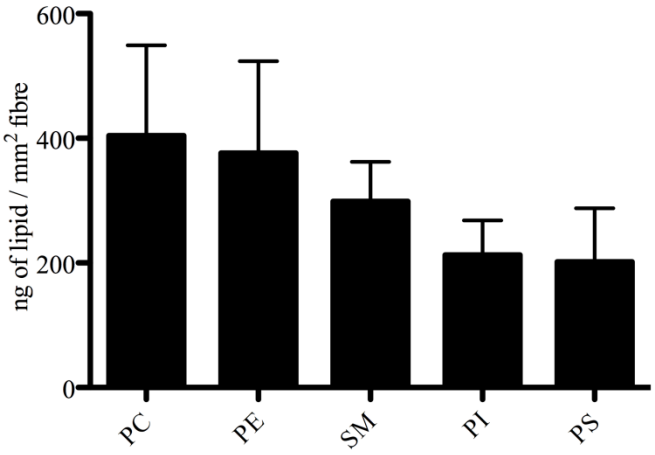


**Figure A3. 3**. Content of major phospholipid species of sarcolemmal membranes from extensor digitorum longus (EDL) skinned fibres (ng/mm$^2$). Values are represented as means ± standard error (n=5). PC, phosphatidylcholine; SM, sphingomyelin; PE, phosphatidylethanolamine; PI, phosphatidylinositol; PS, phosphatidylserine.

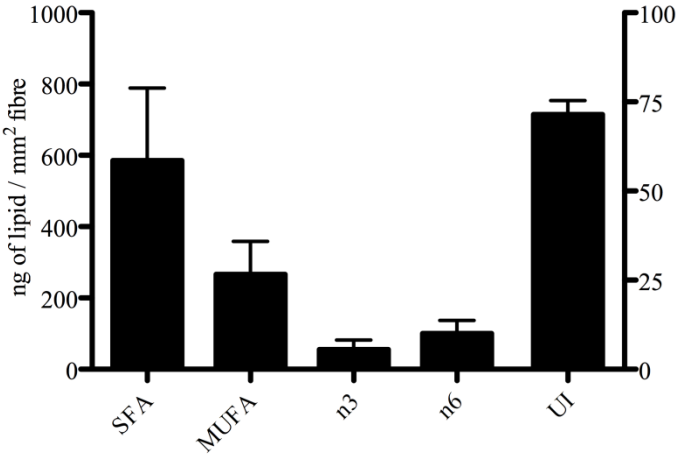


**Figure A3. 4**. Content of total fatty acid subclasses independent of phospholipid species of sarcolemmal membranes from EDL skinned fibres (ng/mm$^2$). Values are represented as means ± standard error with SFA, MUFA, n3, and n6 represented on the left *y*-axis and UI represented on the right (n=5). SFA, saturated fatty acids; MUFA, monounsaturated fatty acids; n3, n3 polyunsaturated fatty acids; n6, n6 polyunsaturated fatty acids; UI, unsaturation index = $\sum m_i$ x $n_i$, where $m_i$ is the ng/mm$^2$ fraction percentage and $n_i$ is the number of carbon–carbon double bonds of the fatty acid.

Representation of data

When converting the results from percent ng/mm$^2$ fraction units to percent mole fraction, the trends (phospholipid species and fatty acid composition) remained constant (Appendix 3 Figures A3.1 & A3.2, Table A3.2). However, after keeping results as absolute (ng/mm$^2$) the phospholipid species order changed with PC (404 ng/mm$^2$) > PE (376 ng/mm$^2$) > SM (298 ng/mm$^2$), > PI (213 ng/mm$^2$) and > PS (202 ng/mm$^2$) (Appendix 3 Figure A3.3). The major FA subclass hierarchy along with UI were similar (Appendix 3 Figure A3.4).

The mechanical skinning technique allows for measurements of skinned fibre length and diameter, which allows for the calculation of total surface area. This is the first study to standardize the lipid analysis results to total surface area of sample analyzed. The representation of the data is still relative to total, and when converting data to the traditional percent mole fraction method, the results did not change (Appendix 3 Figure A3.1). However, when presenting the data in absolute terms, the phospholipid species composition did change with PE being more abundant than SM (Appendix 3 Figure A3.3). This may be a result of the high variability of absolute PC, PE (80% and 87% CV, respectively) and lower variability in SM (47% CV).

These results may inherently outline a limitation to GC analysis specifically where much of the analysis is determined by the external standard (13:0). Specifically, the general formula for converting peaks on a chromatograph to lipid concentrations is:

$$\frac{\text{(AUC of FA)}}{\text{(AUC of 13:0)}} \times \text{(weight of 13:0 injected)} \times \frac{1}{\text{(molecular weight of FA)}} \times \frac{1}{\text{(volume of sample)}}$$

where AUC is the area under the curve. Interestingly, lipid analysis with absolute units is more influenced by AUC of 13:0 than lipid analysis is with relative terms. Absolute total phospholipid weights are non-linearly related to 13:0 AUC ($r^2 = 0.99$) whereby at lower 13:0 AUC (< 300 000) lipid weight is inflated (Appendix 3 Figure A3.5). This effect is more pronounced in PC and PE species, whereby below a 13:0 AUC of 300 000 the lipid weights are much higher than those when AUC > 300 000 (differences of: PC, +573 ng/mm$^2$ ; PE, and +585 ng/mm$^2$) (Appendix 3 Figure A3.6). In contrast, the difference in SM weight between when 13:0 AUC < 300 000 and 13:0 AUC > 300 000 is less pronounced (+200 ng/mm$^2$) (Appendix 3 Figure A3.6). Thus the great differences seen in PC and PE species at the various 13:0 AUC can pull their respective average absolute lipid weights higher. In addition, the great differences in PC and PE account for their high CVs. In contrast, because SM differences are less pronounced across the various 13:0 AUC, the mean absolute lipid weights and variation are not as influenced. This suggests, that in order to present the data in absolute terms, there must be an adjustment factor made for AUC of 13:0. It seems that there is a dynamic range in which the AUC of 13:0 can accurately predict the weight of lipids, and anything beyond this range must be adjusted for.

Of interest, since individual phospholipids shared the same non-linear relationship (Appendix 3 Figure A3.5), there seems to be no effect (linear or non-linear) of 13:0 AUC on the relative amounts of these individual phospholipid species (Appendix 3 Figure A3.7). Furthermore, the variation when presenting data in percent ng/mm$^2$ fraction for all individual phospholipid species is minimal compared to absolute values, with CVs for PC

= 12%, SM = 33 %, PE = 23%, PI = 30% and PS = 32%. Indeed, at a 13:0 AUC ~600 000, SM% is inflated which pulls the average SM% and variation higher, however if the two values were excluded, SM% would still remain ~20% (Appendix 3 Figure A3.7B). This value is still higher than what has been shown in previous studies and thus it is still possible that the mechanical skinning technique is more inclusive of the detergent-resistant domains (Fiehn, et al., 1971; L. E. Stefanyk, 2008).

**Table A3.4**. Fatty acid content of phospholipid species of sarcolemmal membranes from EDL skinned fibres (ng/mm$^2$).

| Fatty acid subclasses | Phosphatidylcholine | Sphingomyelin | Phosphatidylethanolamine | Phosphatidylinositol | Phosphatidylserine |
|---|---|---|---|---|---|
| 12:0 | 4.2 ± 1.7 | 3.5 ± 1.5 | 6.1 ± 2.1 | 1.9 ± 1.4 | 0.7 ± 0.7 |
| 14:0 | 4.8 ± 2.8 | 1.2 ± 0.5 | 4.5 ± 2.1 | 3.3 ± 2.5 | 3.1 ± 1.7 |
| 15:0 | 5.0 ± 1.3 | 7.9 ± 2.2 | 7.9 ± 3.6 | 0.8 ± 0.4 | 1.1 ± 0.9 |
| 16:0 | 82.0 ± 29.1 | 26.1 ± 6.1 | 69.1 ± 33.4 | 35.0 ± 10.8 | 64.3 ± 35.2 |
| 17:0 | 7.0 ± 5.0 | 4.0 ± 2.6 | 6.5 ± 2.1 | 0.4 ± 0.3 | 1.1 ± 1.0 |
| 18:0 | 44.0 ± 20.7 | 19.1 ± 6.5 | 53.3 ± 33.2 | 51.9 ± 13.7 | 15.2 ± 11.3 |
| 20:0 | 9.9 ± 5.0 | 9.0 ± 6.3 | 1.3 ± 0.8 | 1.1 ± 1.1 | 1.0 ± 1.0 |
| 22:0 | 1.4 ± 1.4 | 1.8 ± 1.2 | 3.2 ± 2.3 | 3.2 ± 1.8 | 2.1 ± 1.6 |
| 23:0 | 2.8 ± 2.0 | 0.1 ± 0.1 | 0.3 ± 0.3 | 3.7 ± 3.7 | 9.3 ± 5.4 |
| 14:1 | 12.2 ± 7.5 | 3.4 ± 1.4 | 5.5 ± 2.9 | 0.8 ± 0.6 | 0.5 ± 0.3 |
| 15:1 | 0.7 ± 0.6 | 2.2 ± 2.2 | 1.7 ± 1.0 | 1.1 ± 1.0 | nd |
| 16:1 | 21.5 ± 13.0 | 13.8 ± 8.3 | 17.1 ± 9.0 | 12.4 ± 6.9 | 5.4 ± 3.3 |
| 17:1 | 11.1 ± 3.9 | 1.9 ± 1.3 | 7.4 ± 3.5 | 1.7 ± 0.6 | 1.9 ± 1.5 |
| 18:1 | 45.9 ± 16.2 | 1.9 ± 1.3 | 32.6 ± 24.6 | 12.2 ± 5.5 | 22.6 ± 11.9 |
| 20:1 | 0.9 ± 0.6 | 4.4 ± 3.2 | 4.8 ± 4.7 | 0.1 ± 0.1 | 3.0 ± 1.7 |
| 22:1 | 2.6 ± 1.8 | 0.4 ± 0.3 | nd | 0.3 ± 0.3 | 1.7 ± 1.0 |
| 24:1 | 1.8 ± 1.8 | nd | 6.3 ± 6.2 | nd | 2.1 ± 1.5 |
| 18:3n3 | 3.1 ± 1.5 | 1.2 ± 0.8 | 5.9 ± 4.0 | 0.5 ± 0.3 | 0.5 ± 0.3 |
| 20:3n3 | nd | 2.7 ± 1.9 | 2.9 ± 2.0 | nd | 4.4 ± 4.4 |
| 20:5n3 | 5.9 ± 4.5 | 0.2 ± 0.2 | 15.2 ± 8.0 | 4.6 ± 2.6 | nd |
| 22:6n3 | 1.1 ± 0.9 | 0.1 ± 0.1 | 1.6 ± 1.1 | 1.2 ± 0.7 | 4.0 ± 2.8 |
| 18:2n6 | 9.9 ± 4.9 | 1.8 ± 0.7 | 4.7 ± 2.3 | 6.1 ± 3.8 | 5.7 ± 4.2 |
| 18:3n6 | 1.9 ± 1.5 | 0.4 ± 0.2 | 19.2 ± 9.7 | 0.8 ± 0.7 | 0.1 ± 0.1 |
| 20:2n6 | 5.6 ± 5.6 | 2.4 ± 1.6 | 0.4 ± 0.3 | 0.7 ± 0.4 | nd |
| 20:3n6 | 0.1 ± 0.1 | nd | 8.7 ± 7.4 | nd | 1.1 ± 1.1 |
| 20:4n6 | nd | 0.9 ± 0.6 | 2.8 ± 2.4 | 0.3 ± 0.3 | nd |
| 22:2n6 | 11.8 ± 7.0 | 3.0 ± 1.3 | 9.3 ± 4.8 | 2.4 ± 1.5 | 0.7 ± 0.7 |
| Total* | 404.3 ± 145.1 | 298.7 ± 63.6 | 376.2 ± 147.7 | 212.7 ± 55.5 | 201.8 ± 85.7 |
| Total saturates | 161.1 ± 58.0 | 72.8 ± 14.7 | 152.3 ± 66.2 | 101.3 ± 25.4 | 98.1 ± 45.1 |
| Total monoenes | 96.7 ± 36.6 | 28.1 ± 9.1 | 75.5 ± 27.4 | 28.6 ± 11.3 | 37.2 ± 12.5 |
| n3 polyenes | 10.2 ± 3.4 | 4.2 ± 1.8 | 25.7 ± 14.1 | 6.3 ± 2.3 | 8.9 ± 7.0 |
| n6 polyenes | 29.3 ± 12.4 | 8.5 ± 1.0 | 45.0 ± 21.8 | 10.4 ± 3.9 | 7.6 ± 3.7 |
| n6/n3 | 2.7 ± 0.7 | 4.1 ± 1.8 | 2.1 ± 0.7 | 1.7 ± 0.3 | 3.1 ± 0.9 |
| U/S | 0.8 ± 0.1 | 0.5 ± 0.1 | 1.1 ± 0.2 | 0.6 ± 0.3 | 0.7 ± 0.1 |
| UI | 72.3 ± 7.4 | 48.1 ± 2.5 | 102.3 ± 6.7 | 57.1 ± 9.1 | 56.6 ± 3.6 |
| Chain length | 17.3 ± 0.1 | 17.1 ± 0.2 | 17.5 ± 0.3 | 17.4 ± 0.2 | 17.7 ± 0.3 |

Values are represented as means ± standard error (n=5). SFA, saturated fatty acids; MUFA, monounsaturated fatty acids; n3, n3 polyunsaturated fatty acids; n6, n6 polyunsaturated fatty acids; UI, unsaturation index = $\sum m_i \times n_i$, where $m_i$ is the mole percentage and $n_i$ is the number of carbon–carbon double bonds of the fatty acid. *Total lipid content was calculated by multiplying the sum of fatty acid subclasses by respective phospholipid factors PC, 1.36g of PC / g of fatty acid (FA); SM, 2.63 g of SM / g of FA; PE, 1.26 g of PE / g of FA; PI, 1.45 g of PI / g of FA; PS, 1.33 g of PS / g of FA.

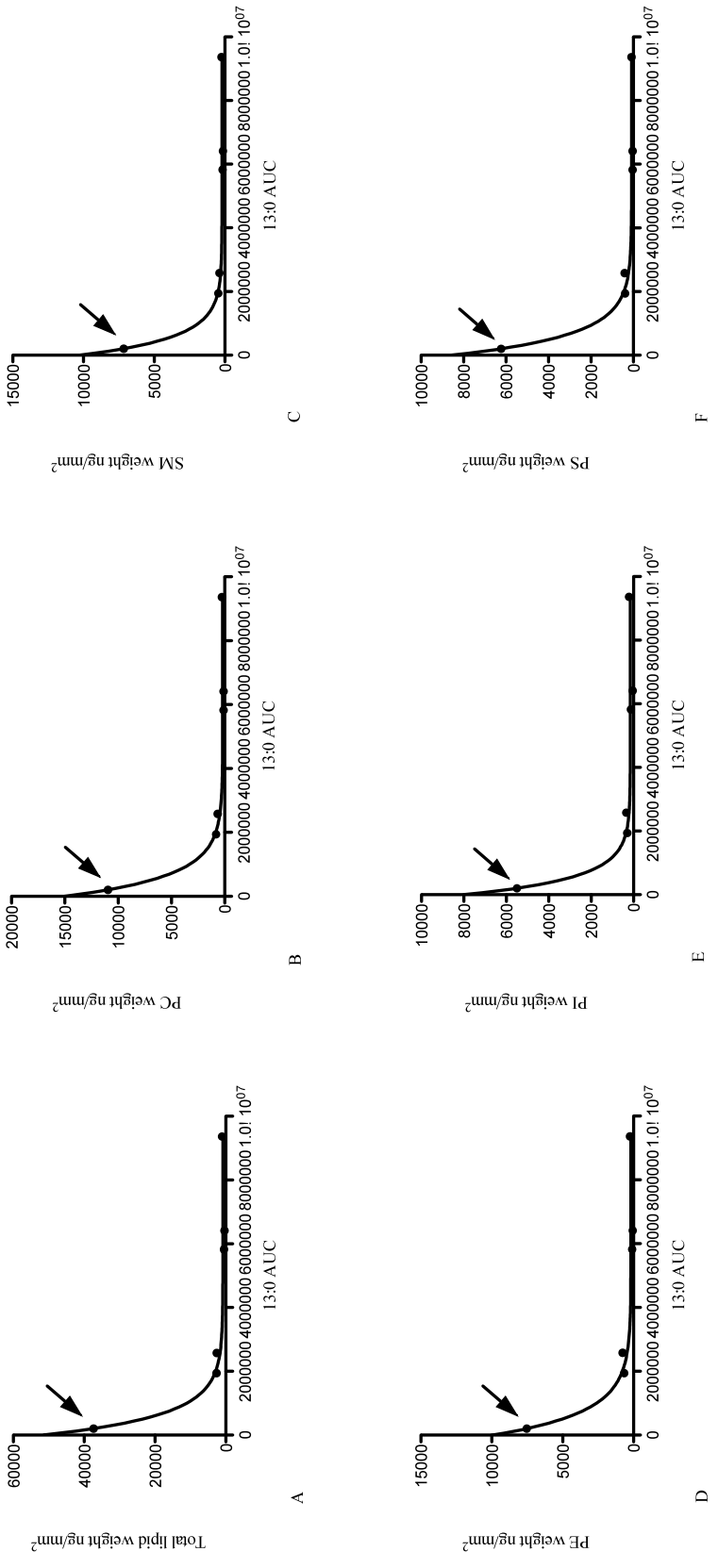


**Figure A3. 5**. Non-linear relationships (one-phase decay model) of 13:0 AUC with total and individual phospholipid weight (ng/mm$^2$). PC: phosphatidylcholine, SM: sphingomyelin, PE: phosphatidylethanolamine, PI: phosphatidylinositol, PS: phosphatidylserine, AUC: area under the curve. All figures A-F fit the one-phase decay model with $r^2 = 0.99$. Arrows are pointing to the extreme values that were excluded from analysis at absolute terms producing the n of 5.

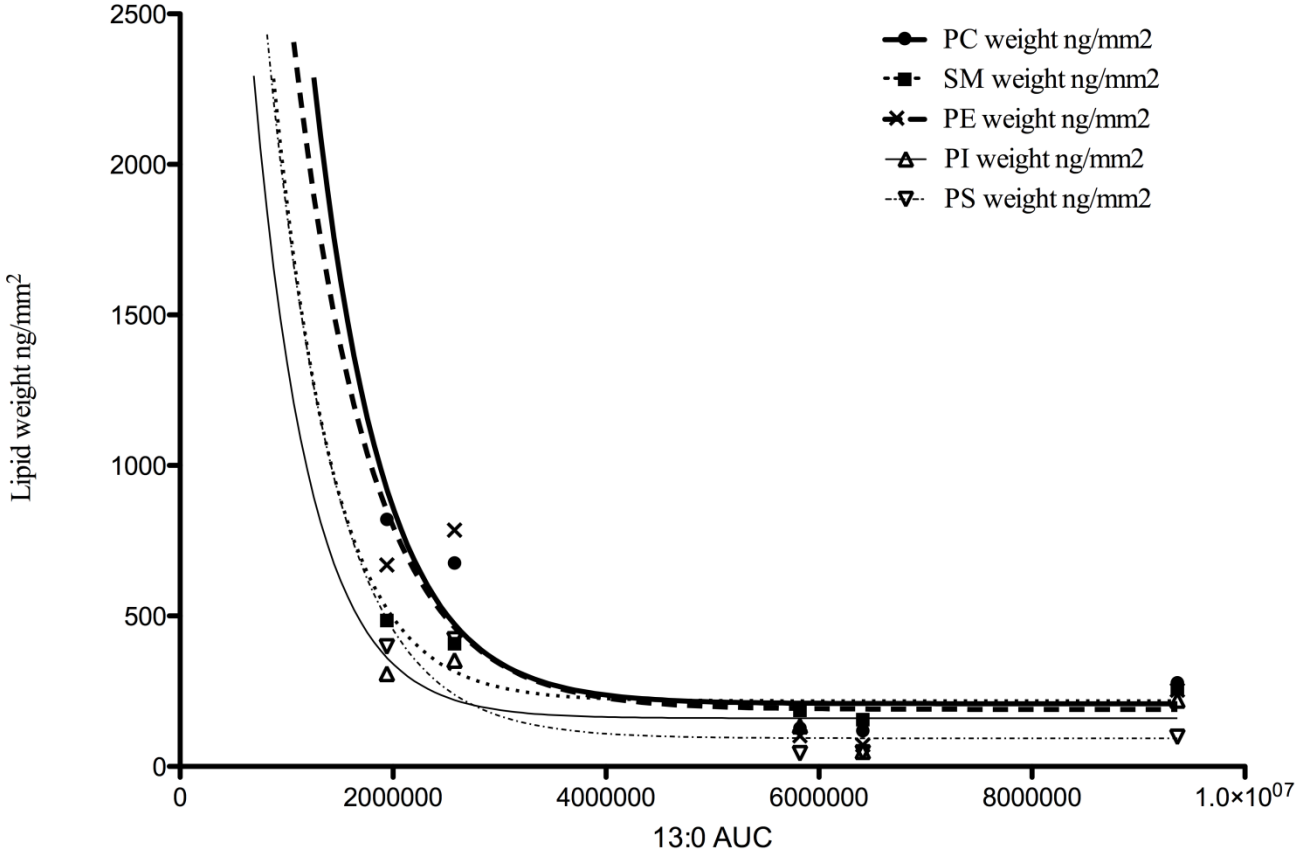


**Figure A3. 6.** Overlay of non-linear relationship from individual phospholipid species excluding the extreme value from 13:0 AUC of ~20 000 (n=5). PC: phosphatidylcholine, SM: sphingomyelin, PE: phosphatidylethanolamine, PI: phosphatidylinositol, PS: phosphatidylserine, AUC: area under the curve.

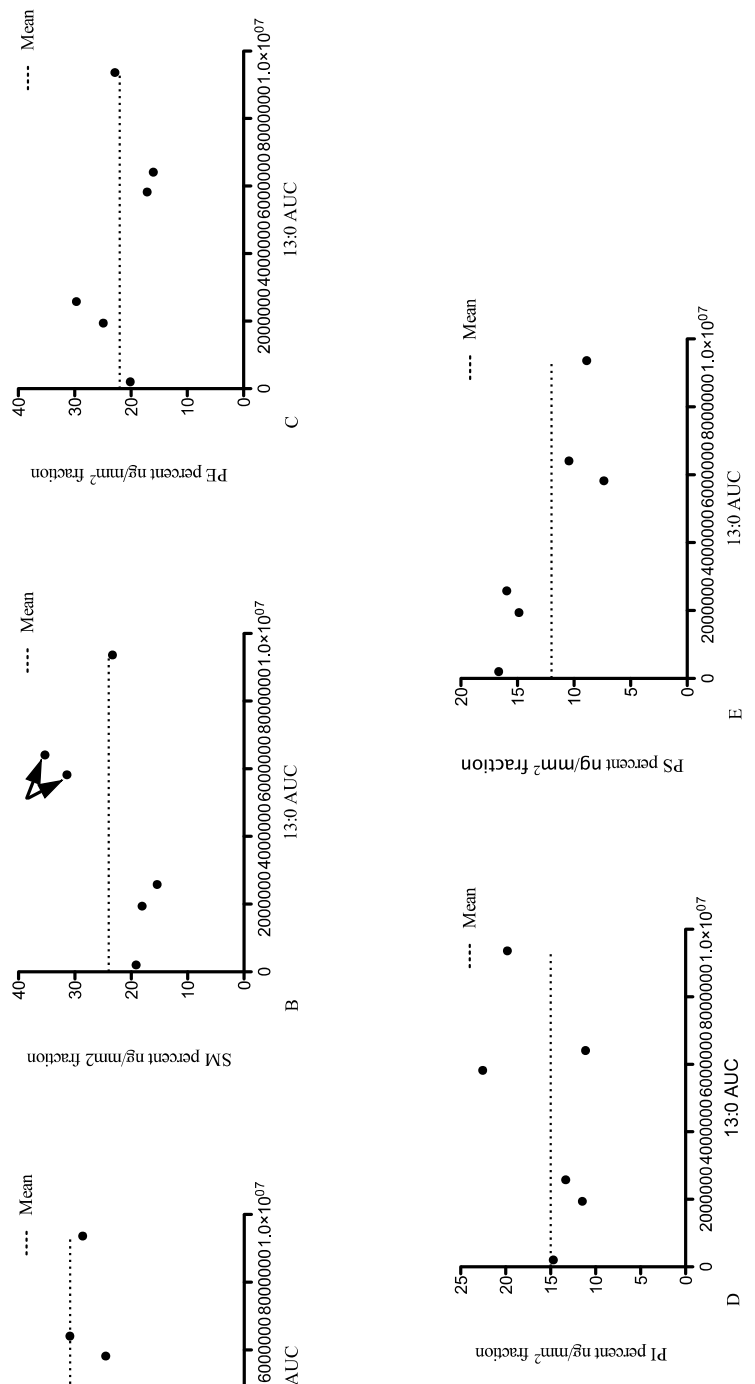


**Figure A3. 7**. Individual phospholipids presented in relative terms (percent ng/mm$^2$ fraction) plotted against 13:0 AUC (n=6). PC: phosphatidylcholine, SM: sphingomyelin, PE: phosphatidylethanolamine, PI: phosphatidylinositol, PS: phosphatidylserine, AUC: area under the curve. The two arrows on SM (B) indicate values that may pull up the average percent of SM.

REFERENCES

Fiehn, W., Peter, J. B., Mead, J. F., & Gan-Elepano, M. (1971). Lipids and fatty acids of sarcolemma, sarcoplasmic reticulum, and mitochondria from rat skeletal muscle. *J Biol Chem, 246*(18), 5617-5620.

Stefanyk, L. (2008). *Skeletal Muscle Fibre-Type Comparison of Whole tissue and Subcellular Phospholipids and Fatty Acids.* Brock University, St. Catharines.

**APPENDIX 4: List of fatty acids**

| FA | Acid name |
|---|---|
| 12:0 | Lauric acid |
| 14:0 | Myristic acid |
| 14:1 | Myristoleic acid |
| 15:0 | Isopalmitic acid |
| 15:1 | Pentadecenoic acid (systematic name) |
| 16:0 | Palmitic acid |
| 16:1 | Palmitoleic acid |
| 17:0 | Margaric acid |
| 17:1 | Margaroleic acid |
| 18:0 | Stearic acid |
| 18:1 | Oleic acid |
| 18:2n6 | Linoleic acid (LA) |
| 18:3n6 | γ-Linolenic acid |
| 18:3n3 | α-Linolenic acid (ALA) |
| 20:0 | Arachidic acid (AA) |
| 20:1 | Gondoic acid |
| 20:2 | Eicosadienoic acid (systematic name) |
| 20:3n6 | Dihomo-γ-linolenic acid |
| 20:3n3 | Eicosatrienoic acid (systematic name) |
| 20:4n6 | Arachidonic acid |
| 20:5n3 | Eicosapentaenoic acid (EPA) |
| 22:0 | Behenic acid |
| 22:1 | Erucic acid |
| 22:2 | Brassic acid |
| 23:0 | Tricosanoic acid |
| 22:6n3 | Docosahexaenoic acid (DHA) |
| 24:1 | Nervonic acid |